Auto- and cross-regulation of the hnRNPs D and DL
&
Hypoxia-driven gene expression changes in human cancer cells

PhD Thesis

TECHNISCHE
UNIVERSITÄT
DARMSTADT

Dem Fachbereich Biologie der
Technischen Universität Darmstadt
zur Erlangung des akademischen Grades eines
Doctor rerum naturalium
(Dr. rer. nat.)

eingereichte Dissertation von

Frau M. Sc. Sandra Fischer

Erstgutachterin: Prof. Dr. Beatrix Süß
Zweitgutachter: Prof. Dr. Alexander Löwer

Darmstadt 2019

Fischer, Sandra: Auto- and cross-regulation of the hnRNPs D and DL & Hypoxia-driven gene expression changes in human cancer cells
Darmstadt, Technische Universität Darmstadt,
Jahr der Veröffentlichung der Dissertation auf TUprints: 2020
URN: urn:nbn:de:tuda-tuprints-91393
Tag der mündlichen Prüfung: 28.11.2019

Veröffentlicht unter CC BY-SA 4.0 International
https://creativecommons.org/licenses/

This thesis is based on the following publications (in chronological order):

Kemmerer K*, **Fischer S*** and Weigand JE. (2018) Auto- and cross-regulation of the hnRNPs D and DL. RNA 24, 324-331. (* Shared first author)

Braun J, **Fischer S**, Xu ZZ, Sun H, Ghoneim DH, Gimbel AT, Plessmann U, Urlaub H, Mathews DH and Weigand JE. (2018) Identification of new high affinity targets for Roquin based on structural conservation. Nucleic Acids Research 46, 12109-12125.

Di Liddo A, de Oliveira Freitas Machado C, **Fischer S**, Ebersberger S, Heumüller AW, Weigand JE, Müller-McNicoll M and Zarnack K. (2019) A combined computational pipeline to detect circular RNAs in human cancer cells under hypoxic stress. Journal of Molecular Cell Biology, Epub ahead of print, doi: 10.1093/jmcb/mjz094.

Fischer S, Di Liddo A, Taylor K, Sobczak K, Zarnack K and Weigand JE. (2019) Muscleblind-like 2 controls the hypoxia response of cancer cells. RNA. (*in revision*)

Contents

1 Abstract

RNA-binding proteins (RBPs) control all steps of mRNA processing, including pre-mRNA splicing, mRNA localization, stability and translation efficiency. Auto- and cross-regulation of RBPs is essential for RBP homeostasis and the prevention of pathologies. Consequently, deregulation of RBPs is prevalent in diseases, in particular during tumorigenesis. A profound understanding of RBP regulation is thus indispensible to open up new approaches in cancer therapy.

HnRNP DL is a ubiquitous RBP that is overexpressed in prostate cancer and chronic myeloid leukemia. HnRNP DL was suggested to regulate its own expression in a negative feedback loop via usage of a poison exon in its 3' UTR. In this study, hnRNP DL autoregulation by binding to its own pre-mRNA was confirmed and cross-regulation between hnRNP DL and its well-studied paralog hnRNP D (AUF1) was demonstrated. Strikingly, *hnRNP DL* is a crucial factor for endothelial cell function, such as migration and angiogenesis. This highlights the influence of hnRNP DL, and RBPs in general, on cellular key processes.

The cellular environment has an influence on the levels of RBPs and their functionality. Oxygen starvation (hypoxia) is a common cellular stress. It appears physiologically at high altitudes or during embryonic development, but hypoxia is also typical for diseased tissue. In particular in solid tumors, the hypoxic microenvironment influences gene expression and promotes cancerogenesis leading to poor patient outcomes. The transcriptional response to hypoxia is well studied and controlled by hypoxia inducible factor (HIF) proteins. However, the posttrancriptional response to hypoxia is still poorly understood. Thus, this study focused on hypoxia-driven changes in RBP levels and alternative splicing (AS) in human cancer cells. Transcriptome analyses showed correlated gene expression changes in human lung and breast cancer cells after chronic hypoxia treatment, but AS changes were highly divergent, demonstrating the cell type-specificity of AS. Strikingly, muscleblind-like 2 (MBNL2) was specifically induced under hypoxia, while RBPs were predominantly reduced. Subsequent transcriptome analyses after MBNL2 depletion showed that MBNL2 controls hypoxia-driven AS and the transcript abundance of typical hypoxia-induced genes, such as vascular endothelial growth factor (*VEGFA*). Strikingly, this control is specific for MBNL2 and not shared by its paralog MBNL1, showing the importance of MBNL2 for cancer cell adaptation to hypoxia. In addition, MBNL2 depletion led to reduced cancer cell proliferation and migration, indicating that deregulated RBPs might be new targets for cancer therapy.

2 Zusammenfassung

RNA-Bindeproteine (RBPs) regulieren alle Schritte der mRNA Prozessierung. Typisch für RBPs ist, dass sie sich selbst (Autoregulation) oder gegenseitig (Crossregulation) regulieren, was wichtig für die RBP Homöostase ist. Entsprechend sind RBPs in vielen Krankheitsbildern dereguliert, u.a. bei Krebserkrankungen. Das Verständnis der RBP Regulation ist daher wichtig, um neue Ansatzpunkte für Therapien zu liefern.

HnRNP DL ist ein ubiquitäres RBP, welches bei Prostatakrebs und chronischer myeloischer Leukämie überexprimiert wird. HnRNP DL reguliert seine eigene Expression durch eine negative Rückkopplungsschleife, durch Inklusion eines sogenannten *„poison“* Exons. In dieser Arbeit wurde die Autoregulation von hnRNP DL durch die direkte Bindung der eigenen prä-mRNA bestätigt. Außerdem konnte die Crossregulation zwischen hnRNP D und DL gezeigt werden. Es ist bemerkenswert, dass *hnRNP DL* maßgebend für endotheliale Funktionen wie Migration und Angiogenese ist. Dies unterstreicht die Rolle von hnRNP DL, und RBPs im Allgemeinen, bei wichtigen zellulären Prozessen.

Sauerstoffmangel (Hypoxie) ist ein häufig auftretender Stressfaktor und tritt in großen Höhen oder bei der Embryonalentwicklung auf. Sie spielt aber auch eine Rolle bei vielen Krankheiten. Typisch ist Hypoxie für solide Tumore, in welchen sie die Genexpression beeinflusst und so schwere Krankheitsverläufe begünstigt. Sogenannte *hypoxia inducible factor* (HIF) Proteine vermitteln die transkriptionelle Antwort auf Hypoxie. Diese ist bereits gut untersucht, während über die post-transkriptionelle Regulation unter Hypoxie noch sehr wenig bekannt ist. Deshalb beschäftigte sich diese Arbeit mit dem Einfluss von Hypoxie auf RBPs und auf das alternative Spleißen (AS). Transkriptomanalysen nach chronischer Hypoxiebehandlung zeigten korrelierte Genexpressionsänderungen in humanen Lungen- und Brustkrebszellen, AS-Änderungen waren jedoch sehr unterschiedlich. Auffallend war, dass *Muscleblind-like* 2 (MBNL2) spezifisch unter Hypoxie induziert wurde, während andere RBPs hauptsächlich reduziert waren. Nachfolgende Transkriptomanalysen nach *MBNL2-Knockdown* zeigten, dass MBNL2 hypoxie-abhängiges AS und die Transkripthäufigkeit typischer hypoxie-induzierter Gene, wie beispielsweise *VEGFA*, kontrolliert. Diese Kontrolle ist spezifisch für MBNL2 und wird nicht von seinem Paralog MBNL1 ausgeübt, was die Bedeutung von MBNL2 für die Anpassung von Krebszellen an Hypoxie verdeutlicht. Darüber hinaus führte die Reduktion von *MBNL2* zu einer reduzierten Krebszell-Proliferation und -Migration, was darauf hindeutet, dass deregulierte RBPs neue Ziele für die Krebstherapie sein könnten.

3 Introduction

3.1 Hypoxia

In general, hypoxia is the state of insufficient oxygen supply. Although oxygen is indispensible for cell viability, hypoxia plays an important role in many physiological processes. It is implicated in embryonic development, wound healing or occurs at high altitudes.[1,2,3] Nevertheless, hypoxia is characteristic for several diseases. Typically, hypoxia is found in inflamed tissue, during cardiovascular diseases and it is a hallmark of solid tumors.[4,5]

There are five types of tissue hypoxia.[6] Characteristic for hypoxemia is a reduced oxygen partial pressure in the blood, which is caused at high altitude.[7] Anemic hypoxia is typical for a reduced level of hemoglobin in the blood, mostly resulting from an iron deficiency. Ischemic hypoxia results from a reduced blood circulation. Diffusional hypoxia occurs when diffusion distances are increased or when countercurrents in vessels inhibit the correct diffusion. Cells can also lose their ability to use oxygen by intoxication for example by cyanides. This condition is called cytotoxic hypoxia.[6]

Blood vessels are important for the distribution of oxygen and metabolites. Endothelial cells form the inner lining of blood vessels and are therefore the first instance affected by hypoxemic, anemic and ischemic hypoxia.[8,9] In endothelial cells, hypoxia strongly influences gene expression. Hypoxia triggers gene expression programs promoting proliferation, migration and angiogenesis.[8] In hypoxic tumors these gene expression programs are activated as well, promoting tumor growth and metastasis.[62]

3.1.1 Transcriptional regulation under hypoxia

The transcriptional response to hypoxia is orchestrated by the family of hypoxia-inducible factors (HIFs).[10,11] The heterodimeric HIF complex consists of a HIF-α and a HIF-β subunit. There are three HIF-α subtypes: HIF-1α, HIF-2α (also endothelial PAS domain protein 1; EPAS1) and HIF-3α.[12,13] HIF-1α is constitutively synthesized and present in the cytosol.[14] Under normoxic conditions HIF-1α, is hydroxylated at conserved proline residues by prolyl hydroxylases (PHD1-3). Subsequently, HIF-1α is bound by the von Hippel-Lindau tumor suppressor protein (VHL protein) and degraded via the proteasome. Under hypoxic conditions, these prolyl hydroxylases are inhibited and HIF-1α dimerizes with HIF-1β (also aryl hydrocarbon receptor nuclear translocator; ARNT), which is constitutively active in the

nucleus. The dimer diffuses into the nucleus and activates transcription of various target genes by binding hypoxia responsive elements (HREs; **Figure 3-1**).[15] Well-studied HIF targets are for example *lactate dehydrogenase* (*LDHA*), *erythropoietin* (*EPO*) or *vascular endothelial growth factor A* (*VEGFA*).[16,17,18] HIF-2α and HIF-3α are regulated in the same way as HIF-1α. HIF-1α mediates acute responses while HIF-2α is accumulated, promoting a prolonged hypoxic gene activation.[19] Thus, HIF-1α and HIF-2α play different roles in the adaptation to acute or chronic hypoxia.[19] The exact role of HIF-3α in hypoxia adaptation is still under investigation. Interestingly, HIF-3α seems to inhibit HIF-1α and HIF-2α activities.[20]

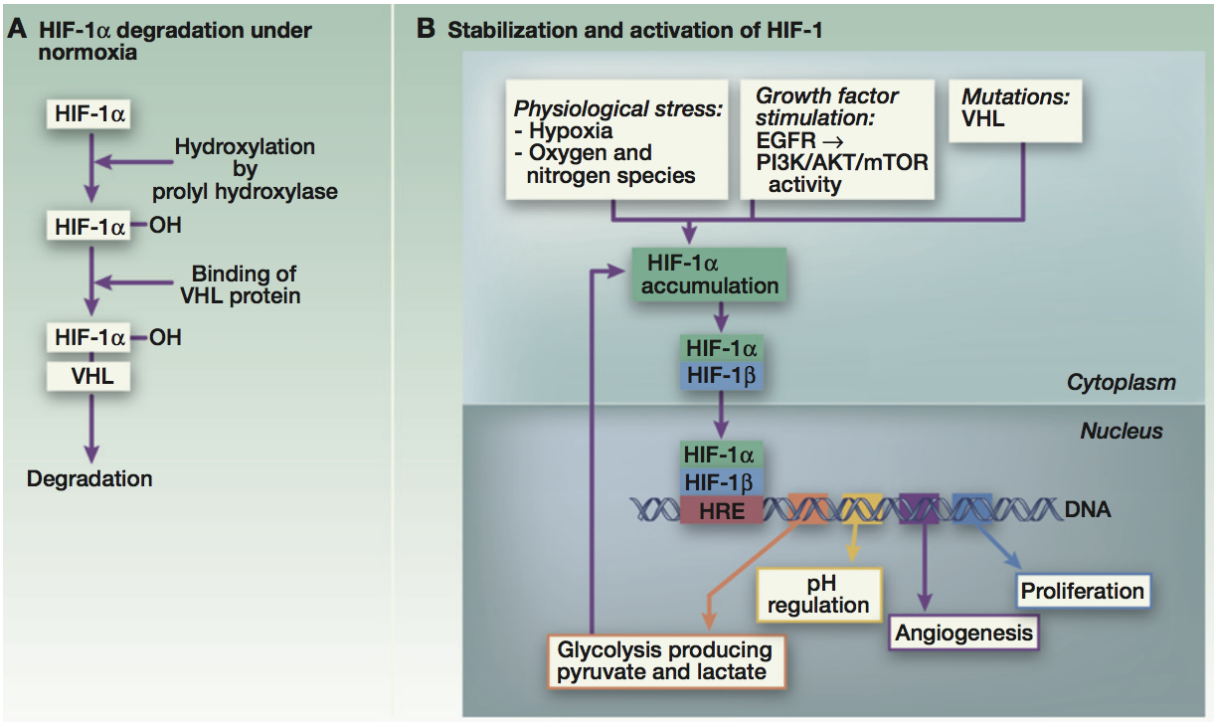

Figure 3-1: HIF transcriptional regulation pathway. (A) Under normoxia HIF-1α is hydroxylated and degraded. **(B)** Under hypoxia HIF-1α accumulates and dimerizes with HIF-1β. Growth factor stimulation or mutations of the VHL protein can also lead to HIF-1α accumulation. The HIF complex activates the transcription of target genes implicated in glycolysis, pH regulation, angiogenesis and proliferation. Figure from [15].

3.1.2 Posttranscriptional regulation under hypoxia

In addition to the transcriptional response, hypoxia impacts on posttranscriptional regulation by modulating alternative splicing (AS; see below), translation efficiency and mRNA stability. This control is often exerted by RNA binding proteins (RBPs). In general, increased mRNA stability results from a decreased mRNA decay rate. Translational efficiency can be altered by influencing the number of ribosomes loaded onto the mRNA, but also by influencing polypeptide synthesis and release. For example, the expression of *HIF-1α* itself is controlled

via mRNA stability[21,22] as well as translation efficiency.[23,24] Human antigen R (HuR) is interacting with the *HIF-1α* 3' UTR, increasing mRNA stability.[25] Additionally, HuR binding in the *HIF-1α* 5' UTR promotes translation.[21,26] Further, polypyrimidine tract binding protein (PTB), which is also called heterogenous nuclear ribonucleoprotein I (hnRNP I), is interacting with the *HIF-1α* 5' UTR increasing translation efficiency.[27] It is likely that HuR and PTB cooperatively promote *HIF-1α* translation by binding at different binding sites.[26]

Another example of a gene exposed to strong posttranscriptional regulation under hypoxia is *VEGFA*. VEGF-A protein is an important regulator under hypoxia since it is a driving force in angiogenesis. Under hypoxia *VEGFA* expression is induced leading to neoangiogenesis, enhancing proliferation and cell migration.[28] *VEGFA* is transcriptionally upregulated by HIF-1α. At the posttranscriptional level, the *VEGFA* 3' UTR is stabilized by both, HuR and PTB.[29,30] In addition, hnRNP L stabilizes *VEGFA* mRNA under hypoxic conditions by displacing several miRNAs.[31]

From a wider perspective, hypoxia is often accompanied by hypoglycemia since the decreased blood flow during ischemia impairs the delivery of both, oxygen and sugar. The mRNAs of several HIF target genes are stabilized by combined oxygen and sugar deprivation.[22] Besides oxygen and sugar, also ATP availability is limited under hypoxia leading to a reduction of canonical protein synthesis. In order to maintain synthesis of proteins needed for hypoxia adaptation alternative translation pathways are activated under hypoxia.[23] There are various mechanisms for mRNA selection and subsequent translation: 1) Upstream open reading frames (uORFs) lie within the 5' UTR and are *cis*-regulatory components, which recruit proteins or ribosomes to promote translation of the main open reading frame (mORF) only under stress conditions.[32,33] 2) Internal ribosome entry sites (IRESs) are sequences or structures in the 5' UTR that recruit ribosomes independent of the cap-binding translation initiation machinery.[34] 3) RNA hypoxia response elements (rHREs) are recognized by the hypoxic translation machinery promoting translation.[35] HIF proteins are well known for their transcriptional activation of target genes, but they can also be part of the hypoxic translation machinery and control translation pathways selective for hypoxia adaptation genes.[23] 4) Selective partitioning of mRNAs to the endoplasmic reticulum (ER) accelerates translation and thus, proteomic hypoxia adaptation.[36] Strikingly, ribosome profiling in human primary hepatocytes revealed that regulation at the translational level is even faster than regulation at the transcriptional level under hypoxia.[37]

Moreover, non-coding RNAs play a role in posttranscriptional regulation under hypoxia. The regulatory role of circRNAs (circular RNAs), lncRNAs (long non-coding RNAs) and miRNAs (microRNAs) has been discovered just recently and is an emerging field of science.[38,39]

The biogenesis of circRNAs differs from the canonical splicing of linear RNAs. CircRNAs are covalently closed loops, which result from back-splicing.[40] CircRNAs do not have 5' to 3' polarity and thus, do not contain a 5' cap or a polyadenylated tail. For that reason, circRNAs have long remained beneath the radar since transcriptome analyses focused on approaches involving poly(A) selection.[40] CircRNAs were previously thought to act as miRNA sponges, but recently it has been discovered that they fulfill diverse biological functions. CircRNA cZNF292, for example, is induced under hypoxia and is implicated in angiogenesis.[41] Further, circDENND4C is HIF-1α-activated and has been shown to promote breast cancer cell proliferation under hypoxic conditions.[42]

LncRNAs can be transcribed from intergenic as well as intragenic regions and are longer than 200 nt.[43] LncRNAs were previously regarded as "junk transcripts", but nowadays it is clear that lncRNAs fulfill diverse biological functions.[43,44] Often lncRNAs control gene regulation by remodeling chromatin structure and thus, the accessibility of genes.[45] Many lncRNAs are induced by hypoxia such as lncRNA LET, RoR, AK058003 or MALAT1, influencing posttranscriptional gene regulation.[46,47,48,49,50] MALAT1, for example, is regulating SR protein phosphorylation and as a result, SR protein activity and SR protein-mediated AS.[51] Furthermore, deregulation of lncRNAs also promotes diseases. For example, lncRNA MALAT-1 was found to promote the onset of various cancers like colorectal, bladder or lung cancer and further facilitates tumor growth and metastasis.[52,53,54]

MiRNAs are the product of a multistep maturation process. Firstly, miRNAs are transcribed as long transcripts containing a hairpin loop (pri-miRNA). In the next step these pri-miRNAs are processed by Drosha into pre-miRNAs.[55] Alternatively, pre-miRNAs can be formed over the miRtron pathway without processing by Drosha.[56] The resulting pre-miRNAs are exported to the cytoplasm, where Dicer converts them into double stranded and approximately 22 nt long miRNA/miRNA* complexes. These complexes include the mature miRNA and a complementary strand, which is usually degraded.[57] In general, miRNAs can bind complementary sequences in 3' UTRs, sometimes blocking specific binding sites for RBPs. Usually, miRNA binding leads to destabilization of the mRNA and subsequently to its degradation. HypoxamiRs are miRNAs induced in response to hypoxia. One of the best-studied examples for a hypoxamiR is miRNA-210 (in short miR-210).[58,59,60] MiR-210 inhibits

receptor tyrosine kinase ligand ephrin-A3 and modulates endothelial cell response to hypoxia by enhancing VEGF-induced chemotaxis.[58] The *VEGFA* 3' UTR further contains a so-called CA-rich element (CARE), which is bound by several miRNAs.[61] MiRNAs miR-297, miR-299, miR-567 and miR-609 can bind to the CARE leading to mRNA degradation under normoxia. Under hypoxia these miRNAs are displaced by hnRNP L leading to an increase in *VEGFA* mRNA levels.[61]

3.1.3 Hypoxia and cancer

In solid tumors, hypoxia is the result of rapidly proliferating cells, which outgrow the vascular system.[62] Typically tumors exhibit varying oxygen pressures ranging from approximately 5% O_2 in external cells, which are still connected to the blood supply, to total anoxia (0% O_2), in parts that are located distal of the blood supply and mostly show necrotic properties.[62,63] These hypoxic regions often show resistance towards chemotherapies since they are not accessible for drugs.[63,64] For efficient radiotherapy free radicals from oxygen are needed to destroy targeted cells, making hypoxic cells also resistant to radiotherapy.[64] Hypoxia further inhibits the T cell-mediated immune response, increasing the immunoresistance of the tumor.[65] Thus, hypoxia is typical for persistent tumors, implicating a poor diagnosis for patients.

In cancer therapy, currently there are mainly two approaches to kill hypoxic cells: Bioreductive prodrugs that are activated only under hypoxia, and inhibitors, that target specific proteins in hypoxic cells. Both approaches underlie the assumption that drugs are still transported to the hypoxic cells in contempt of the disorganization of the vascular network in tumors. Proteins that are already targeted in cancer therapies mostly belong to the HIF, UPR (unfolded protein response) and to a lesser extent the mTOR (mechanistic target of rapamycin kinase) pathway.[66] The HIF target *VEGFA*, with its pro-angiogenic properties, has been identified as potential therapeutic target in hypoxic tumors as well.[67]

3.2 Pre-mRNA splicing

Splicing is a crucial step in the process of gene expression. At first, a precursor mRNA (pre-mRNA) is transcribed from the genomic DNA. This pre-mRNA contains exonic and intronic sequences. During splicing the introns are removed giving rise to the mature mRNA.[68] A

multiprotein complex called the spliceosome catalyzes the complete process of splicing. GURAGU motifs indicate the 5' splice sites (5' SS) within the introns. The 3' SS contains a polypyrimidine tract and a terminal YAG motif at the end. Further, introns contain a branch point sequence with an invariant adenosine 18-40 nt upstream of the 3' SS. All three sites together serve as recognition sites for the splicing machinery. The splicing reaction includes two transesterifications (**Figure 3-2**). In the first step the 5' end of the intron is ligated with the branch point adenosine through a nucleophilic attack of the 2' OH group on the 5' SS. In a second step the free 3' OH of the 5' SS reacts with the phosphate of the 3' SS, whereby the exons are connected and the intron is removed in a lariat structure.[69,70]

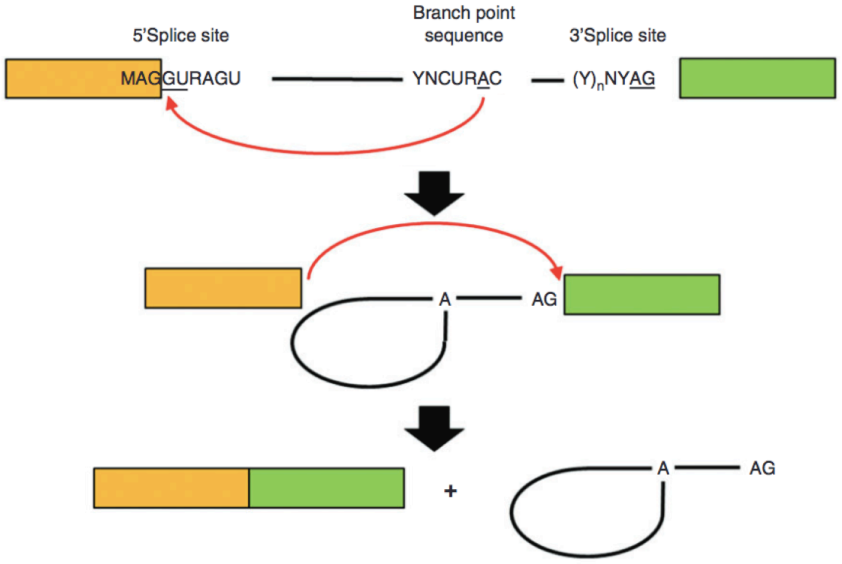

Figure 3-2: Pre-mRNA splicing. The splicing reaction is carried out in two subsequent transesterifications as described in the text. Modified figure from [69].

Essential components of the U2-dependent spliceosome are the five small nuclear ribonucleoproteins (snRNPs): U1, U2, U4, U5 and U6. Each snRNP contains a uridine-rich snRNA, a set of seven (L)Sm proteins and numerous snRNP specific proteins.[71,72] The splicing process is highly dynamic. Thus, the spliceosome configures its conformation several times during the whole process. If the spliced intron does not exceed 200-250 nt, the spliceosome is directly constituted across the intron. However, if it exceeds a size of 200-250 nt, which is the case in most higher eukaryotes, the spliceosomal complex is formed across an exon. These processes are called intron or exon definition, respectively.[73] During intron definition the U1 snRNP is recruited to the 5' SS. The splicing factors SF1/mBBP and U2 auxiliary factor (U2AF) recognize the branch site, the polypyrimidine tract and the 3' SS, respectively. In the next step U2 snRNP binds the branch point, building complex A. By attaching the pre-assembled

U4/U5/U6 tri-snRNP, the precatalytic complex B is created. The following RNA-RNA as well as RNA-protein interactions lead to destabilization of the snRNPs U1 and U4 and to the activation of the spliceosome, which then catalyzes the first splicing step. The catalysis gives rise to complex C, which completes the splicing process by exerting the second catalytic step. Afterwards, the spliceosome is disassembled and the involved snRNPs are available for further catalyses.[68] During exon definition the U1 snRNP binds the 5' SS downstream of the exon and recruits U2AF to the polypyrimidine tract of the 3' SS. The U2 snRNP is recruited to the branch point upstream of the exon. This complex is stabilized by serine and arginine-rich (SR) proteins, which bind exonic splicing enhancer (ESE) elements within the exon. Subsequently, the complex shifts from the exon definition complex to the cross-intron complex to catalyze splicing. However, this shifting process is not yet fully understood.[68]

3.2.1 Alternative splicing

Alternative splicing (AS) enables the generation of multiple mRNA isoforms from just one gene. AS occurs in approximately 95% of all human, multiexonic genes and thus, increases mRNA and finally protein diversity enormously.[74] AS is important for tissue-specific gene expression and enables the implementation of different gene expression programs in different cell types.[75] These gene expression programs can be activated also by spontaneous stimuli from the environment, e.g. hypoxia or pH conditions. Here, AS can act as a switch, activating regulatory pathways, which sustain cell survival.[76] AS is also evolutionarily relevant. Vertebrates show a higher amount of AS than invertebrates, indicating that the amount of AS can be a measure of organismal complexity.[76] Strikingly, AS can lead to significant differences in protein function.[77] Accordingly, deregulated AS promotes pathogenesis.[78]

There are different types of AS (**Figure 3-3**). The most common AS event in mammals is exon skipping. There, a so-called cassette exon is either included in the mature mRNA or excluded. In some cases two neighboring cassette exons can be mutually exclusive. Thereby either the first or the second exon can be included in the mature mRNA. AS can also lead to the retention of introns in the mature mRNA. In addition, alternative 5' or 3' SS can be used. [79]

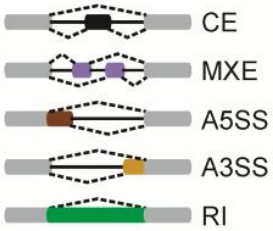

Figure 3-3: Different types of AS. CE = cassette exon, MXE = mutually exclusive exon, A5SS = alternative 5' splice site, A3SS = alternative 3' splice site, RI = retained intron.

The splicing decision is mediated by splicing factors. Not only the core spliceosome, but also regulatory RBPs, mainly SR proteins and hnRNPs, modulate splicing. SR proteins and hnRNPs bind to splicing regulatory elements (SREs). Exonic and intronic splicing enhancers (ESEs and ISEs) enhance splicing, while exonic and intronic splicing silencers (ESSs and ISSs) inhibit splicing.[80,81,82] SR proteins and hnRNPs are involved in constitutive, but also in alternative splicing and are described in chapter 3.3 in more detail.[81,82]

3.2.2 Alternative splicing coupled to NMD

Besides increase in protein diversity, AS can also be used to control protein levels. Here, the mechanism of nonsense-mediated decay (NMD) can be used to degrade the resulting mRNA.[83] NMD is an mRNA quality control mechanism, which leads to the degradation of mRNAs containing a premature termination codon (PTC; **Figure 3-4**). A PTC is a stop codon that is located more than 50-55 nt upstream of an exon-junction complex (EJC), which is present at the mRNA after splicing. PTCs can be introduced to the mRNA by mutations that occur during transcription or by errors during mRNA processing.[84] In addition, the natural stop codon of a transcript can also be used as PTC, when a cassette exon from the 3' UTR is included in the mRNA. Coupling of AS to NMD is called AS-NMD and is used to regulate protein amount at the posttranscriptional level.[85]

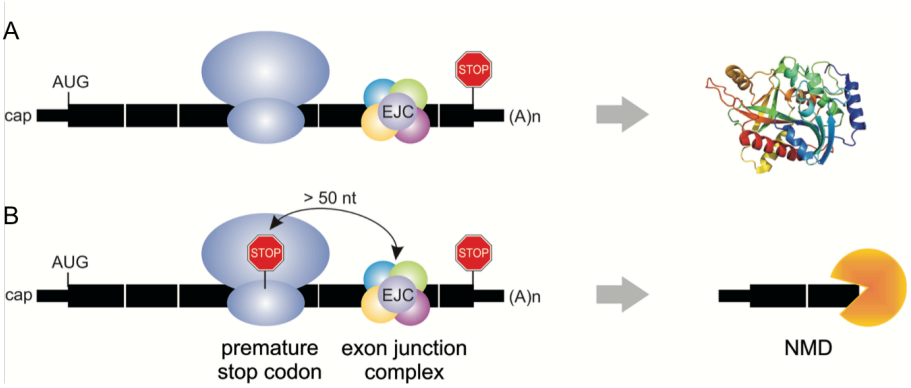

Figure 3-4: Nonsense-mediated decay mechanism. (A) Normal translation with termination signal (STOP in figure) in last exon. **(B)** The premature termination codon (PTC; STOP in figure) leads to degradation of the mRNA trough NMD. Figure by K. Kemmerer.

Originally, it was assumed that about one third of all human genes are regulated by AS-NMD[86], but this assumption was not confirmed by up-frameshift (UPF) protein 1 knockdown studies.[87,88] UPF proteins are the core component of the NMD machinery and participate in the decision whether an mRNA is degraded or translated.[85] Nowadays it is clear that NMD regulates the level of approximately 10% of human mRNAs.[89] Nevertheless, AS-NMD plays an important role in the autoregulation of many SR proteins and hnRNPs.[90,91] Thereby, AS-NMD contributes to the homeostasis of these splicing factors and their regulation in negative feedback loops.[92] Examples for splicing factors that are regulated by AS-NMD are: SRSF10[93], SRSF3[94], neural hnRNP I (also called polypyrimidine tract binding protein 2; PTBP2 or nPTB)[95] or hnRNP D[96]. HnRNP D regulates its own expression in a negative feedback loop through inclusion of an exon in its 3' UTR to the mRNA (see also chapter 3.3.1).[97] This exon is referred to as poison exon since its inclusion leads to degradation of the mRNA through NMD. Sometimes the AS-NMD mechanism is also used for the cross-regulation between protein paralogs, as it is known for PTB (hnRNP I) and nPTB (neural hnRNP I)[98], hnRNP L and hnRNP LL[99] and shown here, in this study, for hnRNP D and hnRNP DL.

3.2.3 Alternative splicing and cancer

Aberrant AS is involved in the pathogenesis and progression of various diseases including cancer.[100,101] Mostly, mutations of the splice sites lead to splicing inhibition and exclusion of the adjacent exon. Changes in highly conserved regions usually cause severe mutations like frameshifts leading to truncated proteins or the inclusion of PTCs leading to mRNA degradation via NMD and depletion of the corresponding protein.[102,103] For example, the mutation of AA to AG within the *BRCA1* gene creates a cryptic 3' SS and is a known molecular

marker for breast cancer.[104,105] The mutation leads to the additional inclusion of eleven nucleotides and subsequently to translation of a truncated protein.[104] Another example is the tumor suppressor phosphatase and tensin homolog deleted on chromosome TEN (PTEN), which is often mutated in cancer.[106,107] In breast cancer, it was found that PTEN different segments from intron 3 and 5 can be retained in the mRNA creating PTCs and leading to pathogenesis.[108]

Deregulated expression of RNA-binding proteins (RBPs, see also 3.3) can also cause aberrant splicing. For example, overexpression of hnRNP M is promoting breast cancer metastasis by activating AS programs favoring epithelial-mesenchymal transition (EMT).[109]

Another example how AS contributes to cancer progression is *VEGFA*. The functions of VEGF-A proteins are modulated by AS, which in turn is determined by splicing factor levels. VEGF-A is an important regulator of angiogenesis during tumor hypoxia and has several protein isoforms, which differ in their C-terminal domains.[110] All pro-angiogenic isoforms are referred to as VEGF-A_{xxx}, while anti-angiogenic isoforms are called VEGF-A_{xxx}b, with xxx being the number of the amino acids in the mature protein. The different isoforms are generated by mutually exclusive splicing of *VEGFA* exon 8a and 8b. Each isoform binds the vascular endothelial growth factor receptor 2 but only VEGF-A_{xxx} can activate it. The splicing decision, whether the 5' SS of exon 8a or exon 8b is used, is governed by the splicing factors SRSF1 and SRSF6. SRSF1 favors inclusion of exon 8a, while SRSF6 promotes the inclusion of exon 8b.[111] Thus, deregulation of SRSF1 or SRSF6 risks the balance between VEGF-A isoforms and might promote tumor angiogenesis.

Besides cancer, aberrant AS was also found to drive Parkinson's disease, cystic fibrosis, retinitis pigmentosa, spinal muscular atrophy and myotonic dystrophy, to name only few examples.[112,113]

Moreover, aberrant AS is already therapeutically exploited.[114] Hereby, either the splicing machinery, RBPs or splice sites themself are targeted.[115] Splice-switching oligonucleotides (SSOs) interfere with *cis*-elements at the mRNA and thus with the *trans*-acting factors, modulating the targeted splicing event.[116] SSOs are already approved by the US Food and Drug Administration for therapy of Duchenne muscular dystrophy as well as spinal muscular atrophy.[117,118]

3.3 RNA-binding proteins

RNA-binding proteins (RBPs) can be divided into several subclasses, depending on which RNAs they bind to: mRNAs, (pre-)rRNAs, tRNAs, snRNAs (small nuclear RNAs), snoRNAs (small nucleolar RNAs) or other ncRNAs (non-coding RNAs).[119] This study focuses mainly on mRNA-binding proteins, which represent almost 45% of all known human RBPs (**Figure 3-5**). Therefore, in this work, the term RBPs refers to mRNA-binding proteins.

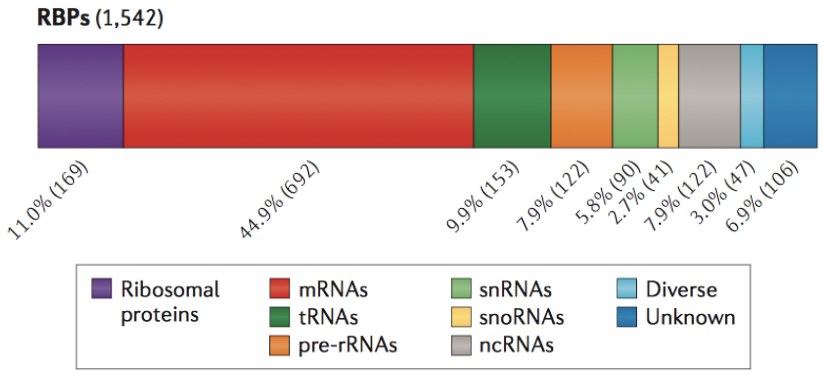

Figure 3-5: Absolute and relative numbers of RBPs in different subclasses. MRNA-binding proteins represent the biggest group of RBPs. Modified figure from [119].

As already mentioned, RBPs are key players for splicing regulation. RBPs show intensive interplay between one another since target mRNAs are usually bound by multiple RBPs simultaneously. Besides splicing regulation, RBPs are also implicated in mRNA localization, modification, polyadenylation, stability and translation regulation (**Figure 3-6**).[120,121]

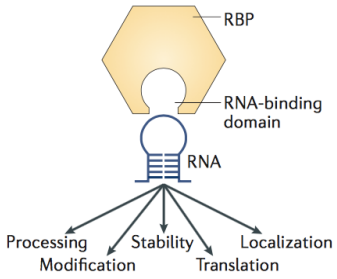

Figure 3-6: RBP functions. RBPs contain RNA-binding domains. Binding of RNA influences RNA processing, modification, stability, translation as well as localization. Figure from [120].

RBP subclasses can further be divided into RBP families with similar features.[121] Highly important for splicing regulation are the families of SR proteins and hnRNPs.

The SR protein family consists of 12 members: SRSF1-12. All SR proteins contain one or two RNA recognition motifs (RRMs) at their N-terminus and a C-terminus with several serine and arginine dipeptide repeats.[122,123]

HnRNPs are named alphabetically from hnRNP A1 to hnRNP U.[124] The hnRNPs have divers structural components increasing their functional diversity. HnRNPs can contain RRMs, quasi-RRMs (qRRM), K-Homology domains (KH) or RGG boxes as well as glycine, proline or acidic rich domains (**Figure 3-7**).[124] Many hnRNPs have paralogs, which share 20-70% of their sequence and have redundant or supplementary functions.[119] Usually, hnRNPs contain a nuclear localization signal (NLS) and are present in the nucleus, but many hnRNPs are also able to shuttle from the nucleus to the cytoplasm, upon stimulation or by recruitment by other RBPs.[125]

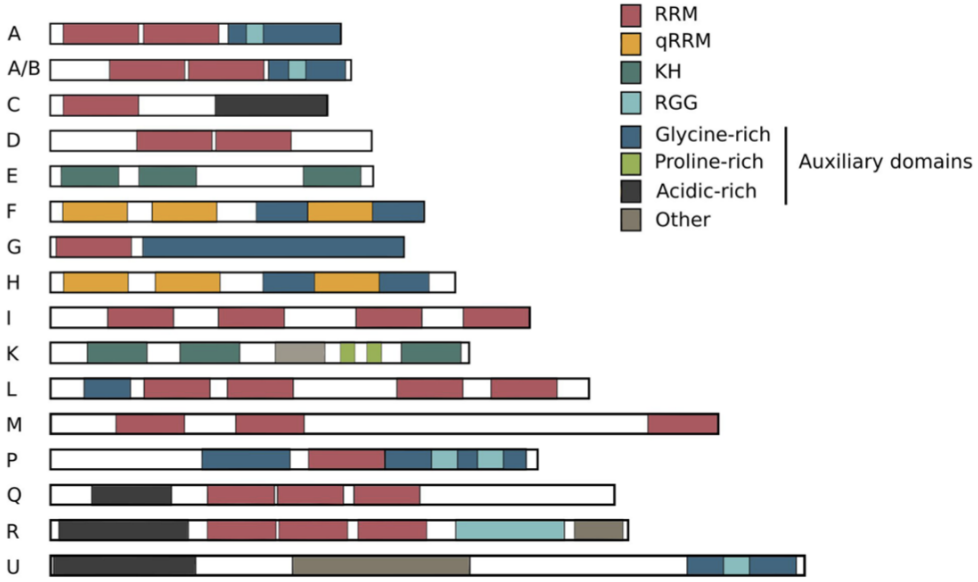

Figure 3-7: Selected members of the hnRNP family. HnRNPs show unique, but also shared structural components. HnRNP molecular weights range from 34 to 120 kDa (sizes are drawn relative to each other). Figure from [124].

Besides SR proteins and hnRNPs, also Nova, FOX, TIA, CUGBP and MBNL proteins are involved in splicing.[126,127,128] As already mentioned in chapter 3.2.2, cross-regulation between RBPs is very common. Splicing regulation is a highly orchestrated process and it is never governed by just one RBP. The combined action of RBPs is essential for fine tuning posttranscriptional regulation.[129] Sometimes RBPs act as antagonists such as MBNL proteins and CUGBPs during myotonic dystrophy.[130] In addition, RBPs also compete with miRNAs as described in chapter 3.1.2 for the *VEGFA* mRNA.[131]

3.3.1 Heterogenous nuclear ribonucleoprotein D-like

Heterogenous nuclear ribonucleoprotein D-like (hnRNP DL or JKTBP1) belongs to the family of hnRNPs. HnRNP DL is the paralog of hnRNP D, also known as AUF1 (AU-rich element

RNA-binding protein 1). HnRNP D and DL are ubiquitously expressed and show a closely related gene organization with two RRMs at the N-terminus [132] and a glycine- and tyrosine-rich domain at the C-terminus.[133] HnRNP D is known to destabilize its target mRNAs containing AU-rich elements (AREs) in their 3' UTR.[134] Like hnRNP D, also hnRNP DL seems to bind AREs.[135]

To this day, there is only one confirmed hnRNP DL target, which is the NF-κB-repressing factor (*NKRF*) mRNA.[136] NKRF is a transcription factor, which represses the transcription of cytokines, interferon β (IFN- β), interleukin-8 (IL-8) and inducible nitric oxide synthase (iNOS).[137,138,139] Here, hnRNP DL functions as enhancer of IRES (internal ribosome entry site)-dependent translation. In addition, hnRNP DL stabilizes the *NKRF* mRNA by binding the 3' UTR.[140] HnRNP DL also binds an exonic silencing sequence (ESS) containing the sequence 5'-AUAGUA-3' within the *human papillomavirus type 16* (*HPV-16*) mRNA. HPV-16 is the most common type of papillomavirus in the human population and increases cancer risk.[141] There, binding of hnRNP DL leads to blocking of a 5' SS. Subsequently, the *L1 late gene* mRNA is reduced. This might help HPV to evade the immune system and remain in the host, increasing cancer risk. HnRNP DL also plays a role in the transcriptional regulation of muscle differentiation in mice.[142] Mouse and human hnRNP DL differ only by one aa within the GY-rich region.[143] In myoblasts ZBP-89 and YY-1 repress the transcription of *COX Vb* (cytochrome C oxidase Vb). In myotubes a 10-fold induction of hnRNP DL leads to activation of COX Vb expression.[142]

HnRNP D and DL are mainly located in the nucleus. However, both can also shuttle to the cytoplasm.[144,145] Interestingly, both, hnRNP D and DL contain an alternatively spliced cassette exon in their 3' UTRs: exon 9 and exon 8, respectively. Inclusion of these exons turns the natural termination codon into a PTC. Consequently, hnRNP D and DL undergo AS-NMD and afflicted mRNAs are degraded through NMD.

HnRNP DL exon 8 is ultraconserved (uc. 144 in UCbase 2.0 ultraconserved sequences database[146]; **Figure 3-8 A**).[97] Previous works from K. Kemmerer (Weigand group), performed prior to this study, have confirmed the NMD-sensitivity of *hnRNP DL* mRNAs containing exon 8.[147] Treatment with the translation blocker puromycin led to increased inclusion of exon 8 into the *hnRNP DL* mRNA (**Figure 3-8 B**). In addition, a *UPF1* knockdown was performed. UPF1 is an important component of the NMD machinery. Knockdown of *UPF1* led to enrichment of the *hnRNP DL* isoform containing exon 8, while the mRNA level of the exon

skipping isoform was not influenced (**Figure 3-8 C**), confirming the NMD-sensitivity of the *hnRNP DL* isoform containing exon 8 (NMD isoform).

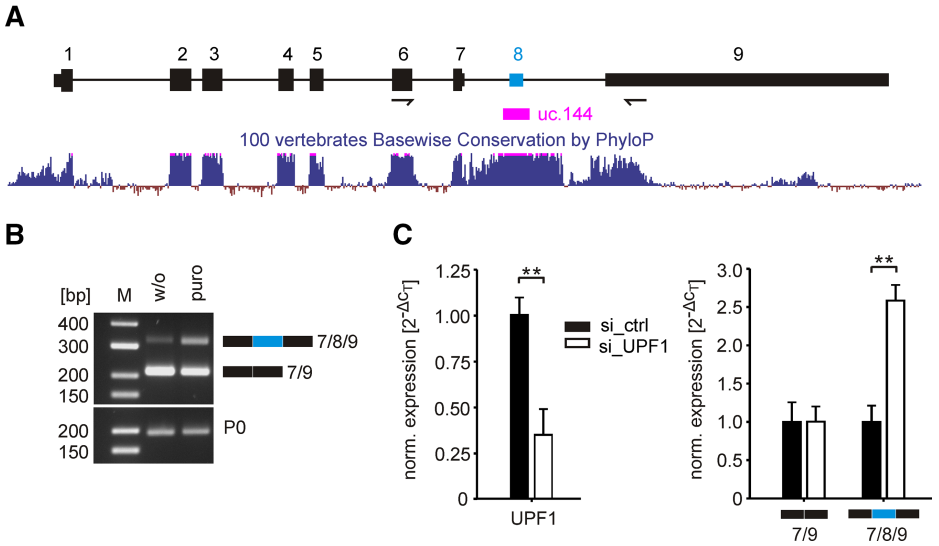

Figure 3-8: The 3' UTR of *hnRNP DL* contains an alternatively spliced, NMD-sensitive exon. **(A)** *hnRNP DL* exon 8 is ultraconserved. **(B)** Treatment with puromycin leads to increased inclusion of *hnRNP DL* exon 8 into the mRNA. **(C)** *UPF1* knockdown leads to increased mRNA level of the *hnRNP DL* isoform containing exon 8, while the mRNA level of the exon 8 skipping isoform is not changed. Figure from [97].

Further, K. Kemmerer demonstrated that hnRNP DL undergoes an autoregulatory feedback loop by controlling inclusion of exon 8 into its own mRNA.[97,147] For that purpose, a luciferase minigene system containing the luciferase gene and the *hnRNP DL* 3' UTR in a dual luciferase vector was established (**Figure 3-9 A**).[97,147,148] After transfection of the minigene construct and transient overexpression of hnRNP DL in HeLa cells the mRNA level of the NMD isoform was increased, while the mRNA level of the exon skipping isoform was decreased (**Figure 3-9 B and C**). Overexpression of GFP as a control, did not influence *hnRNP DL* mRNA splicing (**Figure 3-9 B and C**). Additionally, luciferase activity was dramatically reduced, when hnRNP DL was overexpressed (**Figure 3-9 D**).

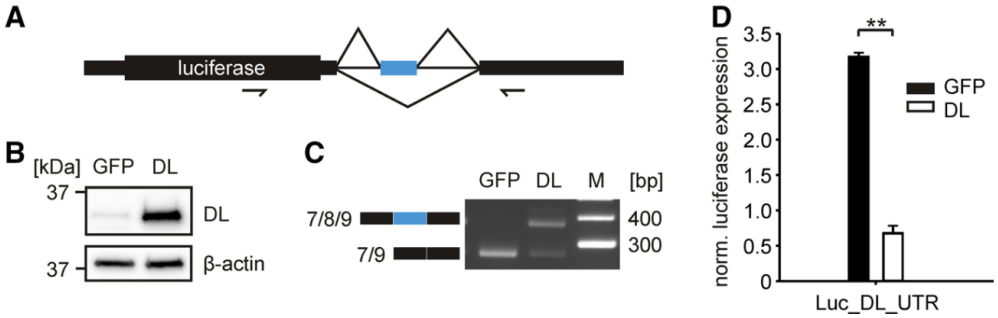

Figure 3-9: HnRNP DL autoregulation in a luciferase minigene system. (A) The complete *hnRNP DL* 3' UTR containing exon 8 (blue) was cloned downstream of the luciferase gene. Arrows indicate oligonucleotide positions for further studies. **(B)** Overexpression of GFP or hnRNP DL. **(C)** RT-PCR showing different *hnRNP DL* splicing patterns after overexpression of GFP or hnRNP DL. **(D)** Luciferase reporter gene assay showing reduced luciferase activity after overexpression of hnRNP DL. Figure from [97].

K. Kemmerer also established stable HeLa cell lines overexpressing GFP or a GFP-hnRNP DL-fusion protein (GFP-DL).[97,147] The HeLa cell line overexpressing GFP-DL showed a reduced endogenous hnRNP DL protein level (**Figure 3-10 A**). In addition, mRNA levels of the hnRNP DL isoforms are also affected by GFP-DL overexpression. The mRNA level of the exon skipping isoform is reduced, while the mRNA level of the NMD isoform is increased leading to mRNA degradation and proving the hnRNP DL autoregulation (**Figure 3-10 B**).

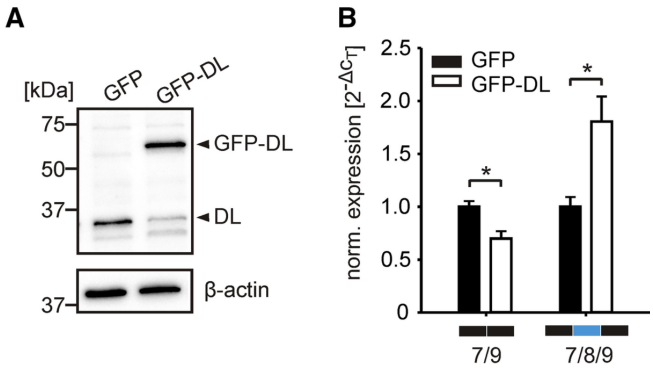

Figure 3-10: HnRNP DL autoregulatory feedback loop. (A) Endogenous hnRNP DL protein level is reduced after GFP-DL overexpression. **(B)** MRNA level of the exon 8 containing isoform is increased and mRNA level of the exon 8 skipping isoform is decreased after GFP-DL overexpression. Figure from [97].

Cross-regulation between RBP paralogs is common as described earlier. A potential cross-regulation between hnRNP DL and its paralog hnRNP D was part of this study and is described in chapter 4.1.2.

An exon array in HUVEC after $CoCl_2$ treatment as hypoxia mimic showed increased inclusion of hnRNP DL exon 8.[149] Previous works from K. Kemmerer confirmed these findings also under hypoxic conditions (1% O_2).[150] The increased inclusion of exon 8 under hypoxic conditions led to reduced hnRNP DL mRNA and protein levels.[147]

3.3.1.1 HnRNP DL and disease

Deregulation of hnRNP DL is associated with cancer and other diseases. Overexpression of hnRNP DL is found in prostate cancer.[151,152] Here, hnRNP DL promotes proliferation and thus cancer progression through activation of epidermal growth factor receptor (EGFR).[152] Further, hnRNP DL is overexpressed in chronic myeloid leukemia contributing to increased cell proliferation.[153,154] Recently, deregulation of hnRNP DL was identified as risk factor for the progression of endometrial cancer.[155] Here, hnRNP DL seems to regulate AS events, which affect endometrial cancer prognosis.[155] Further, a defect of hnRNP DL causes limb-girdle muscular dystrophy 1G (LGMD1G).[156] LGMD is a hereditary muscle disease leading to paralysis of the musculature of the shoulder and the pelvic girdle. Genome sequencing of three patients showed that two point mutations in the same codon are responsible for the hnRNP DL defect. Both cases are missense mutations, where aspartate is either changed to asparagine (D378N) or histidine (D378H).[156]

3.3.2 Muscleblind-like protein 2

The family of muscleblind-like proteins (MBNLs) consists of the three paralogs MBNL1, MBNL2 and MBNL3. All three paralogs contain two conserved zinc finger domains (**Figure 3-11**), which bind clustered 5'-YGCY-3' motifs in pre-mRNAs leading to alternative splicing regulation.[157,158,159] The binding location of MBNL proteins determines whether they activate or repress mRNA alternative splicing. Binding of MBNLs downstream of an exon facilitates inclusion of this exon while binding of MBNLs within or upstream of an exon leads to exon exclusion.[160] This splicing regulation pattern is also common to other splicing factors like hnRNP L or NOVA.[161] The binding efficiency depends on the RNAs structural context.[162] More recently, MBNL proteins were also found to be implicated in mRNA localization[163] as well as stability regulation[164,165], translation regulation[166], alternative polyadenylation[167] and miRNA biogenesis.[168] MBNL1 and MBNL2 are ubiquitously expressed, while expression of MBNL3 is restricted to the placenta.[169] MBNL proteins are often functionally redundant but they have different capacity for AS regulation with MBNL1 being the strongest splicing regulator.[170]

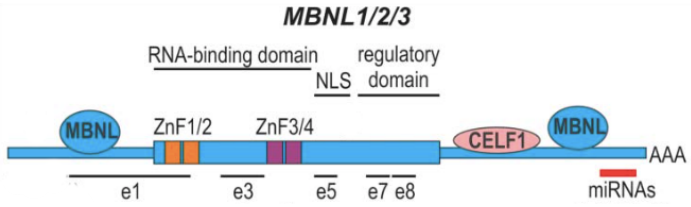

Figure 3-11: Schematic representation of MBNL transcripts. The zinc finger domains (ZnF) encoded by exon 1/2 and exon 3/4, respectively, are shown in orange and violet. MBNL, CELF (CUGBP) and miRNA binding sites are indicated. Alternatively spliced exons (e) are: e1, e3, e5, e7 and e8. e1 to e4 encode the RNA binding domain, e5 encodes the NLS and e7 and e8 encode the regulatory domain. Modified figure from [171].

Interestingly, all three paralogs undergo auto- and cross-regulatory loops influencing the expression of one another by binding to the first coding exon.[171] In general, MBNL proteins undergo extensive alternative splicing, which fine-tunes their expression pattern and also their functionality since inclusion or exclusion of specific exons influences their localization and also binding preferences.[170] MBNL2 in particular has four isoforms ranging from 38 to 41 kDa. The isoforms MBNL2-38 and MBNL2-39 are present in the cytoplasm, while MBNL2-40 and MBNL2-41 are restricted to the nucleus. The localization is determined by the NLS that is encoded in the alternatively spliced exon 5.[171]

3.3.2.1 MBNL proteins and disease

Deregulation of MBNL proteins is related to myotonic dystrophy (DM). Here, MBNL proteins are distracted from their natural targets by expanded CUG or CCUG repeats within the 3' UTR of dystrophia myotonica protein kinase (*DMPK,* DM type 1) or CCHC-type zinc finger nucleic acid binding protein (*CNBP*, DM type 2), respectively (**Figure 3-12**).[172,173] Thus, DM1 and DM2 are RNA-mediated disorders.[174] The expanded CUG or CCUG repeats are the product of mutations. Repetitive DNA sequences are common in the human genome and can have regulatory functions. Short tandem repeats (STRs) fine-tune the regulation of the STR host gene. Expansion of STRs by mutation is toxic and leads to STR expansion diseases as in the case of DM.[174] Repetition of CUG and CCUG leads to formation of 5'-YGCY-3' motifs, which are bound by MBNL proteins. Subsequently, MBNL proteins are sequestered in RNA foci leading to the same consequences as an MBNL depletion. RNA foci are RNP complexes, which result from expanded RNA repeats. DM is associated with muscle malfunctions, heart defects and cognitive decline.[174]

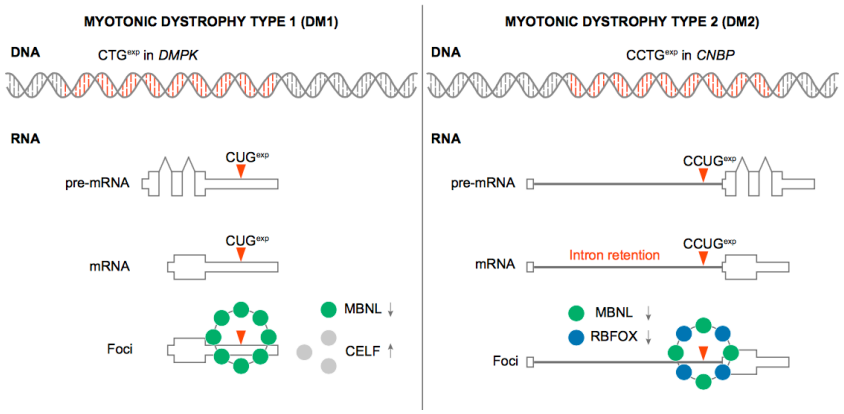

Figure 3-12: DM1 and DM2 disease mechanisms. DM1 is caused by expanded CUG repeats in the 3' UTR of *DMPK* (left side). *DMPK* pre-mRNA is correctly spliced, but sequesteres MBNL proteins and increases CELF1 protein levels. DM2 is caused by expanded CCUG repeats in an intron of *CNBP* (right side). The respective intron is retained and MBNL and RBFOX proteins are sequestered. The deregulation of these splicing factors leads to DM symptoms. Modified figure from [174].

Just recently, MBNL proteins have also been associated with cancer and several studies supposed contrasting roles for MBNL proteins. MBNL1 was found to support colorectal carcinogenesis by interfering with Dicer1 recruitment to miRNA precursors.[175] In contrast, MBNL1 suppresses metastasis in breast and colorectal cancer by regulating the mRNA stability of metastasis suppressor transcripts like drebin-like protein (*DBNL*) and transforming acidic coiled-coil containing protein 1 (*TACC1*).[176,177] These opposing roles might be due to different isoform distributions. The MBNL1 isoform containing exon 7 is upregulated in cancer, while the overall level of MBNL1 is reduced.[178] Also for MBNL2, controversial functions were documented. While MBNL2 was identified as oncogenic driver in a murine model of breast cancer, MBNL2 acted as tumor suppressor in human hepatocellular carcinoma.[179,180] There, overexpression of MBNL2 led to inhibited tumor growth and invasion. Furthermore, MBNL2 is overexpressed in human clear cell renal cell carcinoma (ccRCC) and contributes to deregulated gene expression promoting cancerogenesis.[181] In this study, MBNL2 target genes were identified that belong to the HIF signaling pathway, which is the main transcriptionally activated pathway under hypoxia.[181] However, neobractatin-mediated MBNL2 upregulation in breast and lung cancer cells inhibits tumor metastasis.[182] MBNL3 is promoting hepatocellular carcinoma via alternative splicing of lncRNA-PXN-AS1, which increases paxillin (PXN) expression.[183] In sum, the previously identified functions of MBNL proteins in cancer are contradictory, making further studies necessary.

3.4 Project aim

3.4.1 Auto- and cross-regulation of the hnRNPs D and DL

Deregulated expression of splicing factors and subsequent aberrant splicing are associated with the pathogenesis of various diseases including cancer.[81,100] HnRNP DL itself is overexpressed in prostate cancer and chronic myeloid leukemia.[152,153] Previous work by K. Kemmerer has shown that hnRNP DL regulates its own expression in a negative feedback loop by AS of a poison exon in its 3' UTR.[147] In this study, the investigation of the hnRNP DL autoregulation was continued. Aim was to confirm binding of hnRNP DL to its own pre-mRNA using RNA-binding protein immunoprecipitation (RIP) analyses. Further, cross-regulation between the endogenous hnRNP DL and its paralog hnRNP D was investigated in RNAi experiments, in which either *hnRNP DL* or *hnRNP D* are depleted. For that purpose, an *hnRNP D* knockdown had to be established. Moreover, I aimed to demonstrate a role of hnRNP DL in endothelial cell migration and angiogenesis in human endothelial cells.

3.4.2 Hypoxia-driven gene expression changes in human cancer cells

Hypoxia is a common characteristic of solid tumors and triggers widespread changes in gene expression. It also influences posttranscriptional regulation mechanisms including AS.[184] By now, there are only few genome-wide analyses of hypoxia-driven transcriptome changes. The studies focused on endothelial cells[184], mesenchymal stem cells[185] and hepatocellular carcinoma[186]. Comparison of these studies is difficult since different hypoxic conditions and different analysis methods have been used. A better understanding of hypoxia-driven changes in the RBPome and in AS in cancer cells could open up new approaches in cancer therapy.

Aim of this study was to achieve a comparable data set of hypoxia-driven gene expression and AS changes in different cancer types. For this purpose, I wanted to establish a suitable hypoxia test system for different cancer cell lines. Aim was to identify hypoxia-responsive splicing factors and hypoxia-driven AS changes in transcriptome analyses and to verify mRNA and protein level changes in RT-qPCRs and Western blots, respectively. In addition, I focused on the characterization of splicing factor target genes and the regulation mechanism by performing RT-PCRs, actinomycin D, ELISA and luciferase assays. Further, I aimed to understand the contribution of hypoxia-responsive splicing factors to tumorigenesis. For that purpose I wanted to investigate cancer cell proliferation and migration in loss-of-function studies.

4 Results

The Results chapter **4** of this study is divided into two sections. Chapter **4.1** deals with the auto- and cross-regulation of the hnRNPs D and DL. Here, I describe the binding of hnRNP DL to its own pre-mRNA. Further, I demonstrate the cross-regulation of hnRNP D and DL in knockdown studies. In addition, I show that hnRNP DL is implicated in migration and angiogenesis in endothelial cells.

Chapter **4.2** is about hypoxia-driven gene expression changes in human cancer cells. Transcriptome analyses were performed in order to elucidate how hypoxia impacts on transcript abundance and AS events in cancer cells. Strikingly, MBNL2 could be identified as major regulator of transcript abundance and AS in hypoxic cancer cells. Transcriptome analyses after siRNA-mediated knockdown of *MBNL2* further revealed novel MBNL2 target genes. In addition, a role of MBNL2 in cancer cell proliferation and migration was demonstrated.

4.1 Auto- and cross-regulation of the hnRNPs D and DL

Previous studies by K. Kemmerer indicated an autoregulation of hnRNP DL in a negative feedback loop (see chapter 3.3.1). HnRNP DL contains an alternatively spliced poison exon in its 3' UTR (exon 8). Inclusion of this exon leads to degradation of the mRNA trough NMD. In this study, I could show that hnRNP DL binds to its own pre-mRNA. In addition, I demonstrated the cross-regulation between endogenous hnRNP D and DL in RNAi experiments. Further, I revealed a key function of hnRNP DL in endothelial cell migration and angiogenesis.

4.1.1 Autoregulation of hnRNP DL

Autoregulation of splicing factors is essential for splicing factor homeostasis and is often exerted in a negative feedback loop.[92] Several splicing factors control their own expression via the mechanism of AS-NMD. Hereby, the splicing factors bind to their own pre-mRNA and influence splicing decisions. Examples for autoregulatory splicing factors are neural hnRNP I (nPTB)[95] or hnRNP L.[99] The regulation of these hnRNPs via AS-NMD suggests that hnRNP DL is also subject to this mechanism.

Binding of hnRNP DL to its own pre-mRNA is a prerequisite for the predicted AS-NMD autoregulation. RNA-binding protein immunoprecipitations (RIPs) were performed in order to investigate whether hnRNP DL targets its own pre-mRNA. For that purpose, HeLa cell lines stably expressing either GFP as a control or a GFP-hnRNP DL fusion protein (GFP-DL) were used. These cell lines were previously established by K. Kemmerer.[147] Either GFP or the GFP-DL fusion protein with bound RNA were precipitated by the use of the corresponding antibody. The U1-70K-U1 snRNA complex was precipitated as a positive control. Proteins were digested by proteinase K and remaining RNA was extracted. RNA was also extracted from an input sample, corresponding to 10% of the input used in the different samples. In RT-qPCR analyses the mature *hnRNP DL* mRNA (DL mRNA), the *hnRNP DL* pre-mRNA (DL pre-mRNA_1/_2) and the *U1* snRNA were detected. The two oligonucleotide pairs for the detection of the *hnRNP DL* pre-mRNA were designed in the way that one pair leads to the amplification of a fragment within hnRNP DL intron 8 (DL pre-mRNA_1) and the other pair leads to the amplification of a fragment ranging from exon 8 over the intron-exon junction to intron 8 (DL pre-mRNA_2; **Figure 4-1 A**). To gain the yield in % input, values were normalized to values obtained in the input sample. Strikingly, the GFP-DL fusion protein preferentially bound the *hnRNP DL* pre-mRNA in comparison with the mature *hnRNP DL* mRNA when the GFP antibody was used for the RIP in HeLa cells overexpressing GFP-DL (**Figure 4-1 A**). These findings demonstrate that hnRNP DL binds its own pre-mRNA, confirming its autoregulation. Both fragments, DL pre-mRNA_1 and DL pre-mRNA_2 were highly enriched in the RIP. As expected, none of the tested RNAs were enriched in the RIP of GFP in HeLa cells overexpressing GFP. Further, the *hnRNP DL* pre-mRNA and the *U1* snRNA, but not the mature hnRNP DL mRNA were enriched when the snRNP U1-70K antibody was used for the RIP. This is in line with the expectations since snRNP U1-70K is a part of the core spliceosome and thus binds to pre-mRNAs. Western blot analyses were performed for each RIP in order to verify equal RIP efficiencies. GFP was immunoprecipitated as a control to ensure that GFP-DL and not GFP alone is binding to mRNAs. Mouse IgG was used as negative control and did not show enrichment of GFP-DL or GFP. GFP-DL and GFP were equally enriched by the use of an anti-GFP antibody (**Figure 4-1 B**).

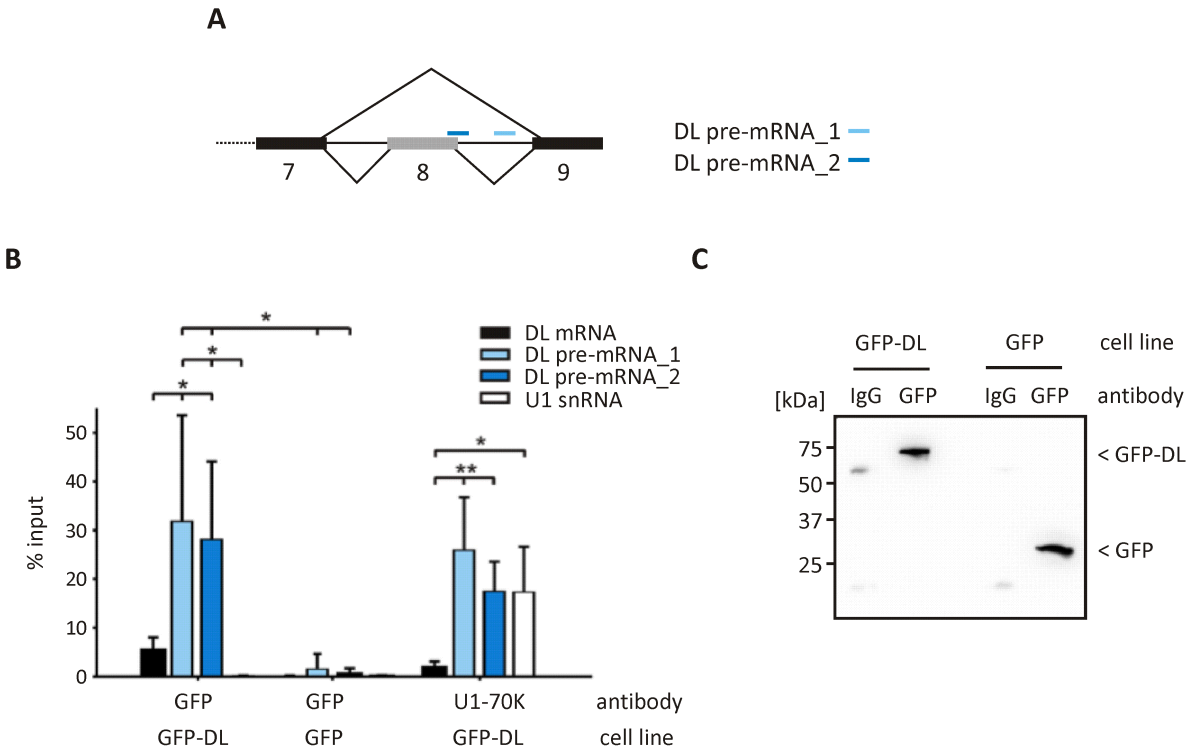

Figure 4-1: HnRNP DL preferentially binds its own pre-mRNA. (A) Scheme of the *hnRNP DL* pre-mRNA ranging from exon 7 to 9. The fragment DL pre-mRNA_1 is located in intron 8. Fragment DL pre-mRNA_2 is located at the exon-intron junction between exon 8 and intron 8. **(B)** HeLa cell lines stably expressing GFP or a GFP-hnRNP DL fusion protein (GFP-DL) were used. A GFP antibody was used for RIP of GFP and the GFP-DL fusion protein. In RT-qPCR, the mature, fully spliced *hnRNP DL* mRNA (DL mRNA), the *hnRNP DL* pre-mRNA (DL pre-mRNA_1/_2) and the *U1* snRNA were detected. An snRNP U1-70K antibody was used as positive control. Values were normalized to the input sample. n=5. **(C)** Western blot verified a comparable RIP efficiency of GFP-DL fusion protein and GFP. Anti-GFP was used to detect both, GFP-DL and GFP. Mouse IgG (IgG) was used as negative control. n=5. (**) P value < 0.01, (*) P value < 0.05.

4.1.2 Cross-regulation between hnRNP D and DL

Cross-regulation between paralogs is common in the family of hnRNPs. For example PTB and nPTB or hnRNP L and LL cross-regulate each other.[98,99] If hnRNP DL and its paralog hnRNP D cross-regulate each other in a negative feedback loop, we would expect that hnRNP DL can control the inclusion of exon 9 into the *hnRNP D* mRNA (**Figure 4-2 A**). Further, hnRNP D should be able to control the inclusion of exon 8 into the *hnRNP DL* mRNA. Inclusion of these exons leads to degradation of the mRNA via NMD and thus, to a decrease in protein amount. To target the question, whether hnRNP D and DL cross-regulate each other, I analyzed protein and mRNA levels after performing RNAi experiments in which either *hnRNP D* or *DL* were depleted. I established an efficient *hnRNP D* and *DL* knockdown in HeLa cells. Knockdown of *hnRNP D* led to a strong induction of hnRNP DL (**Figure 4-2 B**). Albeit to a lesser extent,

knockdown of *hnRNP DL* led to an induction of hnRNP D. In addition, knockdown of one of the paralogs had a strong influence on splicing of the other paralog. Knockdown of either *hnRNP D* or *DL* led to induction of the protein-coding mRNA level of the other paralog (**Figure 4-2 C and D**). Additionally, the NMD-sensitive isoform containing exon 8 in *hnRNP DL* or exon 9 in *hnRNP D* was dramatically reduced. Both findings represent an explanation for the increase in protein quantities. All together, the RNAi experiments prove the cross-regulation between hnRNP D and DL.

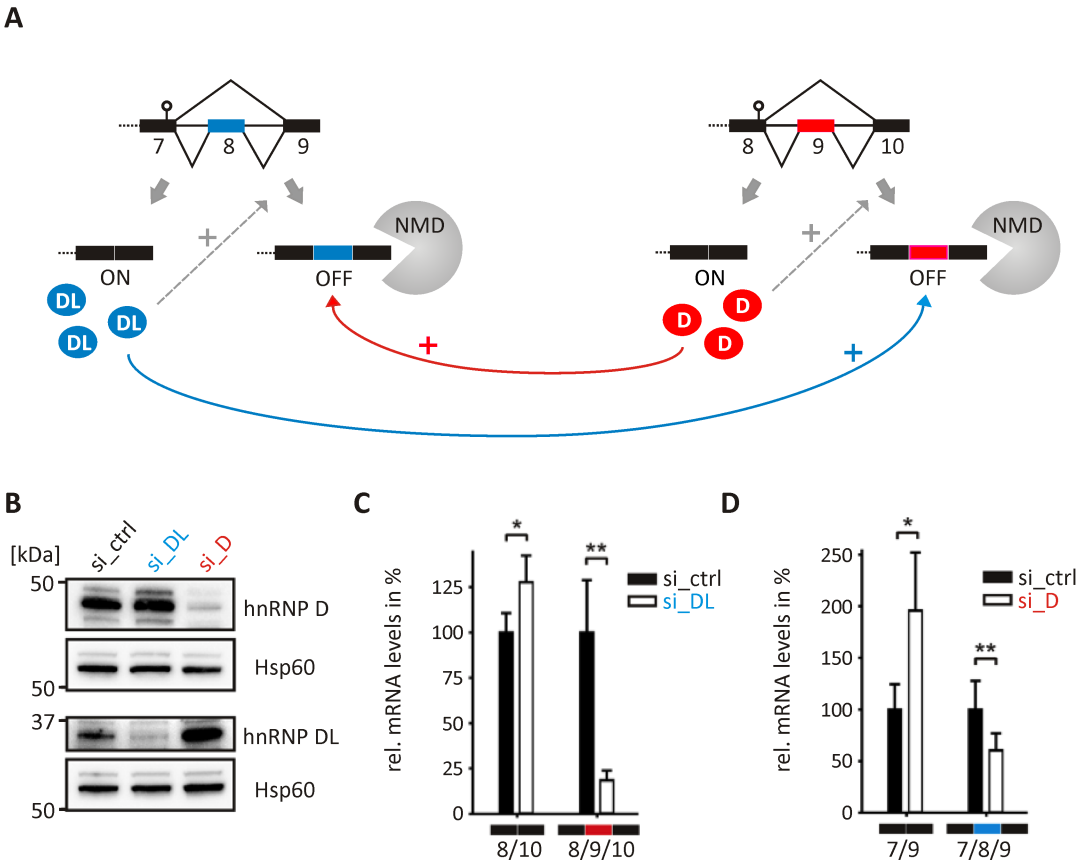

Figure 4-2: HnRNP D and DL cross-regulate each other. (A) Scheme of the hypothesized cross-regulation between hnRNP D and DL. HnRNP D is shown in red. HnRNP DL is shown in blue. Grey arrows show the autoregulation of hnRNP D and DL, respectively. Both hnRNPs regulate their own expression in a negative feedback loop by controlling the inclusion of a poison exon (*hnRNP D* exon 9 in red and *hnRNP DL* exon 8 in blue) in their 3' UTR into the mRNA. Colored arrows indicate the cross-regulation between hnRNP D and DL. **(B)** HnRNP D and DL protein levels are increased after knockdown of the other paralog. Anti-hnRNP D and anti-hnRNP DL antibodies were used to verify protein levels. Anti-HSP60 was used as loading control. n=3. **(C) and (D)** MRNA levels of *hnRNP D* isoforms 8/10 and NMD-sensitive isoform 8/9/10 (**C**) and of *hnRNP DL* isoforms 7/9 and NMD-sensitive isoform 7/8/9 (**D**) after knockdown of the respective paralog. Values are normalized to the housekeeping gene *RPLP0*. n=5. (**) P value < 0.01, (*) P value < 0.05.

4.1.3 Role of hnRNP DL in migration

A transcriptome analysis after *hnRNP DL* knockdown in human umbilical vein endothelial cells (HUVECs), which was performed in our working group prior to this study, predicted a role of hnRNP DL in proliferation, cytoskeleton remodeling and angiogenesis.[187] To study the predicted role of hnRNP DL in endothelial cell migration, I established a transwell endothelial cell migration assay in our laboratory. Endothelial cell migration was dramatically reduced, when *hnRNP DL* was depleted (**Figure 4-3**), proving a promoting role of hnRNP DL in endothelial cell migration.

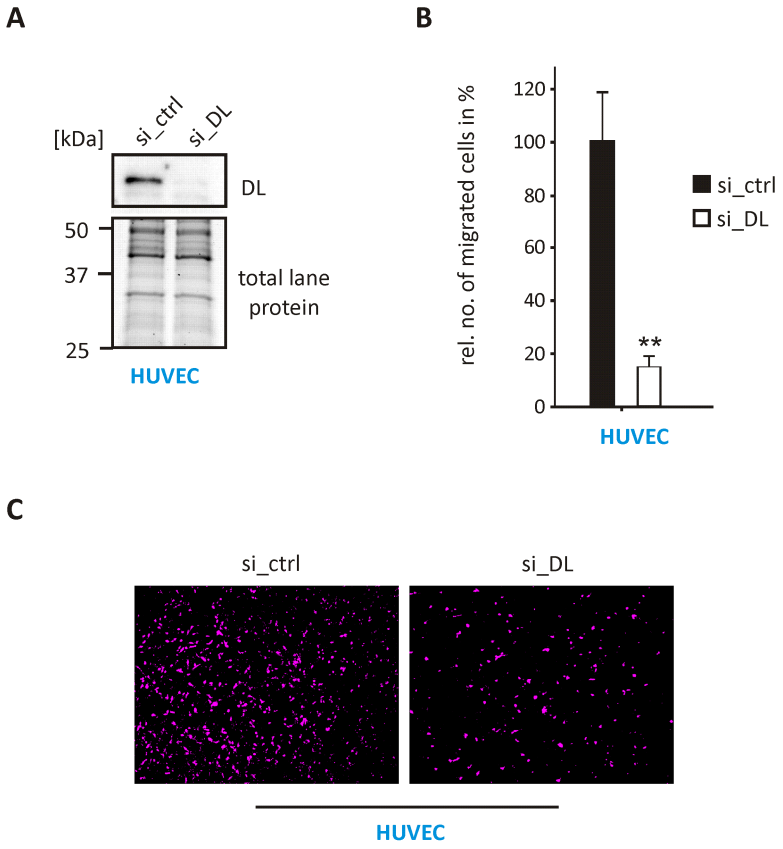

Figure 4-3: HnRNP DL affects endothelial cell migration. (A) Knockdown of *hnRNP DL* leads to hnRNP DL protein depletion in HUVECs. **(B)** Quantification of migrated HUVECs in a transwell assay after knockdown of *hnRNP DL*. n=4. **(C)** Representative pictures of migrated HUVECs. Original images were colored in magenta to visualize crystal violet staining. (**) P value < 0.01.

4.1.4 Role of hnRNP DL in angiogenesis

Endothelial cells build the inner lining of blood vessels and are responsible for angiogenesis and neovascularization. To study the predicted role of hnRNP DL in angiogenesis[187], I established a spheroid sprouting assay in our laboratory. During this assay, HUVECs are

transfected with RNAi constructs. 24 h later HUVECs are seeded in hanging drop cultures to enable endothelial spheroid formation. These spheroids have a HUVEC monolayer on their outside. In addition, the spheroids are hollow and match the characteristics of blood vessels. The spheroids are transferred into a collagen matrix, which allows observation of sprout formation. Sprouting is the initial process needed for angiogenesis.

Knockdown of *hnRNP DL* in HUVECs led to a dramatic reduction of sprouting (**Figure 4-4**). VEGF-A is the most important driver for angiogenesis. Stimulation of HUVEC spheroids with VEGF-A led to an increase in sprouting, but strikingly, stimulation could not restore sprouting after *hnRNP DL* knockdown. These data emphasize an important role of hnRNP DL in angiogenesis.

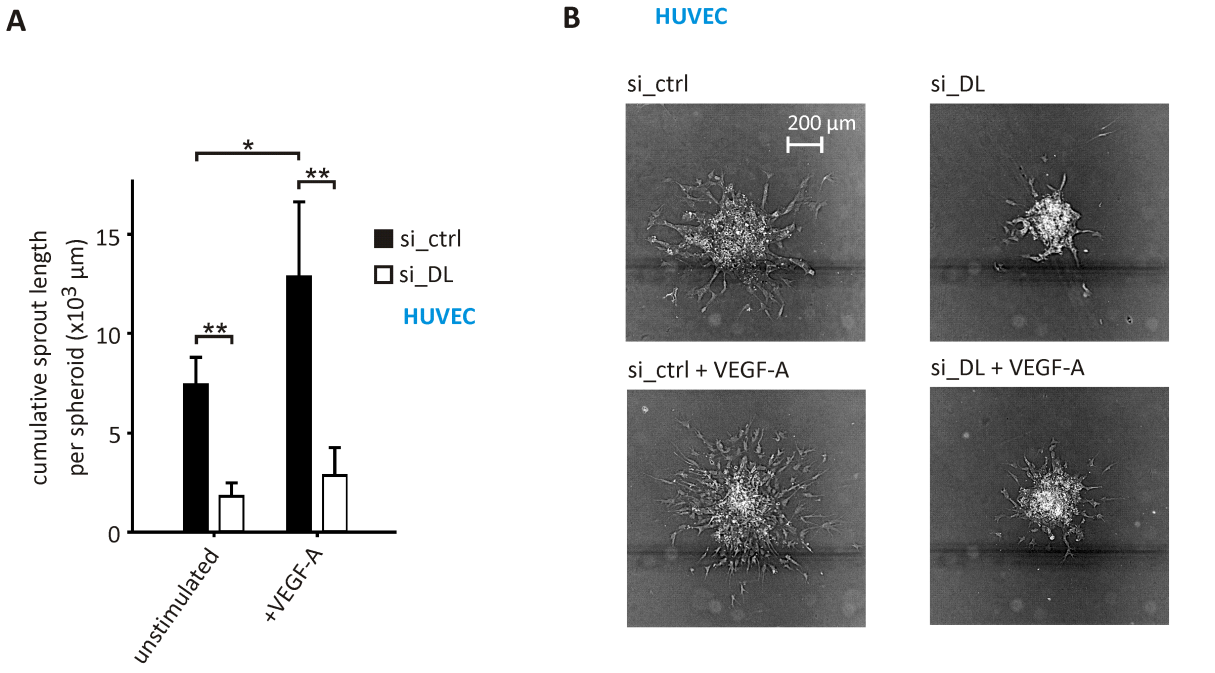

Figure 4-4: HnRNP DL affects endothelial cell angiogenesis. (A) Quantification of the cumulative sprout length per spheroid in HUVECs after knockdown of *hnRNP DL* with or without VEGF-A stimulation (0.05 mg/ml). Sprouting is dramatically reduced after *hnRNP DL* knockdown. n=4. **(B)** Representative pictures of spheroids and sprouts. Knockdown of *hnRNP DL* leads to dramatic reduction in sprouting. (**) P value < 0.01.

Vascular cell adhesion protein 1 (VCAM1) is an important angiogenic factor. VEGF-A increases the transcription rate of VCAM1 during angiogenesis.[188,189] Further, *VCAM1* was identified as potential new hnRNP DL target in the transcriptome analyses after *hnRNP DL* knockdown in HUVECs. To investigate the influence of hnRNP DL on VCAM1 levels, samples were taken from unstimulated HUVECs and HUVECs stimulated with VEGF-A 48 h after

transfection with a nonsilencing siRNA or an siRNA targeting *hnRNP DL*. A.T. Gimbel performed RT-qPCR and Western blot analyses of VCAM1 levels in the context of her master thesis.[190] *VCAM1* mRNA and VCAM1 protein levels were dramatically reduced after *hnRNP DL* knockdown (**Figure 4-5**). While stimulation with VEGF-A led to a dramatic increase of VCAM1 levels in the control cells, it could not restore VCAM1 levels after *hnRNP DL* knockdown. This highlights the role of hnRNP DL in angiogenesis and implicates a *VCAM1* expression control mechanism involving both, hnRNP DL and VEGF-A.

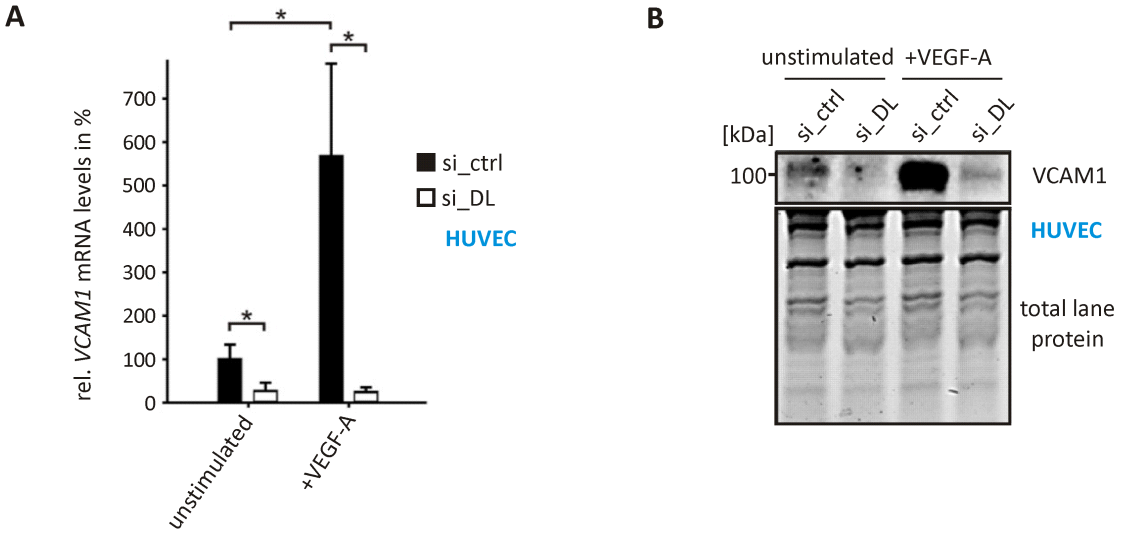

Figure 4-5: Knockdown of *hnRNP DL* leads to reduced VCAM1 levels. (A) RT-qPCR shows reduced *VCAM1* mRNA levels after *hnRNP DL* knockdown. Stimulation with VEGF-A (0.05 mg/ml) does not restore *VCAM1* mRNA levels. Values are normalized to the housekeeping gene *RPLP0*. n=3. **(B)** Western blot analysis shows reduced VCAM1 protein levels after *hnRNP DL* knockdown with or without VEGF-A stimulation. n=2. (*) P value < 0.05.

4.2 Hypoxia-driven gene expression changes in human cancer cells

Solid tumors typically comprise hypoxic regions. Hypoxia influences the gene expression in afflicted cells, promoting cancer cell gene expression programs, which favor cancer cell survival, migration, tumor angiogenesis and thus tumor progression. A profound understanding of hypoxia-driven gene expression changes, especially changes in posttranscriptional regulation like AS, is necessary to address hypoxic tumors in cancer therapy. In this study, I focused on the differential expression of RBPs as well as on splicing changes in cancer cells after hypoxia treatment. Lung and breast cancer cause the most of cancer-related deaths in males and females, respectively.[191,192] Thus, these cancer types were chosen for this study. In the following experiments A549 lung and MCF-7 breast cancer cells were used. After identification of hypoxic conditions that can be applied to both cell types without causing cell death, RNA sequencing analyses were performed. Interestingly, both cancer types exhibit a highly concordant response to hypoxia regarding transcript abundance. In contrast, hypoxia-driven splicing programs differed markedly. The transcriptome analyses further revealed a global reduction in RBP and especially hnRNP levels in both cell types. Strikingly, the splicing factor MBNL2 was one of few upregulated RBPs under hypoxia. A transcriptome analyses after siRNA-mediated knockdown of *MBNL2* enabled me to identify novel MBNL2 target mRNAs. There was a strong intersection between genes induced under hypoxia and downregulated after *MBNL2* knockdown, hypothesizing an mRNA stabilizing role of MBNL2. In actinomycin D mRNA decay assays I could disprove a stabilizing function of MBNL2 for the *VEGFA* mRNA. Instead, I could find that MBNL2 is required for efficient VEGF-A protein secretion under hypoxia. In addition, MBNL2 target gene induction under hypoxia is specific for MBNL2 and not shared by its paralog MBNL1. Importantly, MBNL2 depletion diminished cancer cell proliferation as well as migration in crystal violet and transwell assays, respectively, highlighting the physiological importance of MBNL2. In sum, this study demonstrates an important role of MBNL2 in controlling cancer cell adaption to hypoxic conditions.

4.2.1 Selection of hypoxic conditions

At first, hypoxic conditions, which can be applied to both, A549 and MCF-7 cancer cells, had to be identified. For the achievement of a comparable data set, it is essential to use the same conditions for cohorts that are to be compared later. The usage of different conditions in previous studies in endothelial cells[184], mesenchymal stem cells[185] and hepatocellular carcinoma cells[186] rendered a direct comparison between the studies impossible. In this study, a hypoxia incubation chamber was used to apply hypoxic conditions to human cancer cells. In order to test the response of cancer cells to hypoxia in preliminary experiments, they were cultured for different durations (6 h, 16 h, 24 h, 48 h) under hypoxia (0.5% O_2). Here, 6 h and 16 h can be considered as acute hypoxia, while 24 h and 48 h are referred to as chronic hypoxia. *VEGFA* mRNA level can be used as a measure of hypoxia response since it is highly induced under hypoxia in many cell types. In addition to *VEGFA*, *hnRNP M* mRNA levels were examined under hypoxia. Previous studies in our laboratory have shown that *hnRNP M* mRNA levels are reduced under hypoxia. The consideration of an induced (*VEGFA*) and a reduced mRNA (*hnRNP M*) under hypoxia should give an overview of the hypoxia response of the cancer cells. Analysis of mRNA levels of the known hypoxia-responsive genes *VEGFA* and *hnRNP M* after hypoxia treatment (0.5% O_2) of A549 and MCF-7 cells for different durations (6 h, 16 h, 24 h, 48 h) revealed that chronic hypoxia (48 h) has the greatest effect on the change in mRNA levels in A549 cells (**Figure 4-6**). In addition, chronic hypoxia had the greatest effect on *hnRNP M* mRNA level in MCF-7. Thus, chronic hypoxia (48 h) was chosen for further experiments.

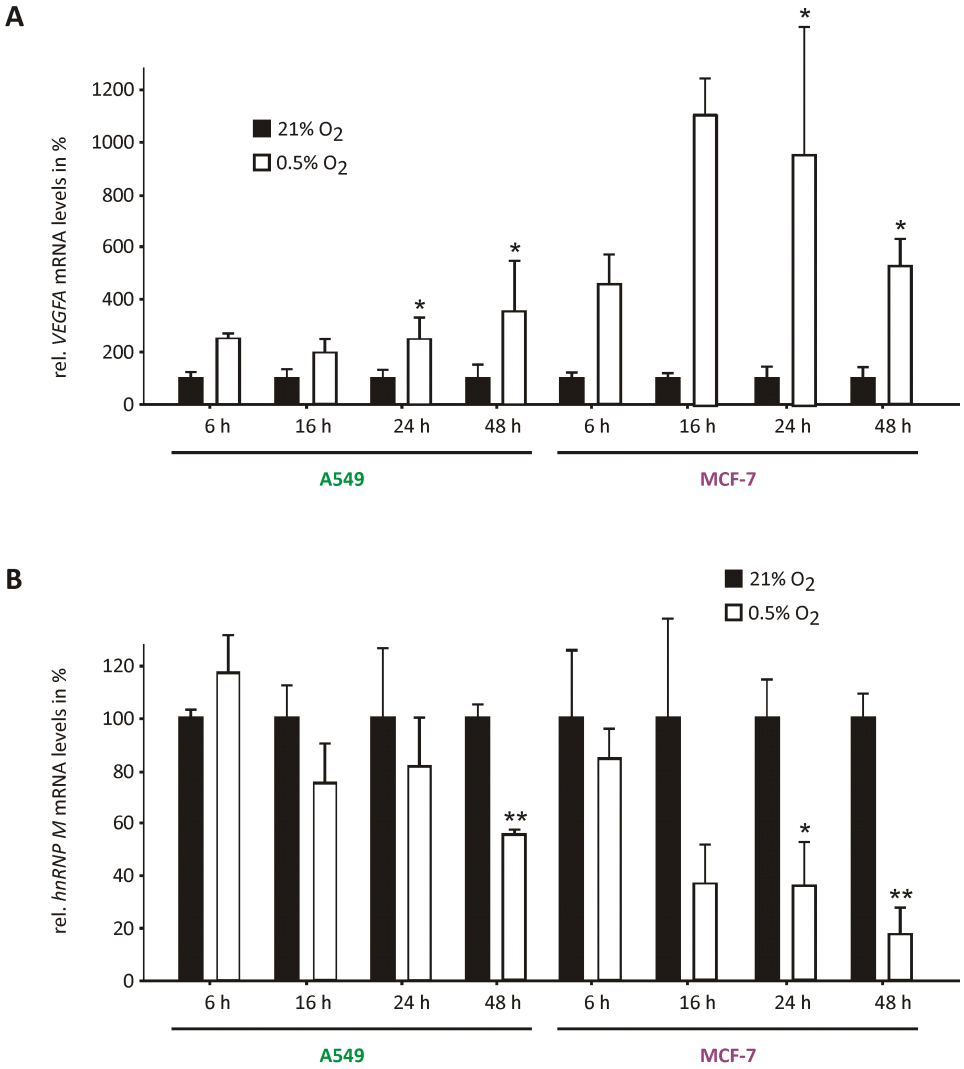

Figure 4-6: Hypoxia leads to *VEGFA* mRNA induction and *hnRNP M* mRNA reduction. (A) and (B) RT-qPCR quantification of *VEGFA* (**A**) and *hnRNP M* (**B**) mRNA levels in normoxic and hypoxic A549 and MCF-7 cells. Values are normalized to the housekeeping gene *RPLP0*. 24 h and 48 h n=3-4, 6 h and 16 h n=2. (**) P value < 0.01, (*) P value < 0.05.

For the investigation of mRNA levels in cancer cells after hypoxia treatment, it is essential that cells are viable and do not induce apoptosis. To ensure that hypoxia treatment with 0.5% O_2 does not impair cell survival, I performed crystal violet assays in A549 and MCF-7 cells after hypoxia treatment with 0.5% O_2 for 48 h. Hypoxia treatment had no influence on hypoxic cancer cell viability in comparison to normoxic control cells as could be seen in the crystal violet assay (**Figure 4-7 A**). Further, it was tested in crystal violet assays, whether lowering the oxygen concentration influences cancer cell survival (**Figure 4-7 B**). Cancer cell proliferation was impaired after treatment with 0.2% O_2 for 48 h. Cell survival is a

prerequisite for further analyses of gene expression and AS changes, therefore, 0.5% O_2 was chosen as condition for further experiments.

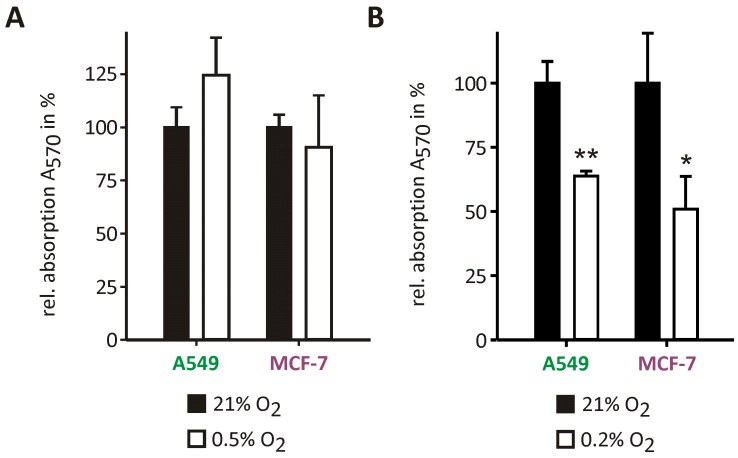

Figure 4-7: Influence of chronic hypoxia on cancer cell viability. (A) and (B) Cell viability of A549 and MCF-7 cells after chronic hypoxia treatment with 0.5% (**A**) and 0.2% (**B**) O_2, respectively. Cell viability was examined in crystal violet assays. Shown is the relative absorption after crystal violet staining. n=3. (**) P value < 0.01, (*) P value < 0.05.

4.2.2 Transcriptome analyses

In order to detect hypoxia-driven changes in gene expression and in AS, deep sequencing was performed. For that purpose, total RNA was extracted from A549 and MCF-7 cells, which were incubated under normoxic (21% O_2) or hypoxic (0.5% O_2) conditions for 48 h (n=2). Ribosomal RNA was depleted, a strand-specific cDNA library was generated and approximately 100 million reads were achieved per sample. A. Di Liddo and K. Zarnack performed bioinformatics and gene ontology (GO) analyses (see also chapter 8.2).

In general, RNA deep sequencing analyses yield a certain number of raw reads per sample. Low-quality reads are discarded and adaptor sequences are trimmed. In this study, reads were mapped to the human genome (GRCh38/hg38 assembly). Reads were counted within genes annotated in GENCODE version 24. DESeq2[193] was used to analyze differential gene expression between hypoxic and normoxic conditions. rMATS[194] was used to detect AS events. RNA sequencing data from normoxic and hypoxic A549 as well as MCF-7 cells is available in the Gene Expression Omnibus Database (GEO, www.ncbi.nlm.nih.gov/geo/) under the accession number GSE131378.

Raw read counts are affected by the total number of reads, sequencing biases and also by transcript length.[195] Therefore, read counts are normalized to the transcript length as well as the total number of transcripts in a sequencing run yielding the transcripts per million (TPM). The following formula can be used to calculate the TPM:

$$TPM = \frac{r_g \, x \, rl \, x \, 10^6}{fl_g \, x \, T}$$

where r_g is the number of reads mapped to a particular gene region g, rl is the read length, fl_g is the feature length and T is the total number of transcripts in a sequencing sample.[196] With this method, the sum of all TPMs in one sample is always 1,000,000. This enables the comparison between several samples and thus, differential gene expression analyses, assuming that the same number of transcripts is present in the samples.[196,197]

During transcriptome analyses in this study, mRNA levels of transcripts with TPMs lower than 1 were not detectable in RT-qPCR experiments, most probably due to technical limitation. Thus, only transcripts with at least one copy per one million transcripts ([TPM] > 1) in at least one sample were considered to increase reproducibility and statistical power.

4.2.2.1 Differential gene expression under hypoxia in cancer cells

Transcripts from 18,214 genes in A549 and from 18,880 genes in MCF-7 cells were detected during deep sequencing. 15,684 transcripts were shared between both cell types. Gene expression was considered as changed, if the expected change in expression level between the normoxic and hypoxic sample was at least 1.5-fold. Differential gene expression analyses after hypoxia treatment revealed significantly changed levels of 2,490 (16%) transcripts in A549 and 4,503 (29%) transcripts in MCF-7 cells. 1,224 differentially expressed transcripts are shared between both cell types and are mainly regulated in the same direction (1109; 91%; **Figure 4-8 A and B**), highlighting the highly correlated response to chronic hypoxia in A549 and MCF-7 cells. A. Di Liddo performed a gene ontology (GO) analysis using the enrichGO function in clusterProfiler in R, which showed an increase in the expression of typical hypoxia response genes implicated in metabolic processes, vasculature development, regulation of blood circulation, positive regulation of cell migration or extracellular matrix organization (**Supplementary Figure 11-1**). GO analysis further showed downregulation of genes

implicated in DNA replication, ribosome biogenesis, RNA splicing, DNA repair or telomere maintenance. For verification, mRNA levels of the known hypoxia response genes *DDIT4* (DNA-damage inducible transcript 4), *LDHA* (lactate dehydrogenase) and *PLOD2* (procollagen-lysine,2-oxoglutarate 5-dioxygenase 2) were investigated. The expected increase of mRNA level could be confirmed in both cell types (**Figure 4-8 C**).

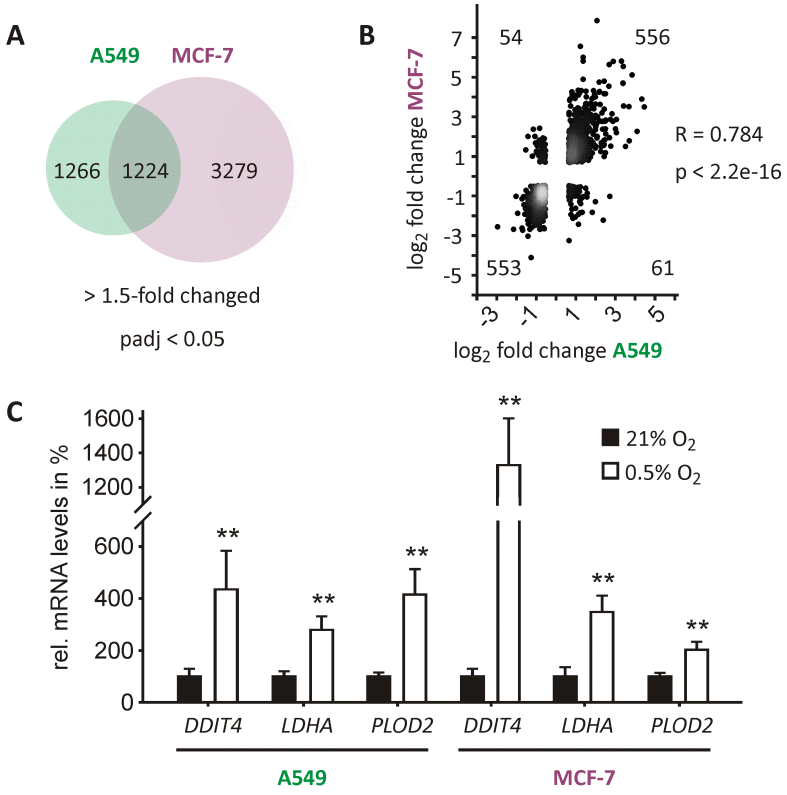

Figure 4-8: Chronic hypoxia treatment causes similar changes in transcript abundance in A549 and MCF-7 cells. (A) 2,490 and 4,503 genes are differentially expressed in A549 and MCF7 cells, respectively. 1,224 differentially expressed genes are shared between both cell types. padj=adjusted P value. **(B)** 1,224 differentially expressed genes are mainly regulated in the same direction. **(C)** RT-qPCR quantification of the mRNA levels of hypoxia-induced genes in normoxic and hypoxic A549 and MCF-7 cells. Values are normalized to the housekeeping gene *RPLP0*. n=5. (**) P value < 0.01, (*) P value < 0.05.

In this study, I focused on the differential expression of RBPs. RBPs are responsible for posttranscriptional regulation and their deregulation is associated with cancer.[81] Interestingly, RBP transcript levels were globally reduced in hypoxic A549 and MCF-7 cells (**Table 4-1**).

Table 4-1: Differential expression of RBPs after hypoxia treatment of A549 and MCF-7 cells. RBPs are mainly regulated in the same direction in A549 and MCF-7 cells. Most RBPs are downregulated under hypoxia.

	Log2FoldChanges	
Gene name	**A549**	**MCF-7**
SAMD4A	1.73	1.61
TIPARP	1.31	0.76
CARHSP1	1.12	0.85
GAPDH	1.06	3.34
CELF5	1.05	1.62
MBNL2	1.03	1.36
SFMBT2	0.85	0.63
RBMS2	0.79	1.08
MEX3D	0.78	1.58
MEX3B	0.75	0.73
ZFP36L1	0.63	0.59
HTATSF1	-0.60	-0.88
PCBP1	-0.60	1.49
LSM4	-0.60	-0.85
SNRPD3	-0.61	-0.78
SNRPC	-0.61	-0.69
POLR2G	-0.62	-0.92
PPRC1	-0.62	-1.09
NIFK	-0.62	-0.61
HNRNPR	-0.63	-0.90
PUM3	-0.66	-0.95
SF3B4	-0.68	-0.93
TRA2B	-0.68	-0.71
PNPT1	-0.72	-1.64
CSTF2	-0.73	-1.77
PNO1	-0.77	-1.64
TOE1	-0.80	-1.32
SNRPD1	-0.82	-1.10
HNRNPAB	-0.82	-1.55
SSB	-0.82	-0.77
ALYREF	-0.86	-1.11
TDRKH	-0.88	-0.98
PDCD11	-0.90	-0.82
HNRNPM	-0.94	-1.00
PPARGC1B	-1.06	-1.85

> 1.5-fold up
padj < 0.05

> 1.5-fold down
padj < 0.05

I further focused on the expression of hnRNPs since hnRNPs are the major splicing regulators. Comparison of the fold changes of hnRNP transcripts in A549 and MCF-7 cells shows for example reduction of *hnRNP L* and *M* in response to hypoxia, with *hnRNP M* reacting most strongly to hypoxia (**Figure 4-9 A**). *HnRNP A1* and *C* mRNA levels show a trend towards reduction under hypoxia. *HnRNP A0* and *DL* mRNA levels were reduced in A549 but slightly increased in MCF-7 cells. The level of *hnRNP E2* mRNA remained almost the same. The strong reduction of *hnRNP M* mRNA level was confirmed by RT-qPCR (**Figure 4-9 B**). The reduced mRNA levels might be due to a reduction of transcription or reduced mRNA stability. In addition, a switch in AS towards NMD-sensitive isoforms might lead to a reduction in mRNA level as could be seen for *hnRNP DL* (**Figure 4-9 C**) in MCF-7 cells. Inclusion of *hnRNP DL* exon 8 was increased under hypoxia in MCF-7 cells and leads to degradation of the mRNA by NMD.

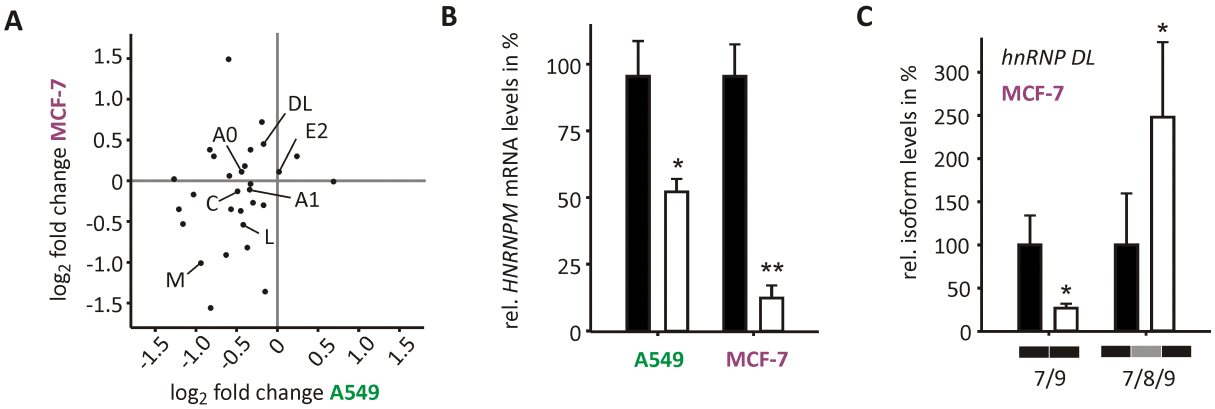

Figure 4-9: Chronic hypoxia leads to reduced *hnRNP* transcript levels. (A) Deep sequencing data reveal reduced hnRNP transcript levels in both, A549 and MCF-7 cells. **(B)** Verification of reduced *hnRNP M* transcript level by RT-qPCR. Values are normalized to the housekeeping gene *RPLP0*. n=3. **(C)** In MCF-7 cells, hypoxia leads to a shift in *hnRNP DL* transcript splicing, promoting inclusion of *hnRNP DL* exon 8, which leads to degradation of the mRNA by NMD. Values are normalized to the housekeeping gene *RPLP0*. n=4. (**) P value < 0.01, (*) P value < 0.05.

Since mRNA levels might not reflect the effects observed at the protein level, I investigated protein levels of hnRNPs. Western blot analyses of hnRNP A0, A1, C, DL, E2, L and M revealed that hnRNP protein levels are reduced in A549 and MCF-7 cells in response to hypoxia (**Figure 4-10**). Parts of the Western blot analyses were performed by M. Fauth in the context of an internship. The transcript level of some hnRNPs, including *hnRNP E2*, did not change in the transcriptome analysis, pointing towards regulation mechanisms other than reduction of transcription or reduced mRNA stability.

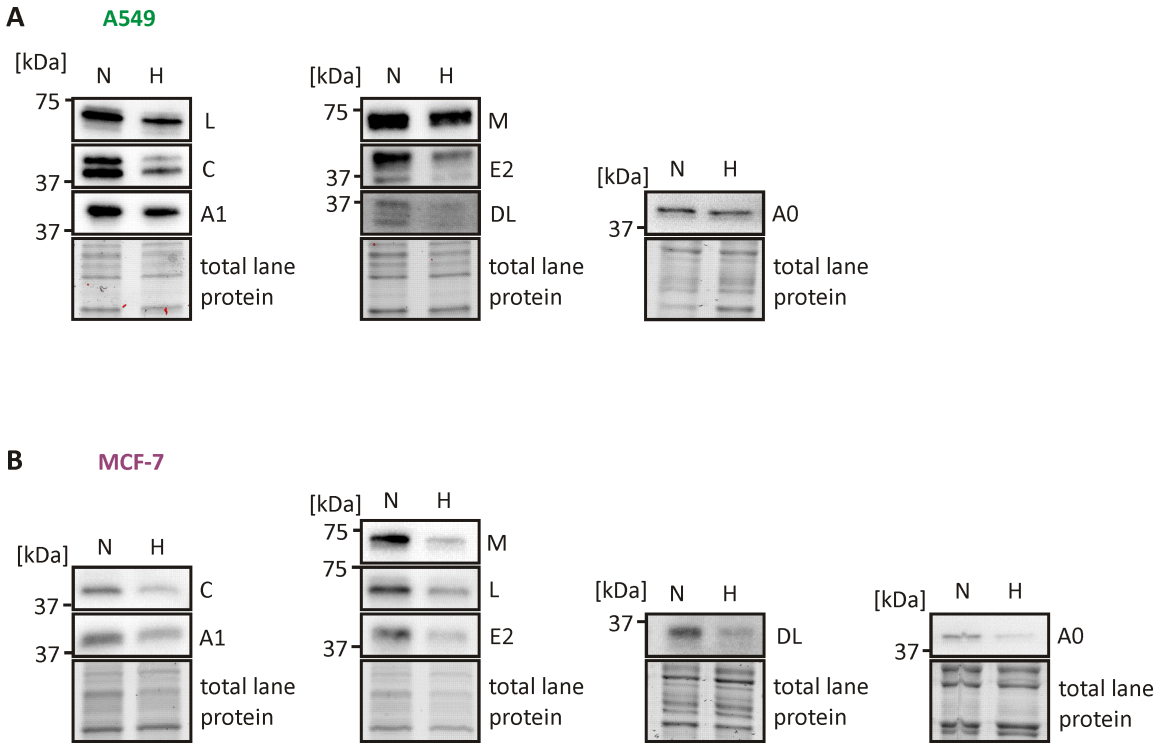

Figure 4-10: Chronic hypoxia leads to reduced hnRNP protein levels. (A) and (B) Protein levels of the hnRNPs A0, A1, C, DL, E2, L and M are reduced in hypoxic A549 (**A**) and MCF-7 cells (**B**). n=2-4.

Strikingly, only few RBPs were induced under hypoxia in the tested cell types. Hypoxia treatment of A549 and MCF-7 cells led to approximately 1.9–fold and 1.5–fold induction of *MBNL2* mRNA level, respectively (**Figure 4-11**). In addition, *PTRF* (polymerase I and transcript release factor, also known as CAVIN1, caveolae associated protein 1) and *SAMD4A* (sterile alpha motif domain-containing protein 4A, also known as SMAUG1) mRNA levels were significantly increased in hypoxic A549 and MCF-7 cells.

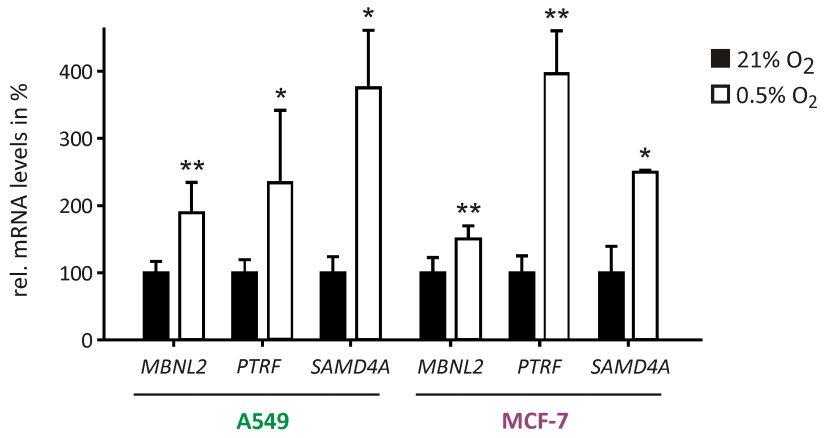

Figure 4-11: *MBNL2*, *PTRF* and *SAMD4A* are specifically induced under hypoxia. RT-qPCR quantification reveals increased *MBNL2*, *PTRF* and *SAMD4A* mRNA levels in hypoxic A549 and MCF-7 cells. Values are normalized to the housekeeping gene *RPLP0*. n=4. (**) P value < 0.01, (*) P value < 0.05.

4.2.2.2 Differential splicing programs under hypoxia in cancer cells

In transcriptome analyses the percent spliced-in (PSI) is used to compare AS events between several conditions. Simplified, the PSI is calculated using the following equation:

$$PSI = \frac{IR}{IR + ER}$$

with IR being the inclusion reads and ER being the exclusion reads.[198] IRs contain features of the exon of interest together with features from the flanking exons, while ERs span the exon-exon junction between the flanking exons of the exon of interest. Constitutive exons have a PSI of 100%.

Hypoxia treatment of A549 and MCF-7 cells extensively changed AS programs. AS events were assumed as changed when the absolute change in PSI (|ΔPSI|) was bigger than 10%. Cassette exons are the most common AS type and represented approximately 50% of all detected AS events in the transcriptome analyses (**Figure 4-12 A**). About 60% of cassette exons were alternatively spliced upon hypoxia (|ΔPSI|>10%). In MCF-7 hypoxia led to preferential exon skipping, while equal amounts of cassette exons were skipped or retained in A549, respectively (**Figure 4-12 B**). Alternative 5' and 3' splice sites as well as retained introns were preferentially skipped in MCF-7 cells, while they were preferentially used in A549 cells. From a total of 2,225 changed AS events in A549 and 4,206 in MCF-7, only 199 changed AS events were shared by both cell types (**Figure 4-12 C**). Moreover, only 123 (63%) of these events were regulated in the same direction in both cell types (**Figure 4-12 D**).

Obviously, the activated AS programs under hypoxia differ markedly between A549 and MCF-7 cells. The same number of changed events was found as for transcript abundance, but the overlap between the two cell types is small for AS changes. Therefore, hypoxia-driven AS changes seem to be much more cell type-specific than the differential gene expression.

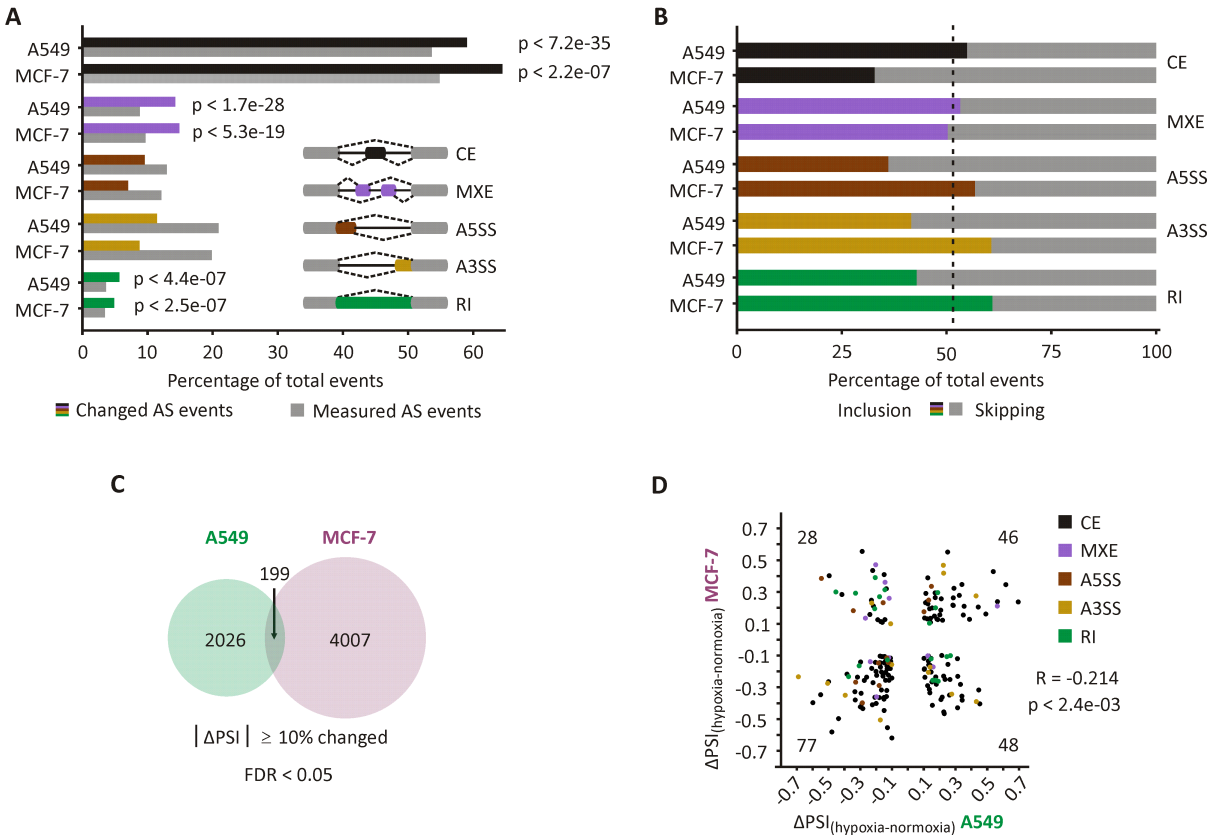

Figure 4-12: Hypoxia-driven AS changes are highly cell type-specific. (A) Detected and changed AS events under hypoxia in A549 and MCF-7 cells. Different event types are color-coded. CE = cassette exon, MXE = mutually exclusive exons, A5SS = alternative 5' splice site, A3SS = alternative 3' splice site, RI = retained intron. **(B)** Inclusion vs. skipping in changed AS events. **(C)** Number of changed AS events in both cell types. Only 199 changed AS events are shared between the two cell types. PSI = percent spliced-in, FDR = false discovery rate. **(D)** Comparison of changed AS events in A549 and MCF-7 cells.

For verification, the splicing patterns of the genes coding for *CENPE* (centromere-associated protein E), PTBP2 and PUSL1 (tRNA pseudouridine synthase-like 1) were examined in response to hypoxia in both cell types. Here, oligonucleotides are located in the exons, which flank the alternatively spliced exon. Oligonucleotides led to amplification of both *CENPE*, *PTBP2* and *PUSL1* isoforms, with or without the alternatively spliced exon, in RT-PCRs. As expected from sequencing data, hypoxia treatment led to decreased inclusion of *CENPE* exon 17 and *PTBP2* exon 10 (**Figure 4-13**). In addition, a slightly increased inclusion of

PUSL1 exon 2 under hypoxia could be shown. RT-PCR analyses of *CENPE* and *PTBP2* splice pattern were performed by J.S. Gerhardus in the context of her bachelor thesis.[199]

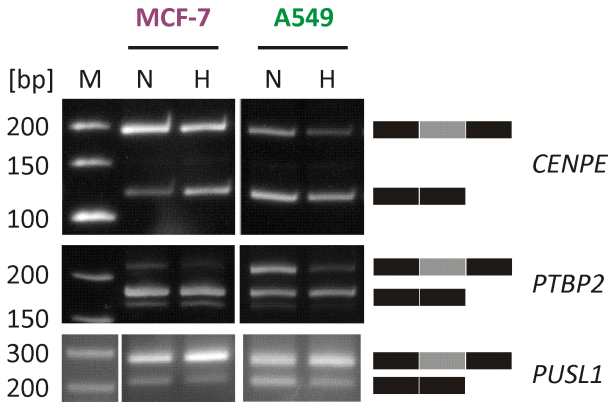

Figure 4-13: Hypoxia-driven AS changes. *CENPE* exon 17 inclusion is reduced after hypoxia treatment in A549 and MCF-7 cells. The short PCR product (118 bp) corresponds to the exon skipping isoform, while the long isoform (192 bp) corresponds to the exon inclusion isoform. *PTBP2* exon 10 inclusion is reduced after hypoxia treatment in A549 and MCF-7 cells. The short PCR product (183 bp) corresponds to the exon skipping isoform, while the long isoform (217 bp) corresponds to the exon inclusion isoform. *PUSL1* exon 2 inclusion is increased after hypoxia treatment in A549 and MCF-7 cells. The short PCR product (215 bp) corresponds to the exon skipping isoform, while the long isoform (273 bp) corresponds to the exon inclusion isoform. Splicing patterns of *CENPE* and *PTBP2* were examined in PAA gels. Splicing pattern of *PUSL1* was examined in an agarose gel. n=2. N = normoxia, H = hypoxia, M = size marker.

4.2.3 MBNL2 controls the hypoxia adaptation of cancer cells

Unlike most of the other splicing factors, which are reduced under hypoxia, MBNL2 is specifically induced under hypoxia. MBNL2 was of particular interest for me, since it is a typical splicing regulator and has recently been shown to be induced in hepatocellular carcinoma.[180] Thus, further experiments focused on MBNL2.

I investigated the MBNL2 protein level under normoxic and hypoxic conditions in A549 and MCF-7 cells. I could show that MBNL2 is induced under hypoxia (**Figure 4-14**), corresponding to its increase at mRNA level.

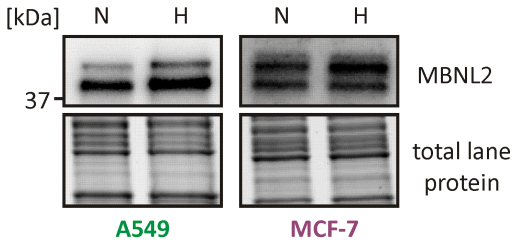

Figure 4-14: MBNL2 is induced under hypoxia. MBNL2 protein is increased under hypoxia in both cell types, A549 and MCF-7.

In order to investigate, how MBNL2 impacts on cancer cell adaptation to hypoxia, I established an *MBNL2* knockdown under hypoxia. The *MBNL2* knockdown under hypoxic conditions efficiently led to a reduction of *MBNL2* mRNA and MBNL2 protein level in A549 and MCF-7 cells (**Figure 4-15**).

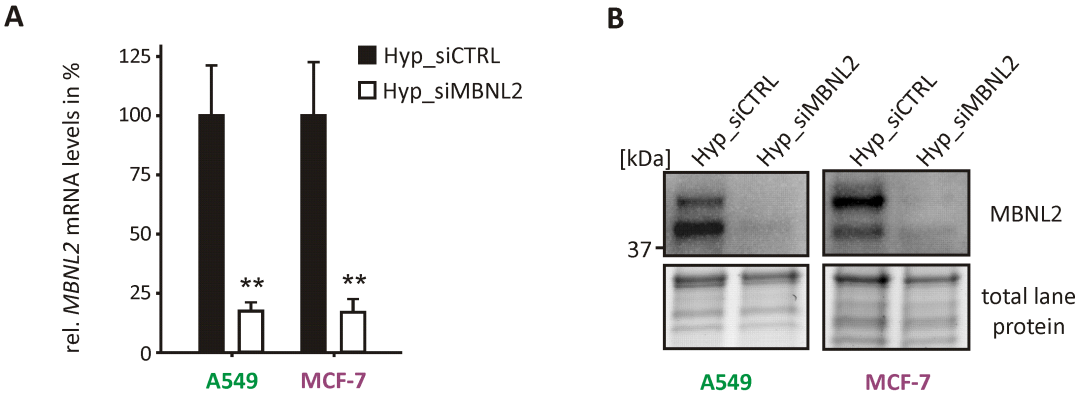

Figure 4-15: Established knockdown of *MBNL2*. (A) and (B) SiRNA-mediated knockdown of *MBNL2* efficiently decreases MBNL2 mRNA (**A**) and protein (**B**) level.

4.2.3.1 MBNL2 controls transcript abundance of hypoxia-responsive genes

Further, we performed transcriptome analyses after *MBNL2* knockdown under hypoxia in MCF-7 cells to investigate, how MBNL2 impacts on cancer cell adaptation to hypoxia. Here, hypoxic MCF-7 cells serve as control. MCF-7 cells were transfected with a nonsilencing control siRNA or with an siRNA targeting *MBNL2* and incubated under normoxic conditions

(21% O_2). After 24 h cells were transferred to the hypoxia incubation chamber (0.5% O_2). After 48 h, total RNA was extracted from MCF-7 cells (n=2). PolyA-enriched strand-specific cDNA libraries were generated and approximately 80 million reads were achieved per sample. A. Di Liddo and K. Zarnack performed bioinformatics and gene ontology (GO) analyses as already described in chapter 4.2.2. RNA sequencing data from *MBNL2* knockdown experiments is available in the Gene Expression Omnibus Database (GEO, www.ncbi.nlm.nih.gov/geo/) under the accession number GSE136231.

4,370 genes were differentially expressed among *MBNL2* knockdown under hypoxia in MCF-7 cells. In comparison with the differentially expressed genes under hypoxia in MCF-7 cells, 1,528 differentially expressed genes are shared between both cohorts (**Figure 4-16 A**). Comparison of shared differentially expressed genes showed that these genes are preferentially regulated in the opposite direction (1,091; 71%; **Figure 4-16 B**), indicating a role of MBNL2 in hypoxia-dependent gene regulation. To identify target mRNAs that can also be traced in A549 cells and other cancer types, we compared the 4,370 differentially expressed genes among *MBNL2* knockdown under hypoxia in MCF-7 cells with the shared differentially expressed genes in A549 and MCF-7 cells under hypoxia. 351 genes were shared between these cohorts (**Figure 4-16 C**). 65% of the shared genes (227) were regulated in the opposite direction (**Figure 4-16 D**), pointing towards a universal role of MBNL2 in hypoxia adaptation, not only in MCF-7 cells but also in other cancer types. Most of the differentially expressed genes were induced under hypoxia and reduced after *MBNL2* knockdown.

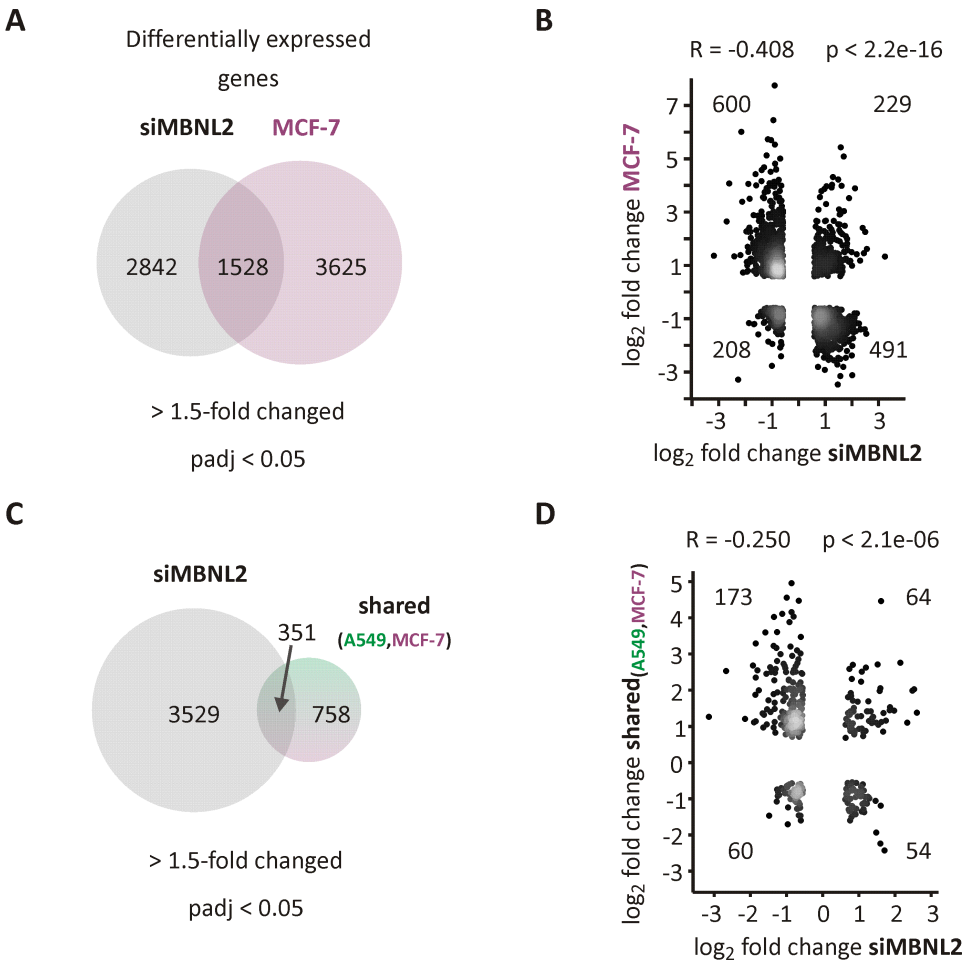

Figure 4-16: MBNL2 affects transcript abundance of hypoxia-responsive genes. (A) Comparison of differentially expressed genes under hypoxia in MCF-7 cells and after *MBNL2* knockdown. 1,528 genes are shared between both cohorts. **(B)** Shared differentially expressed genes from (**A**) are preferentially regulated in the opposite direction. **(C)** Comparison of shared differentially expressed genes under hypoxia in A549 and MCF-7 cells and differentially expressed genes after *MBNL2* knockdown in MCF-7 cells. 351 genes are shared between both cohorts. **(D)** Shared differentially expressed genes from **(C)** are preferentially regulated in the opposite direction.

Further, I identified novel hypoxia-responsive MBNL2 target genes. The expression of *ALDOC*, *ENO2*, *ITGA5* and *LOX* was increased under hypoxia in MCF-7 cells, which was to be expected, as these are HIF targets. Knockdown of *MBNL2* under hypoxia attenuated the HIF target induction, pointing towards participation of MBNL2 in the regulation of HIF targets. Further, *VEGFA* turned out to be an MBNL2 target in our study, which was also recently found by Perron *et al.*[181] *ALDOC*, *ITGA5* and *VEGFA* are likewise regulated by hypoxia and MBNL2 in A549 cells (**Figure 4-17**). The fact that these targets are regulated in several cancer cell types reinforces the hypothesis of a universal function of MBNL2 in the hypoxia adaptation of cancer cells.

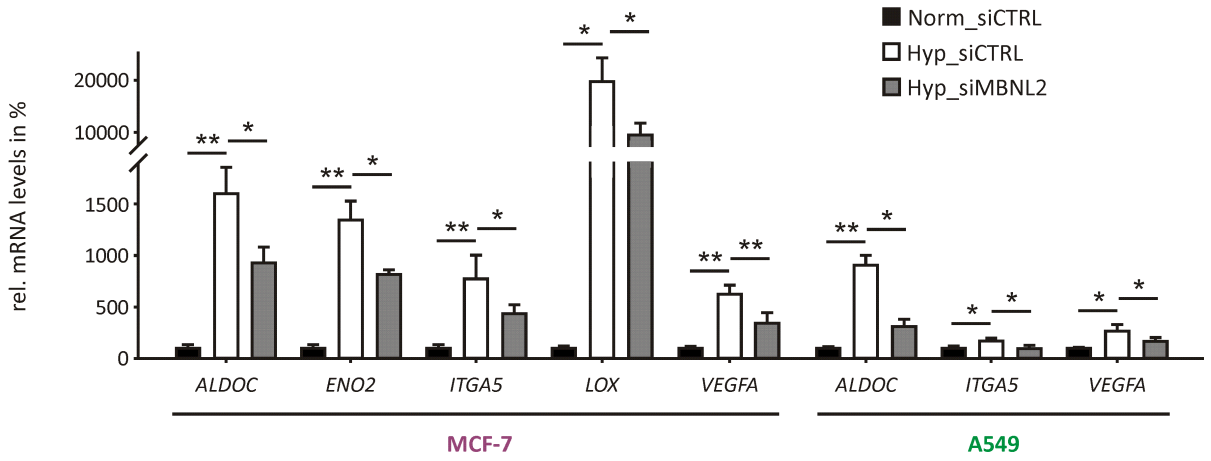

Figure 4-17: MBNL2 influences target gene induction under hypoxia. Verification of hypoxia-responsive MBNL2 target mRNAs by RT-qPCR. Values are normalized to the housekeeping gene *RPLP0*. n=3-6. (**) P value<0.01. (*) P value < 0.05.

4.2.3.2 MBNL2 target gene regulation is specific

Since MBNL2 is known to have similar functions like its paralogs MBNL1 and MBNL3, I also investigated mRNA levels of *MBNL1* and *MBNL3*. The mRNA level of its paralog *MBNL1* was unchanged in A549 and reduced in MCF-7 cells in response to hypoxia. Expression of *MBNL3* was only found in MCF-7 cells and was reduced upon hypoxia (**Figure 4-18 A**). Western blot analysis further revealed unchanged MBNL1 protein levels under hypoxia (**Figure 4-18 B**), while MBNL2 protein level is induced under hypoxia (**Figure 4-14**). These data show that only MBNL2, among the family of MBNLs, is specifically induced under hypoxia.

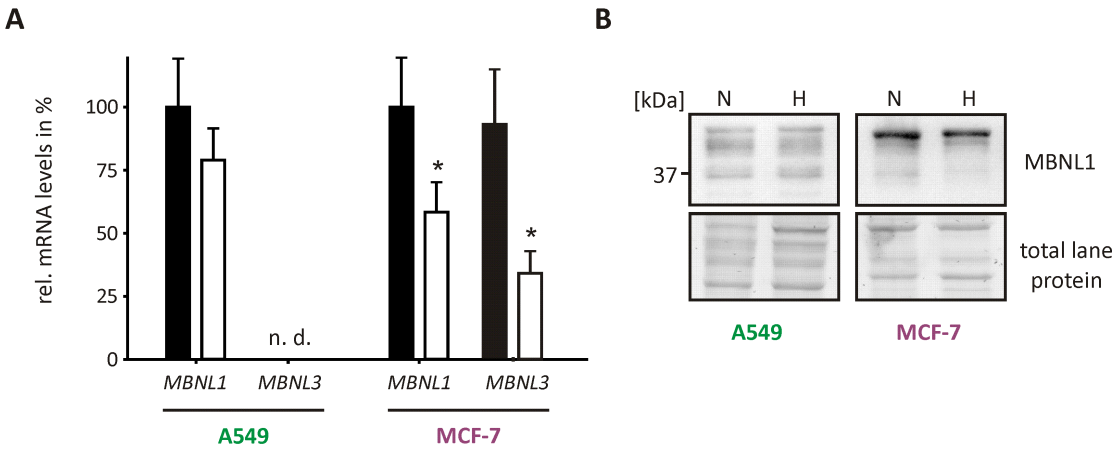

Figure 4-18: MBNL2 is specifically induced under hypoxia. (A) RT-qPCR quantification shows reduced *MBNL1* and *MBNL3* mRNA levels under hypoxia. *MBNL3* mRNA could not be detected in A549 cells. Values are normalized to the housekeeping gene *RPLP0*. n. d. = not detectable. n=4. **(B)** Western blot analyses show that MBNL1 protein level is unchanged under hypoxia. (*) P value < 0.05.

It is known that MBNL2 and its paralog MBNL1 have similar binding preferences and thus, share several targets.[160] I established an *MBNL1* knockdown to investigate whether MBNL2 target regulation in response to hypoxia is specific or shared by its paralog MBNL1. MBNL2 levels are increased at the mRNA and at the protein level (**Figure 4-19 A**) after depletion of *MBNL1*. The induction of MBNL2 in response to MBNL1 depletion might be due to MBNL1 and MBNL2 cross-regulation.[171] Subsequently, MBNL2 induction leads to MBNL2 target gene induction as could be seen for *ALDOC*, *ENO2*, *ITGA5* and *VEGFA* in MCF-7 cells (**Figure 4-19 B**). These findings indicate that specifically MBNL2 and not MBNL1 is necessary for target gene induction under hypoxia.

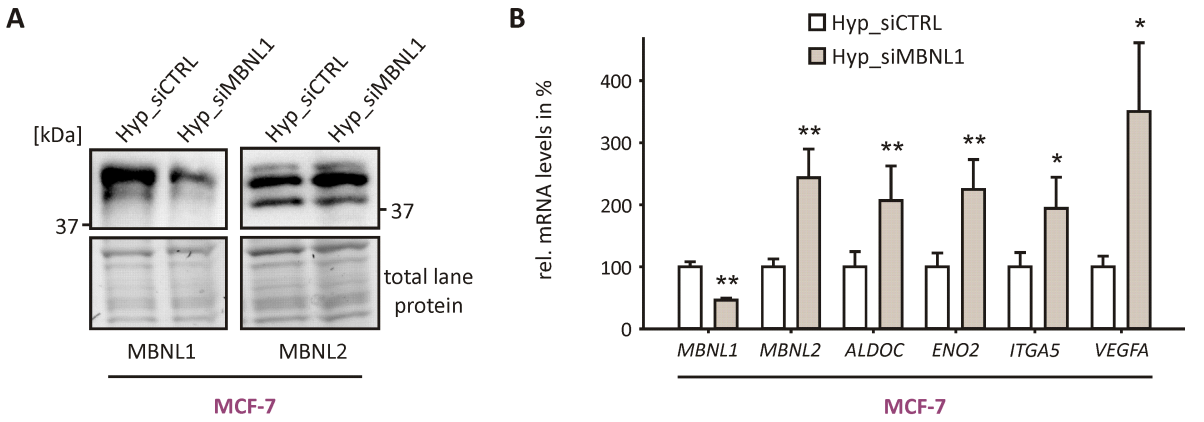

Figure 4-19: MBNL2 mediated induction of target genes is specific and not shared by its paralog MBNL1. (A) Knockdown of *MBNL1* increases MBNL2 protein level. n=2. **(B)** *MBNL1* knockdown does not decrease, but increase MBNL2 target gene mRNA levels. Values are normalized to the housekeeping gene *RPLP0*. n=3. (**) P value<0.01. (*) P value < 0.05.

4.2.3.3 MBNL2 does not control *VEGFA* mRNA stability, but secreted VEGF-A protein levels

The increased mRNA levels of MBNL2 targets under hypoxia and the decreased target mRNA levels after MBNL2 depletion point towards an mRNA stabilizing effect exerted by MBNL2. Previous studies also suggested a putative role of MBNL2 in target mRNA stabilization in several tissues and cell types by correlation of *in vitro* RNA-binding data with *in vivo* levels of putative target mRNAs.[200] For further investigation of MBNL2 target stabilization mechanism, I chose VEGF-A as model target since VEGF-A is a well-known and important regulator in both, hypoxia and cancer. In order to test whether MBNL2 stabilizes *VEGFA* mRNA, I performed actinomycin D mRNA decay assays after *MBNL2* knockdown under hypoxic conditions. Over a time course of 4 h there was no difference between the decay rates of *VEGFA* mRNA in control and *MBNL2* knockdown cells (**Figure 4-20**), disproving an mRNA stabilizing function of MBNL2, here.

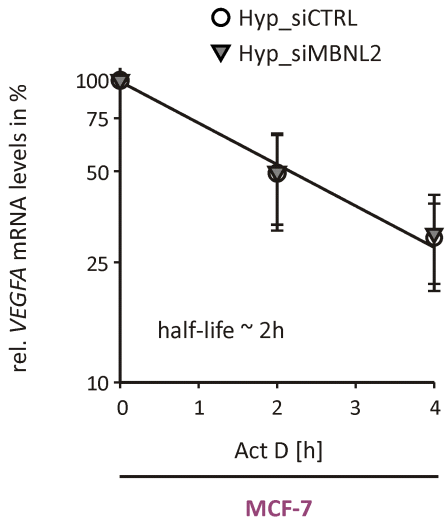

Figure 4-20: MBNL2 does not influence *VEGFA* mRNA stability. *VEGFA* mRNA level was measured after 2 and 4 h in comparison to the initial *VEGFA* mRNA level (0 h) after actinomycin D treatment. The *VEGFA* mRNA decay rates are nearly the same in control and *MBNL2* knockdown cells (MCF-7). *VEGFA* mRNA level was normalized to the housekeeping gene *RPLP0*. n=3.

Further, MBNL2 was supposed to be involved in promoting translation and subsequent secretion of proteins by influencing target mRNA localization.[169] Therefore, I investigated secreted VEGF-A protein levels depending on hypoxia and MBNL2 abundance. For that purpose, I performed enzyme-linked immunosorbent assays (ELISAs) using the supernatant of normoxic and hypoxic A549 and MCF-7 cells, which were transfected either with a nonsilencing control siRNA or an siRNA targeting *MBNL2*. Hypoxia induced secreted VEGF-A protein level by approximately 1.5-fold in MCF-7 and A549 cells (**Figure 4-21**). Normoxic VEGF-A protein level was completely restored when *MBNL2* was knocked down under hypoxia, highlighting the strong influence of MBNL2 on secreted VEGF-A protein level.

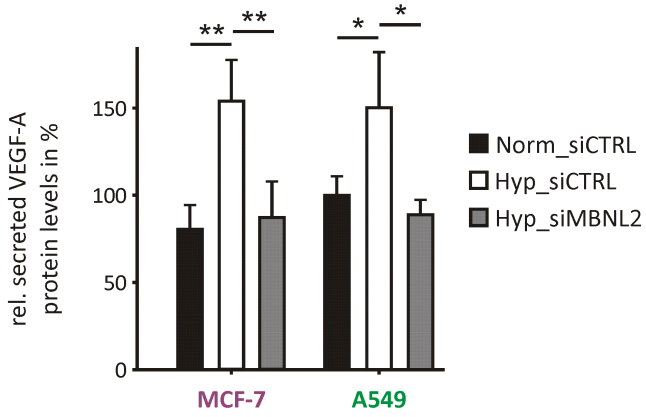

Figure 4-21: MBNL2 controls secreted VEGF-A protein levels. ELISA shows increased secreted VEGF-A protein level after hypoxia treatment and restored VEGF-A protein levels after MBNL2 depletion. n=4. (**) P value < 0.01. (*) P value < 0.05.

4.2.3.4 MBNL2 isoforms

MBNL2 gives rise to several protein isoforms as can be seen in the Western blot analyses (**Figure 4-14** and **Figure 4-19 A**). The four known isoforms differ in AS and have sizes ranging from 38 to 41 kDa (MBNL2-38/MBNL2-39/MBNL2-40/MBNL2-41; **Figure 4-22 A**). DNA sequence alignment is shown in **Supplementary Table 11-1**. The isoforms MBNL2-38 and MBNL2-40 contain exon 8, which has a size of 95 nt. The isoforms MBNL2-40 and MBNL2-41 contain exon 5, which has a size of 54 nt and is responsible for nuclear localization of the MBNL2 protein.[170] To investigate, which MBNL2 isoforms predominate in MCF-7 cells, I performed overexpression experiments, in which either GFP or one of the MBNL2 isoforms were overexpressed. For that, cDNA constructs were cloned into pCMV vectors. Starting vectors, containing the sequences of the several MBNL2 isoforms[170] were a kind gift from K. Sobczak. Overexpression of the MBNL2 isoforms indicates that MCF-7 cells prefer the isoforms MBNL2-38 and 40 or 41 (**Figure 4-22 B**).

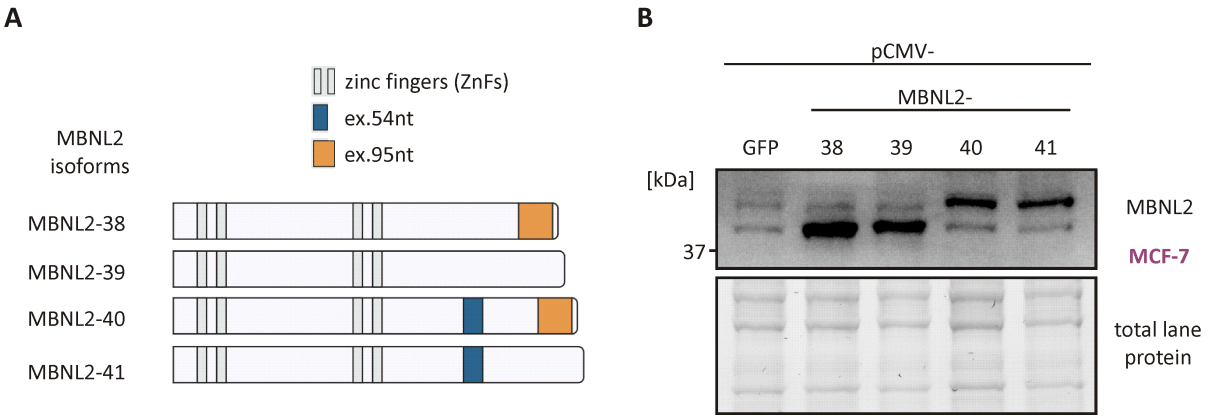

Figure 4-22: MBNL2 isoforms. (A) MBNL2 isoforms are ranging from 38 to 41 kDa and are thus called MBNL2-38, MBNL2-39, MBNL2-40 and MBNL2-41. The isoforms differ in the inclusion of two exons, indicated in blue (54 nt) and yellow (95 nt). Figure modified from[170]. **(B)** Western blot after overexpression of the MBNL2 isoforms MBNL2-38, MBNL2-39, MBNL2-40 and MBNL2-41 suggests preferred expression of *MBNL2* isoforms 38 and 40. n=4.

Since MBNL2 isoforms 40 and 41 could not be well differentiated, I took a look at the RNA sequencing data under normoxia and hypoxia in MCF-7 cells (**Figure 4-23**). MBNL2-40 and 41 differ in the inclusion of exon 8 (95 nt). In normoxic MCF-7 cells 13 (11 and 2) reads were detected, in which exon 8 was included. Exon 8 was excluded in only one read. In hypoxic MCF-7 cells, exon 8 was included in 59 (47 and 12) reads, while it was excluded in only 6 (5 and 1) reads. This indicates the preferred inclusion of exon 8 (95 nt) and thus, preferred expression of isoform MBNL2-40 instead of MBNL2-41. Further, exon 7 (36 nt) could be detected at low levels in MCF-7 cells. This isoform was not described in HeLa cells in the study by Sznajder *et al.*.[170] Due to the profound inclusion of *MBNL2* exon 8 in MCF-7 cells MBNL2 isoforms 38 and 40 were used in further overexpression experiments in MCF-7 cells (see chapter 4.2.3.5).

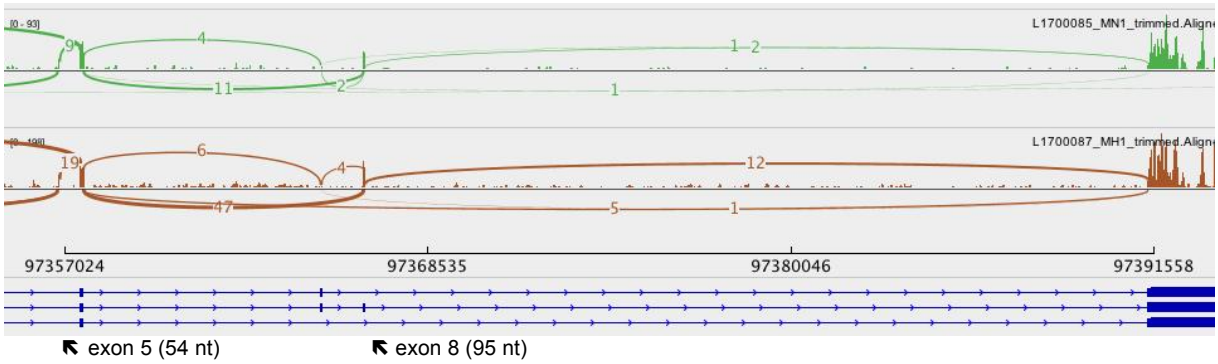

Figure 4-23: Sashimi plot shows preferential inclusion of exon 8 (95 nt) in MCF-7 mRNA. Sashimi plot was plotted using the Intregrated Genome Viewer. Mapped reads data from one replicate from normoxic and hypoxic MCF-7 cells was loaded into the Intregrated Genome Viewer and is representative for both replicates. Shown are detected reads over exon-exon junctions, which give information about the splicing patterns. MN = MCF-7 normoxia, MH = MCF-7 hypoxia.

4.2.3.5 MBNL2 binds to the *VEGFA* 3' UTR

Under hypoxia, both, MBNL2 and VEGFA mRNA and protein levels are induced. Knockdown of *MBNL2* further leads to reduced *VEGFA* mRNA, but also VEGF-A protein levels. To gain more insight into the mechanism by which MBNL2 is regulating *VEGFA*, we identified three potential MBNL2 binding sites within the *VEGFA* 3' UTR (**Figure 4-24**). MBNL2 is known to bind clustered 5'-YGCY-3' motifs with its two zinc finger domains, just like its paralog MBNL1.[201] In the *VEGFA* 3' UTR we found three such potential binding sites. To elucidate whether MBNL2 binds the *VEGFA* 3' UTR, the potential binding sites and their flanking sequences were cloned into an *ATP2A1* (Sarcoplasmic/endoplasmic reticulum calcium ATPase 1) minigene system. Cloning and the following *ATP2A1* splicing assays were performed by K. Taylor in the laboratory of K. Sobczak at the Adam Mickiewicz University in Poznan, Poland.

5′–GCCGGGCAGGAGGAAGGAGCCUCCCUCAGGGUUUCGGGAACCAGAUCUCUCACCAGGAAAGACUGAUACAGAACGAUCGAUACAGAAACCA
CGCUGCCGCCACCACACCAUCACCAUCGACAGAACAGUCCUUAAUCCAGAAACCUGAAAUGAAGGAAGAGGAGACUCUGCGCAGAGCACUUUGG
GUCCGGAGGGCGAGACUCCGGCGGAAGCAUUCCCGGGCGGGGUGACCCAGCACGGUCCCUCUUGGAAUUGGAUUCGCCAUUUUAUUUUUCUUGC
UGCUAAAUCACCGAGCCCGGAAGAUUAGAGAGUUUUAUUUCUGGGAUUCCUGUAGACACACCCACCCACAUACAUACAUUUAUAUAUAUAUAUA
UUAUAUAUAUAUAAAAAUAAAUAUCUCUAUUUUAUAUAUAUAAAAUAUAUAUAUUCUUUUUUUAAAUUAACAGUGCUAAUGUUAUUGGUGUCUU
CACUGGAUGUAUUUGACUGCUGUGGACUUGAGUUGGGAGGGGAAUGUUCCCACUCAGAUCCUGACAGGGAAGAGGAGGAGAUGAGAGACUCUGG
CAUGAUCUUUUUUUUGUCCCACUUGGUGGGGCCAGGGUCCUCUCCCCUGCCCAGGAAUGUGCAAGGCCAGGGCAUGGGGGCAAAUAUGACCCAG
UUUUGGGAACACCGACAAACCCAGCCCUGGCGCUGAGCCUCUCUACCCCAGGUCAGACGGACAGAAAGACAGAUCACAGGUACAGGGAUGAGGA
CACCGGCUCUGACCAGGAGUUUGGGGAGCUUCAGGACAUUGCUGUGCUUUGGGGAUUCCCUCCACAUGCUGCACGCGCAUCUCGCCCCCAGGGG
CACUGCCUGGAAGAUUCAGGAGCCUGGGCGGCCUUCGCUUACUCUCACCUGCUUCUGAGUUGCCCAGGAGACCACUGGCAGAUGUCCCGGCGAA
GAGAAGAGACACAUUGUUGGAAGAAGCAGCCCAUGACAGCUCCCCUUCCUGGGACUCGCCCUCAUCCUCUUCCUGCUCCCCUUCCUGGGGUGCA
GCCUAAAAGGACCUAUGUCCUCACACCAUUGAAACCACUAGUUCUGUCCCCCCAGGAGACCUGGUUGUGUGUGUGUGAGUGGUUGACCUUCCUC
CAUCCCCUGGUCCUUCCCUUCCCUUCCCGAGGCACAGAGAGACAGGGCAGGAUCCACGUGCCCAUUGUGGAGGCAGAGAAAAGAGAAAGUGUUU
UAUAUACGGUACUUAUUUAAUAUCCCUUUUUAAUUAGAAAUUAAAACAGUUAAUUUAAUUAAAGAGUAGGGUUUUUUUUCAGUAUUCUUGGUUA
AUAUUUAAUUUCAACUAUUUAUGAGAUGUAUCUUUUGCUCUCUCUUGCUCUCUUAUUUGUACCGGUUUUUGUAUAUAAAAUUCAUGUUUCCAAU
CUCUCUCUCCCUGAUCGGUGACAGUCACUAGCUUAUCUUGAACAGAUAUUUAAUUUUGCUAACACUCAGCUCUGCCCUCCCCGAUCCCCUGGCU
CCCCAGCACACAUUCCUUUGAAAUAAGGUUUCAAUAUACAUCUACAUACUAUAUAUAUAUUUGGCAACUUGUAUUUGUGUGUAUAUAUAUAUAU
AUAUGUUUAUGUAUAUAUGUGAUUCUGAUAAAAUAGACAUUGCUAUUCUGUUUUUUAUAUGUAAAAACAAAACAAGAAAAAAUAGAGAAUUCUA
CAUACUAAAUCUCUCUCCUUUUUUAAUUUUAAUAUUUGUUAUCAUUUAUUUAUUGGUGCUACUGUUUAUCCGUAAUAAUUGUGGGGAAAAGAUA
UUAACAUCACGUCUUUGUCUCUAGUGCAGUUUUUCGAGAUAUUCCGUAGUACAUAUUUAUUUUUAAACAACGACAAAGAAAUACAGAUAUAUCU
UAAAAAAAAAAAAGCAUUUUGUAUUAAAGAAUUUAAUUCUGAUCUCAAA–3′

Figure 4-24: Potential MBNL2 binding sites in the 3' UTR of *VEGFA*. The potential binding sites of MBNL2 are marked in red. The cloned sequences are highlighted in blue.

The *ATP2A1* minigene system consists of a region from the *ATP2A1* gene ranging from exon 21 to 23 (**Figure 4-25**).[202] Exon 22 is alternatively spliced depending on MBNL protein level. In the absence of MBNL proteins exon 22 is not included into the mRNA. The presence of MBNL1-40 leads to approximately 50 % inclusion of exon 22. The binding site of MBNL1 is located in intron 22 and in the *ATP2A1* minigene system, it can be substituted by other potential binding sites. A stable helical region, which is located at the base of the binding site ensures independent folding of the binding site.

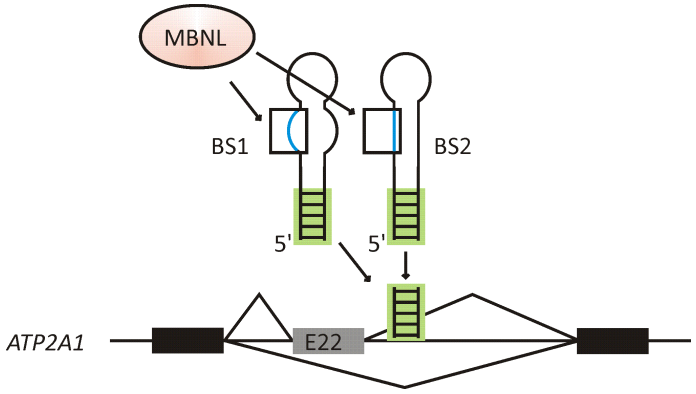

Figure 4-25: *ATP2A1* minigene system. The minigene contains *ATP2A1* exon 21 to 23. A natural MBNL2 binding site is located within intron 22. In the minigene system, this binding site can be substituted by potential binding sites (BS) from other genes. A stable helical region (highlighted in blue) connects the BS with intron 22 to allow independent folding. The exons 21 and 23 are shown in black and are constitutive. Exon 22 (E22) is shown in grey and is an alternatively spliced exon. The inclusion level of E22 is dependent on the binding efficiency of MBNL proteins to the BS.

The observed *ATP2A1* exon 22 inclusion levels in *ATP2A1* splicing assays give information about the binding efficiency of the MBNL protein to the tested binding site. In the following *ATP2A1* splicing assays the binding behavior of MBNL2 and its paralog MBNL1 to the identified binding sites in the *VEGFA* 3' UTR should be examined. Experiments were performed in mouse embryonic fibroblast (MEF) cells with a double knock-out of both, MBNL1 and MBNL2. Plasmid-based expression of one MBNL protein alone allowed independent investigation of MBNL binding behavior. We chose MBNL2 isoform 40 (MBNL-40) for these experiments since it is the most abundant isoform in MCF-7 cells. Expression of MBNL-40 led to 25% inclusion of exon 22 in the positive control with the natural MBNL binding site in the *ATP2A1* minigene (**Figure 4-26**). When the construct without binding site, which serves as a control, was transfected, approximately 12% of mRNAs included exon 22. Insertion of *VEGFA* binding site 1 and 3 into the *ATP2A1* minigene restored the inclusion level observed in the control (25%), indicating that MBNL2-40 is binding here. Insertion of *VEGFA* binding site 2 led to 18% inclusion, indicating that this binding site has a lower affinity for MBNL2 than the others. Accordingly, expression of MBNL2 isoform 38 showed similar results. Overexpression of GFP did not lead to *ATP2A1* exon 22 inclusion (**Figure 4-26 C**). Expression of MBNL1-40 led to 50% inclusion of exon 22 in the positive control and thus, to more inclusion than MBNL2. This is in line with the expectations since MBNL1 is known to be the most potent splicing regulator among the three MBNL paralogs. Exon 22 inclusion was reduced to 24% in the negative control without binding site. Insertion of the *VEGFA* binding sites 1, 2 and 3 into the minigene led to inclusion levels ranging from approximately 32% to 40%. Hence, expression of MBNL1-40 did not restore the inclusion level from the positive control as seen for MBNL2-40, leading to the assumption that MBNL2 has a higher binding affinity to the tested MBNL binding sites in the *VEGFA* 3' UTR than MBNL1.

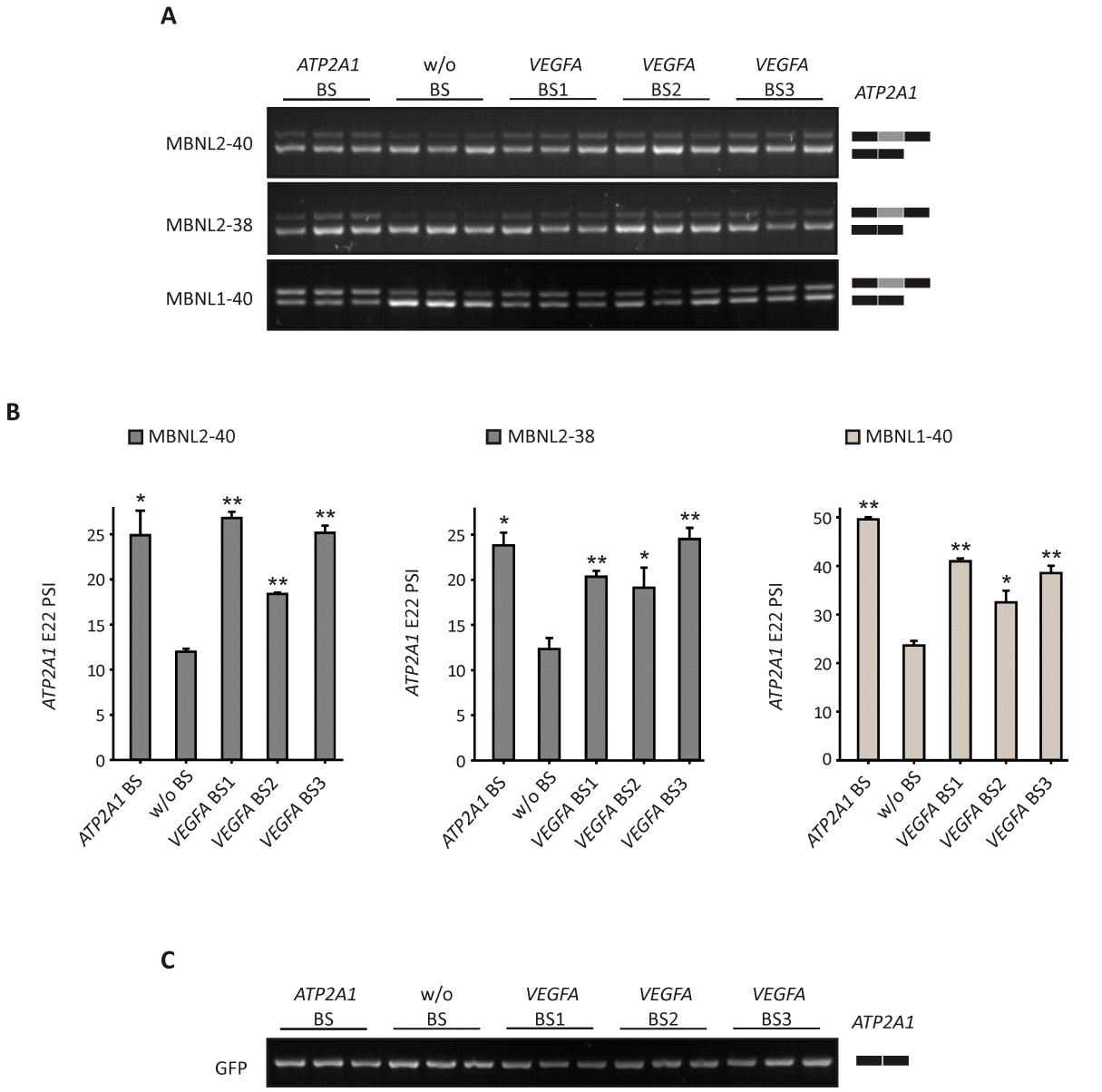

Figure 4-26: MBNL2 binds the *VEGFA* 3' UTR. (A) Splicing pattern of the *ATP2A1* minigene in MEF cells with a double knock-out of *MBNL1* and *MBNL2* after plasmid-based expression of MBNL2-40, MBNL2-38 or MBNL1-40, respectively. BS = binding site. **(B)** Quantification of RT-PCR results shown in **(A)**. Statistical significance is given in reference to the minigene without MBNL binding site (w/o BS). PSI = percent spliced-in. n=3. **(C)** Overexpression of GFP does not lead to *ATP2A1* exon 22 inclusion in the *ATP2A1* splicing assay. (**) P value < 0.01. (*) P value < 0.05.

In order to further investigate the MBNL2 binding behavior in our laboratory, I performed luciferase reporter gene assays. Cloning UTRs either 5' or 3' of the luciferase open reading frame in a luciferase reporter gene construct allows to investigate whether the cloned UTR has an influence on luciferase expression. An altered expression of the luciferase can be caused by an altered mRNA stability or by different translation efficiencies. For that purpose,

the complete 3' UTRs from *ALDOC* and *ITGA5* were cloned 3' of the luciferase in a bidirectional reporter gene construct, which also codes for the *Renilla* luciferase as an internal standard. In addition, also parts from the *VEGFA* and *LOX* 3' UTRs, which contain the predicted MBNL binding sites were cloned into the luciferase reporter gene vector. Several pre-tests in HeLa and HEK cells did not show effects after transfection of the luciferase reporter gene constructs together with MBNL2 overexpression or *MBNL2* knockdown. Here, preliminary results from MCF-7 cells are shown. The cytoplasmic MBNL2 isoform 38 and cytoplasmic GFP, as a negative control, were chosen for overexpression in these experiments.

Expression of the reporter gene constructs combined with MBNL2 overexpression did not result in any changes in luciferase expression (**Figure 4-27 A**). Accordingly, *MBNL2* knockdown had no influence on luciferase expression, when the 3' UTR reporter gene constructs were used (**Figure 4-27 B**). As maybe translation is regulated we also tested 5' UTRs. Therefore, I cloned the complete 5' UTRs of *ITGA5*, *LOX* and *VEGFA* into the luciferase reporter gene vector. Expression of the reporter gene constructs in combination with *MBNL2* knockdown did not have an influence on luciferase expression (**Figure 4-27 C**), indicating that MBNL2 is not binding to these regions under the tested conditions. A role of MBNL2 in the regulation of mRNA stability or translation efficiency cannot yet be excluded, as the experiments shown were only performed once in MCF-7 cells and the experimental setup can be further optimized (see discussion in chapter 5.2.6).

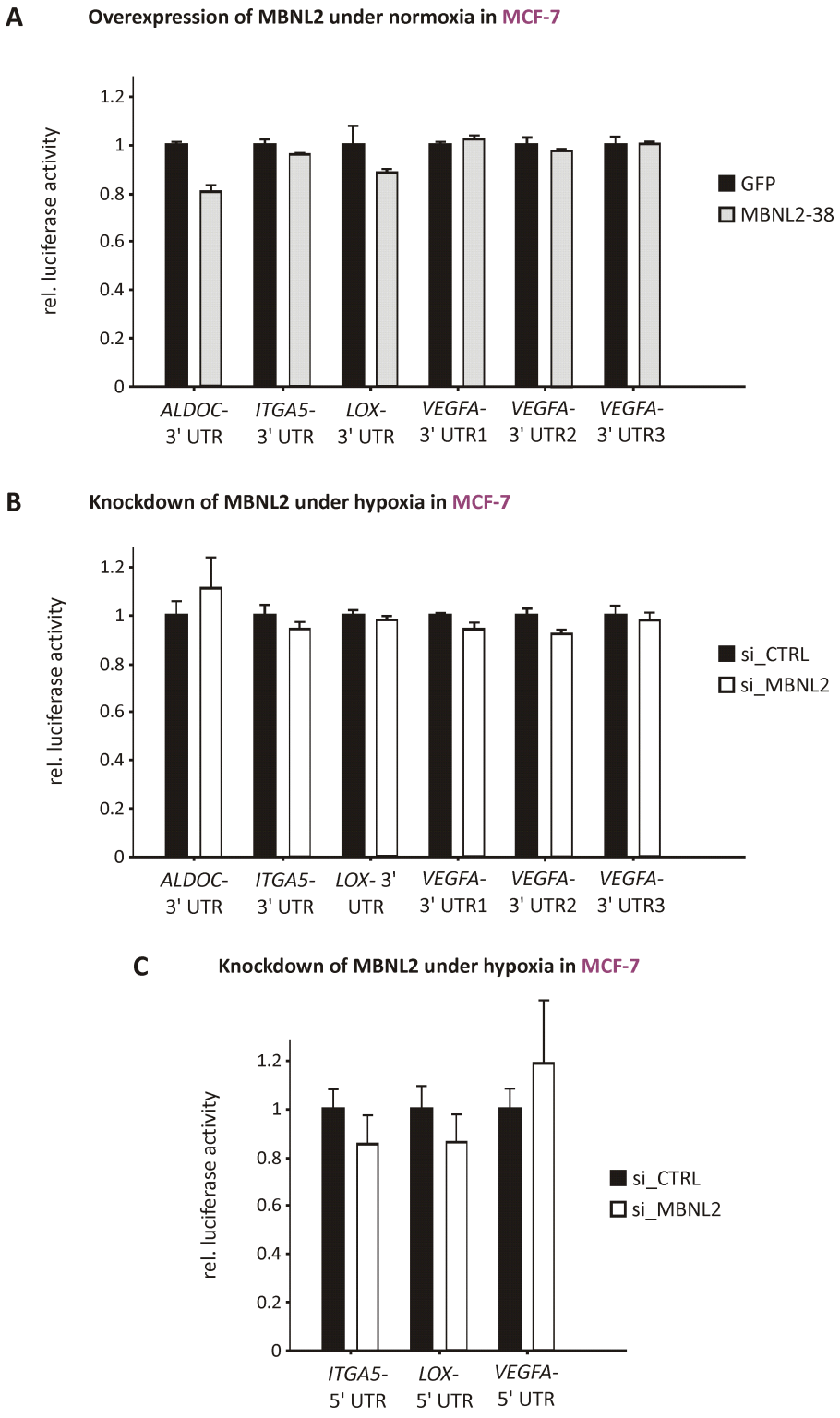

Figure 4-27: MBNL2 does not influence luciferase activity of target UTR fusion constructs. (A), (B) and (C) Luciferase activity is not changed upon overexpression of MBNL2 (**A**) or knockdown of *MBNL2* (**B** and **C**) either when MBNL2 target mRNA 3' UTRs (**A** and **B**) or 5' UTRs (**C**) were cloned 3' of the luciferase reporter gene. The shown standard deviation corresponds to the deviation between the technical duplicates. All values were normalized to luciferase expression observed in control cells, which were transfected with the empty reporter gene vector. n=1.

4.2.3.6 MBNL2 controls alternative splicing of hypoxia-responsive genes

Since MBNL2 is known as splicing regulator, we examined AS changes after *MBNL2* knockdown in our transcriptome analyses. 2,074 AS events were changed upon *MBNL2* knockdown (**Figure 4-28 A**), 393 of which also occurred after hypoxia treatment. The changed AS events after hypoxia treatment and MBNL2 depletion are preferentially changed in the opposite direction (349; 89%; **Figure 4-28 B**), indicating the importance of MBNL2 for hypoxia-induced AS. The majority of changed AS events after *MBNL2* knockdown were cassette exons, which were increasingly included when *MBNL2* was depleted, hinting at a repressive function of MBNL2. RT-PCRs were performed to verify AS changes after *MBNL2* knockdown in hypoxic MCF-7 cells. *PIGN* exon 2 inclusion was reduced under hypoxic conditions in comparison to normoxic conditions (**Figure 4-28 C**). Knockdown of *MBNL2* under hypoxia led to restoration of the splicing pattern observed under normoxia. Here, MBNL2 is sufficient to reverse the hypoxia-induced splicing change in MCF-7 cells, demonstrating the important role of MBNL2 in AS under hypoxia.

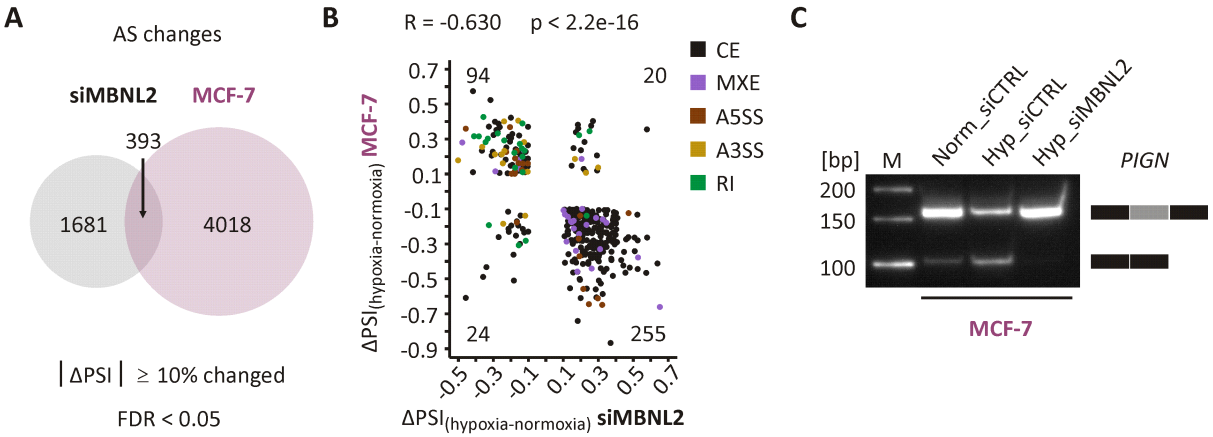

Figure 4-28: MBNL2 controls hypoxia-dependent AS. (A) Comparison of AS changes after hypoxia treatment of MCF-7 cells and AS changes after MBNL2 knockdown. 393 changed events are shared between both cohorts. **(B)** The changed AS events are preferentially regulated in the opposite direction. **(C)** *PIGN* exon 2 inclusion is reduced after hypoxia treatment in MCF-7 cells and is restored after MBNL2 depletion. The short PCR product (100 bp) corresponds to the exon skipping isoform, while the long isoform (160 bp) corresponds to the exon inclusion isoform. n=2. M = size marker.

4.2.4 MBNL2 promotes cancer cell proliferation and migration

The data point towards an important role of MBNL2 in cancer cell adaptation to hypoxia. In order to investigate the role of MBNL2 in physiological cancer cell functions, I performed cell viability as well as cancer cell migration assays. The cancer cell viability was investigated in crystal violet assays after *MBNL2* knockdown and cisplatin treatment of the hypoxic cancer cells. Cisplatin or also called *cis*-diamminedichloroplatinum(II) is commonly used in the chemotherapy of different cancer types including lung, bladder, ovarian or neck cancer.[203,204] Cisplatin reacts with purine bases in the DNA forming crosslinks, which inhibit DNA replication and repair, thus leading to apoptosis.[204] However, DNA damage caused by cisplatin is not irreversible, but can be reversed by mismatch or nucleotide excision repair.[205] In cancer therapy, cisplatin is commonly used in combination with other drugs, promoting therapeutical sensitivity of cancer cells.[205] Furthermore, cisplatin is used in research to sensitize cancer cells for other treatments. Therefore, I combined cisplatin and siMBNL2 treatment in order to investigate whether MBNL2 is implicated in cancer cell proliferation. The combined siMBNL2 and cisplatin treatment of A549 and MCF-7 cells led to a significant reduction in cancer cell proliferation under hypoxia (**Figure 4-29 A and B**), proving the influence of MBNL2 on cancer cell proliferation. Cancer cell viability assays were performed by K. Wlotzka in the context of her bachelor thesis.[206]

In addition, the influence of MBNL2 on cancer cell migration was examined in transwell assays. Knockdown of *MBNL2* dramatically reduced migration of A549 cells (**Figure 4-29 C and D**), demonstrating the importance of MBNL2 for cancer cell function.

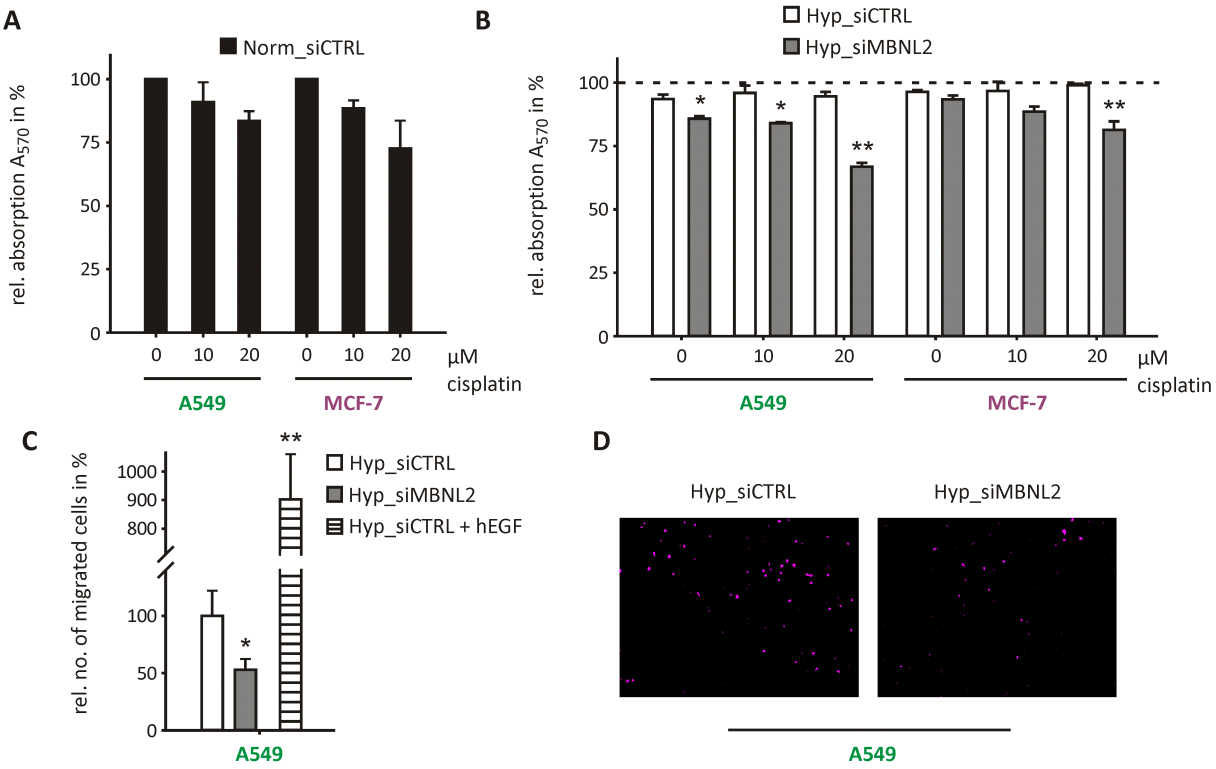

Figure 4-29: *MBNL2* promotes cancer cell proliferation and migration. (A) Cell viability of normoxic A549 and MCF-7 cells transfected with a nonsilencing control siRNA (siCTRL) is only slightly reduced by cisplatin treatment in the indicated concentrations for 24 h. **(B)** Knockdown of *MBNL2* significantly reduces cell viability after cisplatin treatment for 24 h. Absorption was normalized to normoxic control cells with the respective cisplatin concentration. n=3. **(C)** Quantification of migrated A549 cells in a transwell assay after knockdown of *MBNL2*. Cells were stimulated with 100 ng/μl hEGF. n=3. **(D)** Representative pictures of migrated A549 cells. Original images were colored in magenta to visualize crystal violet staining. (**) P value < 0.01, (*) P value < 0.05.

5 Discussion

5.1 Auto- and cross-regulation of the hnRNPs D and DL

RBPs regulate all steps of mRNA processing, including pre-mRNA splicing, localization, stability and translation. The homeostasis in RBP levels is essential for correct mRNA processing and is often achieved by autoregulation in a negative feedback loop. Autoregulation and also cross-regulation by AS-NMD is documented for PTB (hnRNP I) and nPTB (neural hnRNP I)[98] or hnRNP L and hnRNP LL.[99] Autoregulation of hnRNP DL and cross-regulation with its paralog hnRNP D were investigated in this study.

5.1.1 Autoregulation of hnRNP DL

Previous studies suggested that hnRNP DL regulates its own expression in a negative feedback loop.[147] It contains an ultraconserved poison exon in its 3' UTR. Translation inhibition using puromycin led to increased inclusion of this exon into the *hnRNP DL* mRNA. Further, *UPF1* knockdown led to accumulation of the *hnRNP DL* exon 8 inclusion isoform. Overexpression of a GFP-hnRNP DL fusion protein led to increased *hnRNP DL* exon 8 inclusion, while the exclusion isoform was downregulated, indicating hnRNP DL autoregulation. Inclusion of exon 8 into the *hnRNP DL* mRNA leads to the introduction of a PTC and subsequent degradation of the mRNA via NMD. To confirm the splicing regulation by hnRNP DL, RNA binding protein immunoprecipitations (RIPs) were performed in this study. The RIPs clearly showed binding of hnRNP DL to its own pre-mRNA (**Figure 4-1**). In future studies, the exact binding site of hnRNP DL on its own pre-mRNA could be identified.. In general, RIP experiments can give information about the binding position of RBPs. Fragments containing the binding site are usually higher enriched in RIPs because the mRNA is degraded from the sites with the highest distance to the immunoprecipitated protein. In the experimental setup in this study, two different oligonucleotide pairs (DL pre-mRNA_1 and DL pre-mRNA_2) were used to amplify the *hnRNP DL* pre-mRNA fragment from the RIP samples. The designed oligonucleotides are close to one another and do not show differences in enrichment of the pre-mRNA. Oligonucleotides, which are located further apart, for example in intron 7 instead of intron 8, might make it possible to see differences in the fragment enrichment. Further, the exact hnRNP DL binding site could be determined by PAR-CLIP (photoactivatable-ribonucleoside-enhanced crosslinking and immunoprecipitation). This method already enabled binding site

identification for several RBPs.[207] During PAR-CLIP photoactivatable nucleosides are incorporated into nascent RNA, which allows crosslinking between RBPs and bound RNAs. Thymidine to cytidine transitions occur and can be tracked in deep sequencing, indicating RBP binding locations. Further, the hnRNP DL binding site on its own mRNA could be identified in minigene splicing assays, in which the splicing behavior is assessed. Deletion of the hnRNP DL binding site in this assay would inhibit splicing regulation by hnRNP DL. In this way, the binding motif could be defined.

Moreover, there are also autoregulation mechanisms other than AS-NMD. For example, TDP-43 regulates its own expression by binding to its own 3' UTR. Binding leads to inhibition of the proximal polyA site and activation of another polyA site preventing TDP-43 expression.[208] Further, PABPN1 regulates its own expression via intron retention and subsequent nuclear pre-mRNA decay in an NMD-independent manner.[209] These mechanisms seem not to be used in the case of hnRNP DL since *hnRNP DL* exon 8 inclusion isoform is enriched after *UPF1* knockdown, clearly demonstrating the involvement of the NMD machinery in *hnRNP DL* degradation. In addition, no other *hnRNP DL* 3' UTR isoforms were detectable in HeLa cells.

5.1.2 Cross-regulation of the hnRNPs D and DL

RNAi experiments in this study showed increased hnRNP D protein and mRNA levels after *hnRNP DL* knockdown and *vice versa*. In addition, the NMD-isoforms containing *hnRNP D* exon 9 or *hnRNP DL* exon 8 were reduced after knockdown of the other paralog (**Figure 4-2**). These findings show the cross-regulation between hnRNP D and DL via AS-NMD. Interestingly, knockdown of *hnRNP D* has a bigger effect on the *hnRNP DL* protein level than the knockdown of *hnRNP DL* on the *hnRNP D* protein level. Possibly, basal levels of hnRNP D and DL influence the degree of the cross-regulation. The basal levels of hnRNP D or DL and also the basal levels of the poison exons, depend on the cell type and are further affected by stress conditions, for example by hypoxia (see **Figure 4-10**). In HeLa cells for example, the *hnRNP DL* exon 8 inclusion isoform is easily detectable via RT-qPCR, but levels of the *hnRNP D* exon 9 inclusion isoform are hardly detectable in comparison to the exon 9 exclusion isoform. Moreover, cross-regulation without changes in splicing could be observed, when hnRNP D isoform 37 was overexpressed.[97] This isoform is predominantly present in the cytoplasm, indicating that another layer of cross-regulation, independent from NMD, could be

exerted here. Cytoplasmic hnRNP D and DL protein isoforms might bind to AREs in the 3' UTR of the other paralog leading to ARE-dependent decay.[210,211] HnRNP D isoform expression and their distribution within the cell are tissue-specific[212] and can change under stress conditions[213] or can be deregulated in cancer.[214] Thus, hnRNP D and DL isoforms and their localization within the cell could also play a role in the cross-regulation. To further underline the cross-regulation, enrichment of *hnRNP D* pre-mRNA in hnRNP DL RIP samples could be investigated and would prove direct binding. In RIP experiments, it could also be investigated, which *hnRNP D* isoforms are bound by hnRNP DL.

In an RNA sequencing after hnRNP DL knockdown in HUVECs in our laboratory, novel hnRNP DL target genes were identified. These were mainly implicated in cell proliferation, cytoskeleton remodeling and angiogenesis.[187] Comparison of the identified target mRNAs with known hnRNP D targets showed an overlap. For example, *CCND8*, *CDCA8* and *FOS* are known to be destabilized by hnRNP D.[215] Interestingly, these mRNAs are stabilized by hnRNP DL since their mRNA levels are reduced after *hnRNP DL* knockdown.[187] These findings indicate that hnRNP D and DL are not fully redundant, but in part antagonistic. Thus, although hnRNP D and DL seem to complement each other in their splicing function, they might oppose each other in mRNA destabilization. Details of the functional overlap or antagonism remain to be elucidated in further studies. A knockdown of *hnRNP D* was established in this thesis and will help to perform RNAi experiments in HUVECs and HeLa cells to assess their antagonistic function in target mRNA regulation. Hypothetically, target mRNAs like *CCND8* should be decreased after *hnRNP DL* knockdown, but increased after *hnRNP D* knockdown since hnRNP D is expected to destabilize its target mRNAs and our RNA sequencing data point towards a stabilizing function of hnRNP DL in some cases. Further, it could be assessed whether hnRNP D and DL have the same binding site and displace each other when one paralog is predominantly present or if they bind adjacently and define mRNA fate through another mechanism.

5.1.3 Role of hnRNP DL in endothelial cell function

An RNA sequencing after hnRNP DL depletion in HUVECs[187] led to the identification of hnRNP DL target genes, implicated in cell proliferation, cytoskeleton remodeling and angiogenesis. To investigate the role of hnRNP DL in these endothelial cell functions, I have established a transwell HUVEC migration assay as well as a HUVEC spheroid sprouting assay.

Performing these assays, I demonstrated the importance of hnRNP DL in endothelial cell migration and angiogenesis for the first time. Strikingly, depletion of hnRNP DL led to a dramatic decrease of HUVEC migration and HUVEC spheroid sprouting (**Figure 4-3** and **Figure 4-4**).

Previously, the physiological role of hnRNP DL in cancer cell functions was investigated. It could be shown that hnRNP DL is promoting cancer cell proliferation in chronic myeloid leukemia cells.[153,154] HnRNP DL is also regulating cell proliferation in HUVECs, as could be shown in previous studies in our laboratory.[147] Strikingly, a role of hnRNP DL in cell migration or angiogenesis has not been supposed so far, indicating the novelty of my findings.

There are few hnRNPs, which have been shown to be involved in migration and angiogenesis so far. HnRNP K has been identified to promote cell movement and angiogenesis by inducing genes involved in these mechanisms in fibrosarcoma cells, for example the matrix metallopeptidases *Mmp3* and *Mmp10* or *Ctgf* (connective tissue growth factor, thymosin).[216] Further, hnRNP A2 promotes cancer cell migration via AS.[217] PTB (hnRNP I) is implicated in cell migration and attachment in mouse embryonic fibroblasts.[218] A potential role of the hnRNP DL paralog hnRNP D in migration has been proposed in osteosarcoma cells. Here, miR-141 and miR-146b-5p lead to destabilization of *hnRNP D* and subsequently to reduced U2OS cell migration and invasion.[219] Since hnRNP functions are highly cell type-dependent, the role of hnRNP D in HUVEC migration remains to be elucidated. However, if hnRNP D is promoting cell migration, as also shown for hnRNP DL in this study, both paralogs will probably enhance the level of transcripts involved in cell migration. Then, hnRNP D and DL would be redundant, here.

In contrast, a role of the hnRNP DL paralog hnRNP D in angiogenesis has not yet been reported. Nevertheless, hnRNP D is important for inflammatory responses, which could also have an impact on angiogenesis.[220] Interestingly, hnRNP D represses *VEGFA* expression in macrophages,[221] pointing towards an anti-angiogenic function of hnRNP D, since VEGFA is a positive regulator of angiogenesis. These findings might reinforce the hypothesis of hnRNP D and DL being antagonists.

In this study, it was shown that the pro-angiogenic factor *VCAM1* is an hnRNP DL target since its expression is dramatically reduced, when *hnRNP DL* is depleted (**Figure 4-5**). *VCAM1* was also identified as hnRNP D target in bovine aortic endothelial cells.[222] There, overexpression of hnRNP D led to increased *VCAM1* levels. This is interesting since hnRNP D is mainly

repressing its targets by reducing their mRNA stability.[134] However, if hnRNP D and DL share *VCAM1* as a target mRNA, they might act synergistically in the regulation of angiogenesis.

All together, it is not clear by now, whether hnRNP D and DL share their targets and thus, their functions. In addition, the role of hnRNP D in endothelial cell migration and angiogenesis has not yet been demonstrated. In future experiments, the role of hnRNP D in endothelial cell function could be assessed to gain more insight into the interplay between the two paralogs hnRNP D and DL.

5.2 Hypoxia-driven gene expression changes in human cancer cells

Hypoxia is a typical feature of solid tumors. In afflicted cells, hypoxia triggers specific gene expression programs, which sustain cell survival by inducing cell migration, tumor angiogenesis and escaping apoptosis. The transcriptional response to hypoxia by HIFs is well studied. Recent advances focus on posttranscriptional gene expression changes under hypoxia. However, there is still a profound knowledge gap when it comes to AS under hypoxia. Thus, this study focused on changes in splicing factor expression as well as in AS in human hypoxic cancer cells.

5.2.1 RNA sequencing preparation

Before performing RNA sequencing after hypoxia treatment, preliminary decisions concerning the used cancer cell types, cell culture as well as hypoxia and sequencing conditions had to be made. In the following chapters (5.2.1.1 - 5.2.1.4), these decisions on the used conditions are explained and discussed.

5.2.1.1 Cancer cell types

A549 lung and MCF-7 breast cancer cell lines were chosen for this study (see chapter 4.2). These cell lines were chosen, since they do not exhibit mutations or deletions in the HIF pathway and in the major splicing factor families, which are hnRNPs and SR proteins, according to the database www.cBioPortal.org.[223,224] This was a prerequisite for this study, since I wanted to investigate hypoxia-driven changes in the RBPome and in AS within the context of a physiological transcriptional response to hypoxia as well as splicing programms.

This prerequisite should exclude secondary hypoxia-induced effects exerted by deregulated splicing factors or by an abberant HIF signaling. The SR protein SRSF1 (also known as SF2/ASF) is overexpressed in many cancer types and its deregulation has an influence on the AS program.[225] Mutations in the HIF pathway are known for clear cell renal cell carcinomas (ccRCC).[226,227] Analysis of hypoxia-driven changes in the RBPome and in AS require a correct transcriptional response to hypoxia. Thus, cell lines with HIF mutations including ccRCC were excluded from this study. Moreover, breast cancer causes the most cancer-related deaths in women. In addition, lung cancer causes the second most cancer-associated deaths in women and most in men.[191,192] So these are the most severe types of cancer. Among other factors, this is due to hypoxic regions in the tumor, which are hardly accessible to drugs and also resistant to radiotherapy.[228] A broader insight into hypoxia-driven gene expression and AS changes might thus start new approaches in breast and lung cancer research.

In this study, a hypoxia test system for A549 and MCF-7 cells was developed. It is possible and desirable that also other cancer cell types will be implemented in the test system in future studies. Results from these studies could be compared to results from this study. Comparison might give insight into universal gene expression programs, which are initiated in a gros of different cancer cell types. For example, the universal role of MBNL2 in cancer cell adaptation to hypoxia, which I suggest in this study, could be confirmed in cell types, other than A549 and MCF-7. Further, this study showed highly cell type-specific AS programs under hypoxia. The investigation of more cancer cell lines in our test system might lead to identification of cancer types with big overlaps between their hypoxia-driven AS changes. In addition, other lung and breast cancer cell lines could be examined to assess differences in the adaptation to hypoxia between different subclasses of one cancer cell type.

5.2.1.2 Cell culture conditions

For the RNA sequencing, I chose to take samples from 2D cancer cell cultures. 2D cell culture is commonly used in basic research to gain first insight into new mechanisms.[229] In the field of cancer research, recent publications described the use of 2D cancer cell culture, for example of ccRCC [181], different breast cancer cell lines [179,182] or different prostate cancer cell lines.[178] 2D cell culture bares the advantage of high conformity. Hypoxic conditions for example are the same for cells within one sample. This is advantageous for transcriptome analyses since expected variations between individual cells are smaller. Recently, 3D tumor models have

become common as well but usually they exhibit heterogenic areas with varying oxygen or nutrient concentrations or unstable pH conditions, which complicates transcriptome analyses of a 3D cell population. These circumstances might produce hypoxia-independent effects on gene expression. Therefore 3D culture was not chosen as experimental condition in this study. However, new mechanisms or specific targets, identified in 2D cultures, should later be analyzed more in detail in more complex systems like 3D cultures. Hypoxia treatment is sometimes not needed in 3D tumor models since tumor spheroids exhibit hypoxic regions, but only if they exceed a diameter of at least 200 μm.[230] Then, the composition of the spheroids comes close to the actual tumor composition.[231] The characteristics of 3D cultures are especially useful for drug testing since three-dimensional tissues behave way different than two-dimensional cell layers.[232,233] Many scientists take advantage of both approaches, 2D and 3D culture, to examine tumor growth and invasion as was done in hepatocellular carcinoma cells.[180] Another approach to increase physiology of cancer cell cultures includes co-culture of fibroblasts or other cells, which normally surround and intersperse tumor tissue.[234] Comparison of microarray data from hypoxic human bladder cancer cells in 2D cell culture with data from patient samples revealed a concordance between *in vitro* and *in vivo* transcriptomes, showing that 2D cell culture delivers valuable insight into transcriptome changes.[235] However, there were also unique expression patterns in some patients. The tumor spheroid forming capacity of A549 and MCF-7 cells was tested during this study. Both cell lines are suited for 3D culture and have already been used for the formation of tumor spheroids in other studies.[229] In this thesis, the approach was not pursued further since the delivery of RNAi constructs to 3D cultures is challenging. A better approach to perform loss-of-function studies in 3D cell culture involves the generation of stable knock-out cell lines.

The flexibility of 2D cancer cell cultures was used in this study to conduct a transcriptome analysis after chronic hypoxia treatment of lung and breast cancer cells. The aim was to achieve a comparable dataset of hypoxia-driven changes in RBP expression and in AS. As a next step, 3D cell culture techniques can be established with the used cell types for the investigation of tumor growth or invasion.

5.2.1.3 Hypoxia conditions

As a pre-test, in this study, *VEGFA* and *hnRNP M* mRNA levels after hypoxia treatment were observed (**Figure 4-6**). Both mRNAs should change their abundance under hypoxia. The

reduction of *hnRNP M* mRNA level was observed in previous studies and here, a hypoxia-driven change in *hnRNP M* mRNA abundance should assure that changes on the splicing factor level can be detected in our test system. Chronic hypoxia was chosen as condition for experiments in this study (see chapter 4.2.1), since *hnRNP M* mRNA was affected by hypoxia in A549 cells only after 48 h. Chronic hypoxia, especially diffusional hypoxia, is typical for cancer cells, which are located far away from the vascular system within a tumor.[236] Most tumor cells underlie varying oxygen concentrations due to rapidly proliferating cancer cells and tumor angiogenesis.[63] Thus, acute hypoxia affects many cells in the dynamic cancer tissue as well.[237] Acute hypoxia is associated with aggressive tumor phenotypes since it induces tumor growth and metastasis.[237,238] HIF-1α is predominantly present during acute hypoxia. Chronic hypoxia leads to restoration of normoxic HIF-1α levels, while HIF-2α is induced.[239] In future experiments, it could be tested, whether acute hypoxia causes the same or different changes in the RBPome and in AS than chronic hypoxia.

Further, a hypoxia incubator was used in this study. The cells must be removed from the hypoxia incubator for sample preparation. It takes a few minutes until the samples are prepared. During this time the samples are exposed to normoxia. Some proteins are rapidly degraded under hypoxia. The HIF-1α protein for example has a half-life of approximately 5 min under normoxia.[240] Thus, using a hypoxia working bench would be advantages to detect rapidly degraded proteins and might be a profitable investment for the future since the working bench also allows for sample stimulation etc. under hypoxic conditions.

5.2.1.4 RNA sequencing conditions

In general, two main RNA sequencing conditions can be distinguished: Ribosomal RNA depletion (Ribo-Zero) and poly(A)-selected RNA-sequencing.[241] The methods differ in the RNA processing before cDNA library preparation. Both methods aim for the reduction of rRNAs in the samples.[242] RRNAs are the most abundant transcripts in total RNA preparations and might complicate the investigation of mRNAs since most of the sample reads would be rRNAs.[243] During Ribo-Zero ribosomal RNA depletion rRNAs are removed by hybridization capture followed by binding to magnetic beads.[242] During poly(A) selection oligo (dT) primers are used to enrich for polyadenylated [poly(A)] RNA transcripts. This leads to elimination of all non-polyadenylated transcripts, which are partly biological relevant, like circRNAs.

Further, poly(A) enrichment is not suitable for samples containing partially degraded mRNAs, for example formalin-fixed and paraffin-embedded samples from tissues.[242]

For our initial RNA sequencing after hypoxia treatment of A549 and MCF-7 cells, we chose Ribo-Zero as method for rRNA depletion, because we wanted to examine non-coding RNAs, like circRNAs, which would have been removed during poly(A) enrichment. Mature miRNAs are too short to be detected in this experimental setup. It is possible to add linker sequences to miRNAs before sequencing to increase their length. Hypoxia-relevant miRNAs have already been subject of several studies, so they were not the focus of this thesis.

After the identification of MBNL2 as a major regulator of transcript abundance and AS under hypoxia, our focus shifted towards mRNAs. This is why we chose poly(A) enrichment as method for rRNA depletion in our second RNA sequencing after *MBNL2* knockdown in MCF-7 cells.

In both RNA sequencing experiments, we chose to use single-end reads instead of paired-end reads. Using single-end reads, fragments are sequenced from one site. Using paired-end reads one fragment is sequenced from both sites.[244] Usually, paired-end reads are used to identify novel transcripts or to study poorly annotated transcriptomes.[195] Single-end reads are cheaper and the method of choice for well-annotated transcriptomes.[195]

The statistical power of such whole transcriptome approaches depends on the experimental design. Several factors like number of replicates, sequencing depth and effect size influence the statistical power.[195] Two replicates were deep sequenced in this study. The use of only two replicates carries the risk that strong differences between the replicates can be detected and should only be chosen if the effects are easily reproducible. Approximately, 100 million and 80 million reads (initial and second RNA sequencing) were achieved as sequencing depth in this study to allow for the detection of transcripts with low expression level. Further, this study focused on effects greater than 1.5-fold to guarantee statistical power and physiological relevance. Moreover, RNA quality is essential for transcriptome analyses and has been checked in this study. Hypoxia-induced effects on transcript abundance, observed in the transcriptome analyses in this study, could easily be validated as shown for several mRNAs in the results chapter (for example **Figure 4-8** and **Figure 4-16**). However, that was different with the AS changes. Approximately only half of the predicted hypoxia-dependent AS changes could be reproduced in RT-PCRs. Either the level of one of the expected isoforms was too low

or the isoforms were amplified correctly, but there was no difference between the normoxia and hypoxia samples.

As a conclusion from this study, I suggest the chosen sequencing conditions are suitable for the investigation of transcript abundance. Since it was not easy to validate all identified hypoxia-driven AS changes, I would recommend to sequence three replicates in order to assess AS changes. In addition, increasing the sequencing depth, using poly(A) enrichment or paired-end reads could also improve the reproducibility of identified AS changes.

5.2.2 RNA sequencing after hypoxia treatment

The following chapter discusses the results from the RNA sequencing after hypoxia treatment of A549 and MCF-7 cells. The sequencing was conducted using two biological replicates for each condition. RRNA was depleted and approximately 100 million reads were achieved per sample. In this chapter, I will discuss gained insights into differentially expressed transcripts, including non-coding RNAs and hypoxia-driven AS.

5.2.2.1 Differential gene expression under hypoxia

Regarding transcript abundance under hypoxia, A549 and MCF-7 cells react very similarly (see chapter 4.2.2.1). Since HIF response genes should be regulated in A549 and MCF-7 cells under hypoxia, a large overlap was to be expected. RNA sequencing approaches have made it easy to compare whole cancer transcriptomes.[245] The revolution in next generation sequencing techniques opens up new opportunities for the identification of new biomarkers and therapeutic targets.[246] It has also become easier to compare whole transcriptomes with each other. The Oncomine database[247] compares cancer expression profiles and has revealed general hypotheses regarding cancer gene expression comparability: 1) Based on global gene expression pattern cancer cells can be distinguished from normal cells of the same type. 2) Cancer subtypes show distinct gene expression patterns. 3) Gene expression profiles from primary tumors give information about metastasis, survival and treatment response.[248] General differences between A549 and MCF-7 gene expression patterns under normoxia, which are expected according to the second hypothesis, were confirmed in our transcriptome analyses. 15,684 transcripts were shared by both cell types (see chapter 4.2.2.1). Under hypoxia, 1,224 of the shared transcripts were differentially expressed (fold change>1.5 and

padj<0.05), but in addition 1,266 and 3,279 transcripts were differentially expressed only in A549 or MCF-7 cells, respectively. These numbers are higher than the amount of shared differentially expressed transcripts, especially in MCF-7 cells, indicating that investigating the independent response to hypoxia of A549 and MCF-7 cells might yield further RBPs, which might be important in the adaptation to hypoxia. However, stating that the hypoxia response of A549 and MCF-7 is similar, is correct since 91% of the shared differentially expressed transcripts are regulated in the same direction.

In a transcriptome analyses after acute (4 h) and chronic (24 h) hypoxia treatment of MCF-7 cells with 1% O_2, Han *et al.* identified 903 differentially expressed genes under acute hypoxia and 1,420 differentially expressed genes under chronic hypoxia in MCF-7 cells.[249] 397 of them were shared between the two conditions and were mainly regulated in the same direction (378, 95%). Since transcript levels were considered as changed when they were changed at least 1.5-fold, the study by Han *et al*. is in part comparable to our study. However, when comparing with the data by Han *et al*., it is important to keep in mind that only one replicate was sequenced in their study. Interestingly, we found 4,503 differentially expressed transcripts in MCF-7 cells after 48 h of hypoxia treatment, which is a significantly higher amount. This might be due to the lower oxygen level in this study (0.5% compared to 1% O_2 in the study by Han *et al*.) and to the longer incubation time (48 instead of 4 or 24 h). Further, also other factors influence the gene expression such as cell culture confluency, media, pH and others. Thus, transcriptome analyses, which were conducted under different conditions will always be hard to compare.

This study focuses on RBPs as major mediators of posttranscriptional regulation. Under hypoxia, RBPs were mainly downregulated. RNA sequencing revealed changed RBP mRNA levels (**Table 4-1**). In addition, extensive Western blot analyses have shown reduced RBP protein levels for many hnRNPs (**Figure 4-10**). Previously, changed SR protein levels under hypoxia have been shown.[250] Interestingly, hypoxia influences not only the levels of SR proteins, but also increases their phosphorylation, changing their pre-mRNA splicing activities.[251,252] Thus, hypoxia has a major impact on the two splicing factor families and subsequently on AS. It is known that processes like DNA replication, transcription or translation are downregulated under stress conditions, for example under hypoxia, oxidative stress, UV-light or under the influence of stressing substances like heavy metals.[253] This could also be seen in our RNA sequencing (**Supplementary Figure 11-1**). Studies have shown that stress stimuli, for example heat shock, inhibit pre-mRNA splicing and affect the expression of

RBPs.[253] The extent of the shut down of splicing depends on the severity of the stress conditions. In this study, I confirmed that chronic hypoxia treatment (48 h, 0.5% O_2) does not impair cell viability (**Figure 4-7**), but still hypoxia is a strong stress factor. That can be seen from the fact that ribosome biogenesis and DNA replication as well as repair are reduced under hypoxia. Further, Han *et al.* did not state generell reduction of RBPs under hypoxia.[249] They mentioned differential expression of *RBM43*, *RBM24*, *RBPMS2* and *FUS* under hypoxia. RBM42 was induced, while the other three mentioned RBPs were downregulated on the mRNA level upon hypoxia. Western blot analyses revealed only reduction of RBM24 and RBPBS2. RBM43 protein level was unchanged and FUS protein was induced under hypoxia instead of reduced. Here, the authors suggested a role of translation regulation. In addition, Han *et al.* found decreased *MBNL3* mRNA level under hypoxia, but they could not detect MBNL3 protein.

This study focused on shared differentially expressed RBPs under hypoxia and identified MBNL2, PTRF and SAMD4A as the only three RBPs, induced under hypoxia (**Figure 4-11**). PTRF is a component of caveolae structures on plasma membranes and is involved in the release of rRNAs and RNA polymerase I. PTRF was found to suppress the tumorigenesis of colorectal cancers by reducing the phosphorylation of AKT, mTOR and MMP-9.[254] Interestingly, hypoxia inhibits PTRF expression in adipocytes, which is in contrast to our findings.[255] SAMD4A regulates translation and mRNA decay of its target mRNAs by binding to smaug recognition elements.[256] SAMD4A has not yet been connected to hypoxia, but its induction was observed in Topotecan-resistant ovarian cancer cells.[257] Topotecan is a cancer therapeutic, which blocks HIF-1α and VEGF expression.[258] Among the three induced RBPs under hypoxia, MBNL2 stood out since it is the only typical splicing regulator. In addition, MBNL2 was of interest for us since it is also disease-associated. MBNL2 is deregulated during DM and has recently been found to be also involved in tumor progression (see chapter 5.2.8). This is why I focused on MBNL2 in further experiments.

5.2.2.2 Hypoxia-driven AS changes

Hypoxia-driven AS changes in A549 and MCF-7 cells differed strongly (see chapter 4.2.2.2), highlighting the cell type specificity of AS programs. Previous studies concerning hypoxia-driven AS were conducted in endothelial cells[184], mesenchymal stem cells[185] and hepatocellular carcinoma cells[186]. The small overlaps of previous studies pointed towards clear

differences in AS between different cell types. Recently, an AS analysis under hypoxia in MCF-7 breast cancer cells has been published.[249] Here, MCF-7 cells were incubated under acute hypoxia for 4 h or under chronic hypoxia for 24 h with 1% O_2. Han *et al.* chose to conduct RNA sequencing with just one replicate, baring the risk that identified AS changes are hard to reproduce. During acute and chronic hypoxia Han *et al.* discovered 2,005 and 1,685 changed AS events. In A549 and MCF-7 cells after 48 h of chronic hypoxia treatment 2,225 and 4,206 AS events were changed. The changed AS events in our study might be higher since we considered AS events as changed if the change in PSI was 10% or higher and Han *et al.* considered AS events as changed if the change in PSI was 15% or higher. Interestingly, in the study by Han *et al.*, intron retention was the most abundant AS change (62%) in both, acute and chronic hypoxia, which is in contrast to our RNA sequencing data, which showed that exon skipping is the most abundant AS change (54 and 56% in A549 and MCF-7). Possibly, the downregulation of the splicing machinery under hypoxia leads to inhibited splicing and thus, to the observed intron retention after acute (4 h) and short-time chronic (24 h) hypoxia, which has also been observed under other stress conditions such as heat shock.[259] In later chronic hypoxia phases (48 h), as examined in our study, the splicing inhibition might shift towards a cell type-specific AS program and cells adapt to hypoxia, sustaining cell survival. This cellular adaptation phase is also typical for heat shock.[260] In line with our findings, Han *et al.* demonstrated that exon skipping dominates over exon inclusion under hypoxia in MCF-7 cells. Further, Han *et al.* identified differences in the direction of changed AS events between acute and chronic hypoxia, indicating that differences between 24 h and 48 h of hypoxia treatment might be plausible. Additionally, Han *et al.* found differences in AS between MCF-7 and other cancer cell lines, confirming our finding that AS programs are highly cell type-specific.

Sena *et al*. performed an exon aray in hepatocellular carcinoma cells after hypoxia treatment (1.5% O_2, 12 to 16 h).[186] They found that exon skipping is the most commonly changed AS event under hypoxia with 51%, while only 11% of the changed AS events are retained introns, which is in line with our findings.

In this study, I chose *CENPE*, *PTBP2* and *PUSL1* for the validation of hypoxia-driven AS events. All three AS events showed regulation in the same direction in both cell types. In addition, expected differences in exon inclusion (PSI) were above 10%, so that they should be detectable in the gel analyses after RT-PCR. In general, these criteria also met other AS events, which I could not validate via RT-PCR. AS events are very sensitive and thus, harder to

reproduce than changes in transcript abundance. The three validated hypoxia-driven AS events are cancer related. Centromere-associated protein E (CENP-E) is implicated in chromosome alignment and has been identified as potential target for cancer therapy.[261] PTBP2 (polypyrimidinetract-binding protein 2) is an RNA-binding protein itself and a potential oncogene with a positive effect on cancer cell growth.[262] *PUSL1* (tRNA pseudouridine synthase-like 1) expression varies in different stages of liver cancer, indicating that it could play a role in cancer progression, there.[263]

Changed AS events are a potential biomarker and interesting for future therapies. The next step in the investigation of hypoxia-driven AS changes in human cancer cells, would be to identify cancer-driving AS events. Here, AS events in known tumor suppressors and oncogenes might be considered. Further, AS events under hypoxia in cancer cells can be compared with AS changes under hypoxia in non-cancerous cells. For example, hypoxia-driven AS changes in cancer cells could be compared to hypoxia-driven AS changes in endothelial cells, which were identified by Weigand *et al*..[184] Overlapping AS events might be excluded from further analyses since they might be hypoxia-related, but not cancer specific. The identified cancer-related changed AS events under hypoxia in cancer cells might be potential new targets for cancer therapy. AS events are already exploited in therapies, for example for the therapy of Duchenne muscular dystrophy or spinal muscular dystrophy, where antisense oligonucleotides are used to eliminate specific transcripts.[117,118]

Known cancer-related AS events that could be exploited in therapies occur for example in the receptor tyrosine kinase RON. Here, skipping of exon 11 leads to formation of a constitutively active isoform of RON.[264] This isoform is enriched in breast and colon cancer. SF2/ASF is implicated in the formation of the constitutively active isoform and is thus promoting cancer cell migration.[264] Further, *VEGFA* splicing is changed under hypoxia, from anti-angiogenic to pro-angiogenic isoforms.[110,111] The cassette exons 6 and 8 from the CD44 transmembrane glycoprotein are also alternatively spliced under hypoxia, promoting tumor progression and metastasis in breast cancer cells.[265]

5.2.2.3 Non-coding RNAs

In our RNA sequencing after hypoxia treatment poly(A) enrichment was not performed before cDNA library generation to have the possibility to also examine non-coding RNAs.

6,784 non-coding RNAs were expressed in A549 cells (37% of all transcripts) and 7,635 in MCF-7 cells (40% of all transcripts). Among them were 231 (3%) and 539 (7%) transcripts in A549 and MCF-7 cells, respectively, which were differentially regulated under hypoxia (fold change>1.5 and padj<0.05). From all detected non-coding RNAs, 5,720 were shared between both cell lines. 71 from the shared transcripts were differentially regulated (fold change>1.5 and padj<0.05) under hypoxia, mainly in the same direction (64, 90%). All together, non-coding RNAs are regulated to an equal extent in both cell lines. In addition, A549 cells show less detected transcripts as well as less hypoxia-regulated non-coding RNAs, which is in line with results from the whole transcriptome analyses, including protein-coding RNAs (see 5.2.2.1).

Interestingly, the antisense long non-coding RNAs PCAT6 and RP11-274H2.3 (also called lncRNA SRLR, sorafenib resistance-associated lncRNA in renal cell carcinoma) were induced under hypoxia in both cell types and are known to be associated with cancer. PCAT6 has been identified as oncogene and as promoter of cancer cell proliferation and invasion in lung cancer cells.[266,267] LncRNA SRLR has been identified as biomarker for sorafenib resistance in renal cell carcinoma patients.[268]

The examination of circRNAs was done in collaboration with A. Di Liddo, K. Zarnack, C. de Oliveira Freitas Machado and M. Müller-McNicoll. Results are described in Di Liddo *et al.*, 2019[269] and also considered sequencing data from hypoxic HeLa cells. In brief, approximately 12,000 circRNAs were detected in the three cancer types. In addition, 64 circRNAs change their abundance upon hypoxia in a cell-specific manner. The data point towards a role of *trans*-acting factors in circRNA biogenesis. In A549 cells 4,618 circRNAs were detected, from which only one (circASXL1) is slightly induced under hypoxia. In MCF-7 cells 7,561 circRNAs were detected and 26 of them change their abundance under hypoxia. The circRNAs PLOD2 and ZNF292 showed very high induction under hypoxia. It is important to mention that the *PLOD2* and *ZNF292* host genes were induced under hypoxia as well, pointing towards a transcription-related increase in circ RNA abundance, not a switch in AS. Notably, *PLOD2* and *ZNF292* are cancer-related and their corresponding circRNAs might also play a role, here. PLOD2 is promoting proliferation, migration and invasion in glioma cells.[270] ZNF292 is a candidate tumor suppressor and mutations in its gene might promote cancerogenesis.[271] Hypoxia-driven induction of circZNF292 was found in endothelial cells and silencing of circZNF292 led to decreased endothelial cell spheroid sprouting indicating a proangiogenic role of circZNF292.[41]

5.2.3 RNA sequencing after *MBNL2* knockdown

Our RNA sequencing after hypoxia treatment of A549 and MCF-7 cells showed specific induction of MBNL2 under hypoxia, while RBPs were mainly reduced. Induction of MBNL2 was also found in ccRCC patient samples.[181] The HIF pathway is constitutively active in ccRCCs and might cause the induction of MBNL2. Interestingly, *MBNL2* has been suggested as HIF-1α target gene in a ChIP-seq (chromatin immunoprecipitaton DNA sequencing) experiment in HUVECs.[272] Thus, *MBNL2* expression could be initially activated by HIF-1α and *MBNL2* mRNA is stabilized under hypoxia prolonging the HIF response, when HIF-1α is degraded. *MBNL2* could also be a HIF-2α target as HIF-1α and HIF-2α address similar genes. Further, Perron *et al.* identified and suggested several MBNL2 targets. They compared genes upregulated in ccRCC tumor samples with downregulated genes after *MBNL2* knockdown and found that 5 of the 31 shared genes between the two cohorts belong to the HIF-1α network. These were *CXCR4*, *EGLN3*, *HK2*, *NDRG1* and *VEGFA* with *VEGFA* showing the highest correlation. The authors further showed binding of MBNL2 to the *VEGFA* mRNA through pull-down studies.[181] RT-qPCR analyses of the *CXCR4*, *EGLN3*, *HK2*, *NDRG1* and *VEGFA* mRNA levels after *MBNL2* knockdown in our laboratory could not confirm any of the mentioned targets in A549 and MCF-7 cells except for *VEGFA*, which clarified that an RNA sequencing in A549 and MCF-7 cells after *MBNL2* knockdown is indispensible to identify MBNL2 targets in these cell types. Since A549 and MCF-7 cells responded similarly to hypoxia and MBNL2 was induced in both cell types, we decided to perform RNA sequencing in just one of the cancer types and to confirm MBNL2 targets in the other cancer type later via RT-qPCR. I chose MCF-7 cells for the RNA sequencing after *MBNL2* knockdown because in MCF-7, more transcripts were significantly differentially regulated under hypoxia than in A549 (4,503 vs. 2,490), suggesting that a knockdown of *MBNL2* will have stronger effects, here.

5.2.4 Differential gene expression after *MBNL2* knockdown

Knockdown of *MBNL2* under hypoxia (0.5% O_2 for 48 h) in MCF-7 cells led to differential expression of 4,370 genes (fold change>1.5 and padj<0.05; **Figure 4-16**). From these, a large fraction of 1,528 genes was also differentially regulated under hypoxia in MCF-7 cells. 1,091 of these shared genes were regulated in the opposite direction. 600 from these 1,091 genes were induced upon hypoxia and were reduced after *MBNL2* knockdown. 351 shared genes were differentially expressed after *MBNL2* knockdown and after hypoxia treatment in

both, A549 and MCF-7 cells. 227 of these shared genes were regulated in the opposite direction. 173 of them were induced upon hypoxia and were reduced after *MBNL2* knockdown. In both ways of comparison, the largest cohort consists of genes, which are induced upon hypoxia and are reduced after *MBNL2* knockdown. In addition, the GO analyses identified significantly downregulated GO terms after *MBNL2* knockdown, but no significantly induced GO terms (**Supplementary Figure 11-2**), highlighting the activating function of MBNL2 under hypoxia. Together, these data indicate an important role of MBNL2 in the positive regulation of transcript abundance under hypoxia in cancer cells. However, MBNL2 might also fulfill other functions under hypoxia, for example destabilizing certain mRNAs.

From the cohort of differentially expressed genes after *MBNL2* knockdown and after hypoxia treatment in both, A549 and MCF-7 cells, we identified novel MBNL2 target genes, which I could validate in RT-qPCR analyses (**Figure 4-17**). Aldolase C (ALDOC) and enolase 2 (ENO2) are glycolytic enzymes. Integrin subunit alpha 5 (ITGA5) is an integral membrane protein, implicated in cell adhesion, and was found overexpressed in several cancers with poor prognosis.[273] Lysyl oxidase (LOX) is an enzyme, which participates in the crosslinking of collagens and elastins. Depletion of LOX leads to suppression of breast cancer metastasis.[274] These proteins have been shown to be increased under hypoxia before,[275,276,277,278] but their regulation has not yet been linked to MBNL2. The best-characterized of our newly identified MBNL2 targets is the *VEGFA* mRNA. *VEGFA* gives rise to the vascular endothelial growth factor A (VEGF-A), which is an important regulator under hypoxia and which triggers important cell functions like proliferation or angiogenesis. Recently, another study in ccRCC cells suggested *VEGFA* as *MBNL2* target as described above confirming our findings.[181]

VEGFA was shown to be a direct MBNL2 target in pulldown-assays.[181] By now, it is not proven that *ALDOC*, *ENO2*, *ITGA5* and *LOX* are direct MBNL2 targets. To show the direct binding of MBNL2 to the mRNAs an RNA-binding protein immunoprecipitation could be performed. Possibly, MBNL2 could also act indirectly by regulating the direct binding partners of *ALDOC*, *ENO2*, *ITGA5* and *LOX*. In addition, a CLIP-seq (crosslinking immunoprecipitation sequencing) experiment would give us the opportunity to identify direct MBNL2 target mRNAs. CLIP-seq was not the method of choice in this study since we wanted to gain a global overview of gene expression changes caused by MBNL2 depletion. A HITS-CLIP (high throughput sequencing-crosslinking immunoprecipitation) analysis after MBNL2 depletion has already been performed in brain cells.[279] Identified MBNL2 target mRNAs are misregulated in DM. Since the transcription in brain and cancer cells differs completely, I expect that a CLIP in cancer cells

would yield different target mRNAs. A CLIP-seq further allows for the identification of the exact MBNL2 binding site within target mRNAs.

5.2.5 MBNL2 induction under hypoxia is specific

The functions of MBNL2 have a large overlap with the functions of its paralogs MBNL1 and MBNL3. In addition, cross-regulation between MBNL1 and MBNL2 has been shown before.[171] Thus, I also investigated the hypoxia response of MBNL1 and MBNL3. *MBNL3* expression is more restricted than the expression of its paralogs *MBNL1* and *MBNL2*.[169] Therefore, it was not surprising that *MBNL3* expression was only found in MCF-7 cells, but not in A549 cells. MBNL1 is the strongest splicing regulator among the family of MBNLs. Therefore, I focused on MBNL1 in further experiments. I established an *MBNL1* knockdown in MCF-7 cells and I could show that MBNL1 depletion leads to MBNL2 induction and consequently to MBNL2 target gene induction (**Figure 4-19**). Thus, MBNL1 is not necessary for MBNL2 target gene regulation. Nevertheless, MBNL1 might have a repressive function in regulating the identified potential MBNL2 targets. An mRNA destabilizing function of MBNL1 has already been found,[165] while an mRNA stabilizing function of MBNL2 is yet to be confirmed. The hypothesis, that MBNL1 instead of MBNL2 is regulating the identified targets by destabilization is further ruled out by the fact, that MBNL1 protein level is not significantly changed under hypoxia (**Figure 4-18**). If MBNL1 would be responsible for the destabilization of for example *ALDOC* under normoxia, it must have been reduced under hypoxia, which is not the case. However, due to their similar binding preferences,[170,200] MBNL1 and MBNL2 could also be competitors in binding their targets. It is possible that the ratio between both is important for the final regulation outcome instead of the absolute protein amount of each paralog. Such a competition between MBNL1 and MBNL2 has been shown for splicing regulation.[162] In this case, induction of MBNL2 under hypoxia might lead to displacement of MBNL1 and consequently to reversed target mRNA regulation.

The cross-regulation between MBNL1 and MBNL2 could be confirmed in this study. To be absolutely sure, that the adaptation to hypoxia in cancer cells is mediated specifically by MBNL2 and not by its paralog MBNL1, the usage of knock-out cell lines would be advantageous for further studies. Cross-regulation would be inhibited, when both paralogs are depleted and just one paralog is rescued via plasmid-based overexpression. Usage of *MBNL1*, *MBNL2* and double knock-out cell lines in further experiments would further eliminate

experimental variations produced by transient siRNA transfection. The knock-out cell lines also open up new possibilities for the long-term observation for example in 3D tumor growth or invasion assays since continuous siRNA treatment of the cells would not be necessary.

5.2.6 MBNL2 target regulation mechanism

The study by Perron *et al.*[181] further supposed a target stabilizing function of MBNL2. In actinomycin D assays I could rule out that MBNL2 is stabilizing *VEGFA* mRNA (**Figure 4-20**). Further, a stabilizing role of MBNL2 has not yet been experimentally confirmed. Nevertheless, it is possible that MBNL2 is stabilizing other targets than *VEGFA*. This could be tested in further actinomycin D assays. MBNL2 could potentially play a role in *VEGFA* splicing since *VEGFA* undergoes extensive AS, tuning its function.[110] However, AS analyses after MBNL2 knockdown did not reveal changed AS of *VEGFA*. As mentioned above (chapter 5.2.5), the MBNL2 paralog MBNL1 was found to destabilize its target mRNAs.[165] Under hypoxia, MBNL2 might displace MBNL1 leading to stabilization of target mRNAs, which are destabilized by MBNL1 under normoxic conditions. The ratio and the cross-regulation between MBNL paralogs might also play a role here.

Moreover, MBNL proteins can also influence mRNA localization.[169] In particular, MBNL2 was found to transport mRNAs to the endoplasmic reticulum (ER),[169] which is in line with our GO analyses, which shows downregulated protein targeting to the ER and to membranes after *MBNL2* knockdown (**Supplementary Figure 11-2**). MBNL2 was also found to be important for the correct expression of extracellular membrane proteins,[164] which could be connected to its ability to locate mRNAs to the ER. Since targeting of mRNAs to the ER is often followed by promoted translation and secretion of proteins, I investigated secreted VEGF-A protein levels under normoxia, hypoxia and after *MBNL2* knockdown. I could show that VEGF-A protein levels in cell culture supernatants from A549 and MCF-7 cells are increased under hypoxia as expected (**Figure 4-21**). In addition, I could demonstrate that MBNL2 depletion leads to reduction of secreted VEGF-A to the normoxic level. This effect is even higher than the effects observed on the mRNA level. This clearly indicates a role of MBNL2 in the secretion of VEGF-A. The exact mechanism by which MBNL2 promotes protein secretion is not clear so far, but it could be that MBNL2 localizes its target mRNAs to the ER, where they are translated and subsequently transported to the membrane for secretion.

To further elucidate how MBNL2 acts on its target mRNAs, we have identified three potential MBNL2 binding motifs within the *VEGFA* 3' UTR (**Figure 4-24**). All of the identified motifs are clustered 3'-YGCY-5' motifs, as this is the canonical binding motif of MBNL proteins.[157] We could prove the functionality of the potential MBNL2 binding sites and thus, binding of MBNL2 to the *VEGFA* 3' UTR, in an *ATP2A1* minigene splicing assay in cooperation with K. Taylor and K. Sobczak. *VEGFA* and its regulation under hypoxia has been subject of studies prior to this thesis. Numerous RBP binding motifs have already been identified in *VEGFA* 3' UTR. *VEGFA* 3' UTR contains for example a CARE which is bound by miRNAs under normoxic conditions. The miRNAs are displaced by hnRNP L under hypoxic conditions leading to *VEGFA* mRNA stabilization.[61] Next to the CARE, the 3' UTR also contains a GAIT element (interferon-γ-activated translation inhibitor), which is bound by the GAIT complex, suppressing mRNA translation.[280] Under normoxic conditions, IFN-γ leads to proteasomal degradation of hnRNP L and activation of the GAIT complex. However, during hypoxia, hnRNP L binding leads to a conformational change in RNA folding, preventing GAIT complex binding and allowing efficient translation.[281] Strikingly, our newly identified potential MBNL2 binding sites do not overlap with any previously found RBP or miRNA binding sites within the *VEGFA* 3' UTR. Thus, we have identified a new layer in *VEGFA* regulation under hypoxia. In addition, the *VEGFA* binding site binding affinity of MBNL2 seems to be higher as the binding affinity for MBNL1 (**Figure 4-26**). This is in line with our previous findings and indicates that MBNL2 and not MBNL1 is responsible for *VEGFA* regulation under hypoxia in cancer cells.

To further investigate the binding and the regulation by MBNL2, I have cloned the 3' UTRs of *VEGFA*, *ALDOC*, *ITGA5*, and *LOX* into a luciferase reporter gene vector. Unfortunately, I could not detect any influence of MBNL2 isoform 38 overexpression or MBNL2 depletion on the luciferase activity in our test system (**Figure 4-27**). CLIP experiments point towards preferential binding of MBNL proteins in 3' UTRs[279] but still MBNL proteins could regulate translation efficiency through binding in the 5' UTR. For this case, I also cloned the 5' UTRs of *VEGFA*, *ITGA5* and *LOX* into the luciferase reporter gene vector. Depletion of MBNL2 did not influence the luciferase activity, when the 5' UTR or 3' UTR constructs were transfected. In contrast to the results from the minigene splicing assay, the luciferase reporter gene assay results suggest that MBNL2 is not regulating its target mRNAs by binding their UTRs. This might be due to the experimental setup. In this experimental setup, MCF-7 cells underwent two transient transfections on two consecutive days (siRNA and reporter gene plasmid transfection), followed by direct hypoxia treatment. Cells, which were transfected with siRNA,

do not necessarily contain the transfected plasmids as well. Here, knock-out cell lines would be helpful as already stated above (chapter 5.2.5). When MBNL2 is implicated in its targets secretion, it might also be helpful to use secreted luciferases in the reporter gene assay. In addition, in this study, the potential MBNL binding sites in the *VEGFA* 3' UTR were cloned individually. Probably, the presence of all or two binding sites is necessary to recruit MBNL2. Thus, a construct containing all binding sites should be created in following studies.

5.2.7 MBNL2 controls hypoxia-dependent AS

The transcriptome analyses after MBNL2 depletion revealed 2,074 changed AS events in MCF-7 cells. 393 of them were affected by hypoxia in MCF-7 cells as well. Of note, a large proportion of MBNL2-dependent AS events are not hypoxia-related. Nevertheless, almost all hypoxia- and MBNL2-dependent AS events were regulated oppositely, which implicates that hypoxia triggers MBNL2 to regulate AS. This AS regulation is reverted, when *MBNL2* is depleted. MBNL2 preferentially promotes exon skipping, since most of the hypoxia- and MBNL2-dependent exon skipping events are triggered by hypoxia and reverted after MBNL2 depletion. MBNL1 is a stronger splicing regulator as MBNL2.[170] Therefore, cross-regulation between the two paralogs as well as the ratio between MBNL1 and MBNL2 protein amounts might again play a role, here.

In this study, *PIGN* (phosphatidylinositol glycan anchor biosynthesis class N) could be identified as MBNL2 splicing target. Strikingly, decreased inclusion of *PIGN* exon 12 under hypoxia was completely reversed, when *MBNL2* was depleted (**Figure 4-28**), showing that MBNL2 is necessary and sufficient for *PIGN* splicing. PIGN participates in the synthesis of GPI (glycosylphosphatidylinositol) anchor proteins in the membrane. PIGN is important for genetic stability and the reduction of PIGN via AS has been shown to promote acute myeloid leukemia.[282] In addition, another hypoxia-driven AS event in *PIGN* was identified in endothelial cells,[184] highlighting that *PIGN* undergoes extensive AS modulation and might be important in hypoxia adaptation.

5.2.8 Physiological role of MBNL2 in cancer cell function

In this study, I could show impaired cancer cell proliferation after MBNL2 depletion, demonstrating the importance of MBNL2 for cancer cell functions. MBNL2 depletion led to a

decrease in cell viability in A549 cells. In contrast, knockdown of *MBNL2* alone did not result in impaired cancer cell proliferation in MCF-7 cells. To sensitize the cells the chemotherapeutic cisplatin was used. Treatment of A549 and MCF-7 cells with cisplatin impaired cancer cell proliferation only slightly. Nevertheless, combined cisplatin and siRNA treatment resulted in a significant decrease in cell viability in both cell lines (**Figure 4-29**). These findings indicate that MBNL2 is regulating target genes, which are implicated in cell proliferation. To increase observed effects, the cisplatin concentration could be increased or another drug, for example doxorubicin[283], could be used. Doxorubicin is an anthracycline drug, which intercalates into DNA, leading to inhibition of DNA repair.[284] Further, doxorubicin metabolism constantly releases reactive oxygen species, which damage DNA and proteins.[284] In future studies, the influence of MBNL2 on cell proliferation could be further assessed, for example in cell cycle analyses. Perron *et al.* already showed an increase in the sub-G1 cell population and an increase in caspase-3/7 activity in ccRCCs after MBNL2 depletion, indicating a shift to apoptosis.[181] Moreover, direct targets of MBNL2, implicated in cell proliferation might be identified as explained above (chapter 5.2.4).

Further, I could demonstrate impaired migration of A549 cells after *MBNL2* knockdown (**Figure 4-29**). Migration of MCF-7 cells was examined in this study as well, but wild type MCF-7 cells showed no significant cell migration in the established transwell assay in short time periods (up to 24 h). Concerning the assay design, it would be possible to use knock-out cell lines in migration experiments over a longer time period (for example 48 h or one week). Usage of knockdown cells in experiments over 4 days is not recommended since daughter cells do not share the depletion. Further, knock-out cell lines would allow the conduction of tumor growth and invasion assays in 3D cell cultures since continuous siRNA delivery is not possible in 3D tumor models.

Implication of MBNL2 in cancer cell functions has previously been shown in several studies in other cancer types. Overexpression of MBNL2 was found in patient ccRCCs.[181] Here, colony formation was reduced after *MBNL2* knockdown.[181] In addition, MBNL2 was induced after chronic and intermittent hypoxia treatment of PyMT mouse breast cancer cells.[179] Paradoxically, overexpression of MBNL2 led to impaired tumor growth and invasion in hepatocellular carcinoma cells.[180]

Interestingly, MBNL2 was found to suppress cancer cell metastasis in breast and lung cancer cells.[182] That could be because MBNL2 is induced under hypoxia, which is present within solid

tumors. Metastatic cells leave the solid tumor and are oxygenated again via the blood system leading to normoxic (not induced) levels of MBNL2. Thus, metastasis means escape from hypoxia, depleting MBNL2 induction. Nevertheless, in this study, A549 cell migration was reduced after MBNL2 depletion. This is in contrast to the suppressed cancer cell metastasis observed by Zhang *et al.* since cell migration is the precursor for metastasis. In line with our finding, MBNL2 promoted a metastatic phenotype in a murine breast cancer model.[179]

All together, the predicted roles of MBNL2 in cancer progression are contradictory. The role of MBNL2 might depend on the tumor type or on the stage of tumor progression, thus, the tumors susceptibility to oxygen and nutrients. In future studies, levels of MBNL2 in patient tumor samples could be assessed to underline the importance of MBNL2 in solid tumors. Nevertheless, MBNL2 induction under hypoxia in several cancer types points towards a universal function of MBNL2 in cancer cell adaptation to hypoxia. Thus, MBNL2 could be a new target for the treatment of hypoxic cancers.

6 Outlook

6.1 Auto- and cross-regulation of the hnRNPs D and DL

So far, autoregulation of hnRNP DL could be shown in our laboratory. In addition, cross-regulation between hnRNP DL and its paralog hnRNP D could be demonstrated in this study. There is an overlap between hnRNP D and DL target mRNAs. Nevertheless, it remains to be investigated whether hnRNP D and DL act similarly on their targets or if they act antagonistically. As a first step, RNAi experiments could be performed, in which mRNA levels of known hnRNP D and DL targets are assessed. In this way, target mRNAs can be identified that are regulated in a common or opposing way. Another way to identify hnRNP DL targets as well as the binding sites would be an hnRNP DL PAR-CLIP. Yoon *et al*. performed an hnRNP D PAR-CLIP in HEK cells.[285] Consistently, an hnRNP DL PAR-CLIP might also be performed in HEK cells. Results can be compared to the study by Yoon *et al*. to identify individual and shared hnRNP D and DL targets. Further, the role of hnRNP DL in endothelial cell migration and angiogenesis was demonstrated in this study. On that basis the role of hnRNP D in these processes could also be assessed to allow for comparison between both paralogs.

6.2 Hypoxia-driven gene expression changes in human cancer cells

In this study, I have identified MBNL2 as important regulator in the cancer cell adaptation to hypoxia. To further examine the potential of MBNL2 for cancer therapy, it would be necessary to assess MBNL2 expression levels in patient samples from different cancer types. Concerning the MBNL2 regulation mechanism, direct MBNL2 target mRNAs and binding sites could be identified in CLIP experiments. Further, the establishment of stable MBNL1, MBNL2 and double MBNL1/2 knock-out cell lines will open up new opportunities in the investigation of the MBNL2 regulation mechanism. Then, all experiments can be performed independent from MBNL1/MBNL2 cross-regulation. Subsequent transfection of siRNAs and luciferase reporter gene constructs will not be needed anymore, allowing for easier luciferase reporter gene assay design. Luciferase assays allow investigating, if MBNL2 influences mRNA stability or translation efficiency of an mRNA containing a specific UTR. Further, secreted luciferases could be used in reporter gene assays to further investigate the role of MBNL2 in target mRNA translation and subsequent protein secretion. Concerning the role of MBNL2 in cancer cell function, knock-out cell lines would facilitate assessment of tumor growth, invasion and metastasis in 3D cell culture.

Apart from MBNL2, this study has revealed a broad overlap in the hypoxia-driven gene expression changes in lung and breast cancer cells. Nevertheless, there is a large proportion of differentially expressed genes that are uniquely differentially expressed in just one of the cell types. It might be worthwhile to also look for hypoxia-driven changes in the RBPome that are unique for a certain cancer type.

7 Material

7.1 Disposable Material and Kits

Table 7-1: Disposable material and kits used in this study.

Disposable/Kit	Manufacturer
Cell culture dishes 60 mm	Greiner Bio-One
CloneJET PCR cloning kit	Fermentas
DNeasy Blood & Tissue kit	Qiagen
Dual Glo luciferase assay system	Promega
Magna RIP kit	Millipore
miRNeasy Mini kit	Qiagen
Trans-Blot Turbo Transfer Pack Mini, 0.2 μm PVDF membranes	Bio-Rad
QIAprep Miniprep kit	Qiagen
QIAquick gel extraction kit	Qiagen
RNase-free Dnase set	Qiagen
SuperScript III Reverse Transcriptase kit	Thermo Fisher Scientific
Thincert cell culture inserts, pore diameter 8 μm, translucent PET membrane	Greiner Bio-One
Trypane blue staining kit	Bio-Rad
TURBO DNase	Thermo Fisher Scientific

7.2 Chemicals and Enzymes

Table 7-2: Chemicals and enzymes used in this study. Standard chemicals were purchased from Carl Roth, if not stated otherwise.

Chemical/Enzyme	Manufacturer
Actinomycin D	Sigma
Agarose	Peqlab
Ammoniumperoxodisulfate (APS)	Carl Roth
Ampicillin	Carl Roth
Bovine serum albumin (BSA)	Applichem
Bradford reagent	Bio-Rad
Cisplatin	Sigma Aldrich
Crystal violet	Carl Roth
EBM (plus) medium	Lonza
ECL Prime Blocking Reagent	Amersham
ECL Select detection reagent	GE Healthcare
EGM (plus) single quots	Lonza
DMEM medium	Sigma Aldrich

FCS	Thermo Fisher Scientific
GoTaq DNA polymerase	Promega
Glycoblue	Invirtogen
hEGF protein	Peprotech
HindIII-HF	New England Biolabs
Hygromycine B	Invivogen
IGEPAL CA-630	Sigma Aldrich
Lipofectamine 2000 / 3000 / RNAiMAX	Invitrogen
Methylcellulose	Carl Roth
NotI-HF	New England Biolabs
OptiMEM medium	Sigma Aldrich
PBS (10 x)	Sigma Aldrich
Pen Strep	Thermo Fisher Scientific
Pertex	Histolab
Protease inhibitor cocktail	Sigma Aldrich
Q5 High-Fidelity DNA polymerase	New England Biolabs
Random hexameres	Sigma Aldrich
Ribolock RNase inhibitor	Molox
RPMI-1640 medium	Sigma Aldrich
SalI-HF	New England Biolabs
Sodium pyruvate	Thermo Fisher Scientific
Fast SYBR green master mix (2 x)	Thermo Fisher Scientific
T4 DNA ligase	New England Biolabs
Taq DNA polymerase	New England Biolabs
Tetramethylethylendiamin (TEMED)	Carl Roth
TRI reagent / TRIzol	Sigma Aldrich
VEGF-A protein	Peprotech
XbaI-HF	New England Biolabs
XhoI-HF	New England Biolabs

7.3 Technical equipment

Table 7-3: Technical equipment used in this study.

Technical equipment	**Manufacturer**
12-tube magnetic separation rack	New England Biolabs
Axiovert 200	Zeiss
Bacteria incubator	Heraeus Christ
Cell incubator (normoxia) Eppendorf Galaxy 170 S	Eppendorf AG
Cell incubator (hypoxia) Eppendorf Galaxy 48 R	Eppendorf AG
Centrifuges	Heraeus Christ

ChemiDoc Imaging System	Bio-Rad
Gel documentation with UV screen	INTAS
Infinite M200 plate reader	Tecan Trading AG
Milli-Q water purification system with RNase filter	EMD Millipore
Mini-PROTEAN Tetra Cell electrophoresis chamber	Bio-Rad
NanoDrop ND-1000 Spectrophotometer	Peqlab
Spectrophotometer Ultrospec 2100 pro	Biochrom Ltd
StepOnePlus Real-Time PCR system	Thermo Fisher Scientific
T100 Thermal Cycler	Bio-Rad
TC-10 Automated cell counter	Bio-Rad
Thermomixer comfort	Eppendorf AG
Trans-Blot Turbo	Bio-Rad

7.4 Oligonucleotides, Plasmids, siRNAs and Antibodies

Table 7-4: Oligonucleotides used for RT-PCR and RT-qPCR in this study.

Specificity	**forward sequence 5' -> 3'**	**reverse sequence 5' -> 3'**
ALDOC	GCTGTCCCAGGAGTGACCTT	CATTCACCTCAGCCCGCTT
ATP2A1 minigene	GATCTTCAAGCTCCGGGCCCTG	AGCAATCAGCTAGTCAGTTGCC
CENPE	TGATTTGGATGAATTTGAGGCTC	TCCTGTAGCTTCTTAATCTGGTC
DDIT4	GTTTGACCGCTCCACGAG	CATCAGGTTGGCACACAAGT
ENO2	GGCTACACGGAAAAGATCGTTATT	GAAGGATCAGTGGGAGACTTGAA
HNRNPD 8/10	CTTATCCCCAACAGGTGGTG	GGACCCAACGTCATACTTCC
HNRNPD 8/9/10	AATGCTGCCGTTTGGTGGTG	GGACCCAACGTCATACTTCC
HNRNPDL 7/9	AACATTGGAGAAAACAGGAGGAG	TGGCAGCTATATACAGTTGGACA
HNRNPDL 7/8/9	CGCTGTCCTGTGGAGGAG	TGGCAGCTATATACAGTTGGACA
HNRNPDL pre-mRNA_1	GCAAGGCATACACCAGAAAAC	TGAGGCTCCACAATTGAAATAC
HNRNPDL pre-mRNA_2	ACTTGGGTTACTAGAGATGCTTC	TCACCCTGGAGTTCCCAAATG
HNRNPM	GCTGGAAGACTTGGAAGCAC	AGAATGTCTGCTCGGACCAC
ITGA5	TGCCTCCCTCACCATCTTC	TGCTTCTGCCAGTCCAGC
LDHA	TGGGAGTTCACCCATTAAGC	CTCAACCACCTGCTTGTGAA
LOX	ACACAGGGATTGAGTCCTGG	CCAGGTAGCTGGGGTTTACA
MBNL1	CAAATGCAACTAGCCAATGC	CAGGCTTGGAGAAACAGGTC
MBNL2	ACACCACTTCATCCAGTGCC	CCAACTCCAGGGGTTACAGG
MBNL3	GGCCCAAAACTGATGCGTTC	TCAGTAGGGTGAGCATAGCG
PIGN	GTGGAGATTGGAGAATTGGAA	AACATGCTCTCTGCTTTGAAGA
PLOD2	GGGGCCAGAAAGTGAGATTA	CCACTTTGTGGTTTGCCTTT

PTBP2	GCTTCCTGTTGCAGCTGTTC	CTTCACACGCTGCACATCTC
PUSL1	CGCGCGCTATCTTGTGTACT	GGTGTGTGTTGAGGGCCTC
RPLP0	TCGACAATGGCAGCATCTAC	ATCCGTCTCCACAGACAAGG
U1 snRNA	GGGAGATACCATGATCACGAAGGT	CCACAAATTATGCAGTCGAGTTTCCC
VEGFA	CCCTGATGAGATCGAGTACA	AGCAAGGCCCACAGGGATTT

Table 7-5: Oligonucleotides used for cloning in this study.

Oligonucleotide	**Primer sequence 5' -> 3'**
ALDOC_3UTR_NotI_fwd	ATAGACGCGGCCGCGTATCCACTCCATACCACAGCC
ALDOC_3UTR_HindIII_rev	ATAGACAAGCTTTAGAATGTTTTGCTACCATTTATTTGCTGTATGG
ITGA5_3UTR_NotI_fwd	ATAGACGCGGCCGCGTCCTCCCAATTTCAGACTCCC
ITGA5_3UTR_HindIII_rev	ATAGACAAGCTTTTCTAGTTCTGGTCAGTGGGGG
ITGA5_5UTR_BamHI_fwd	ATAGACGGATCCAGTCCAGACAACCGGCTTCCAGC
ITGA5_5UTR_MluI_rev	ATAGACACGCGTAGCGCCCGCTCTTCCCTGTC
LOX_3UTR_mid_NotI_fwd	atagacgcggccgcGATGTCTTGACCTCTGAGGCtag
LOX_3UTR_SalI_rev	ATAGACGTCGACGACACTTGAAATCATTTATTCAAGGCATTTTTATATAATC
LOX_5UTR_BamHI_fwd	ATAGACGGATCCAAAATCTCTCCTCCTTCCTTCACTCC
LOX_5UTR_Mlu_rev	ATAGACACGCGTCACTCCTTTTGCCAGATTGACCC
MBNL2_XhoI_fwd	ATAGACCTCGAGCGGCTTTGAACGTTGCCCC
MBNL2_XbaI_rev	ATAGACTCTAGACTTTCAGAATTATCTGATTGGCTGTG
MBNL2_39_41_XbaI_rev	ATAGACTCTAGACGCATGCAGTTTGTGGCAA
VEGFA_3UTR_NotI_fwd	ATAGACGCGGCCGCGCCGGGCAGGAGGAAGG
VEGFA_3UTR1_HindIII_rev	ATAGACAAGCTTTCCGGACCCAAAGTGCTCTG
VEGFA_3UTR2_NotI_fwd	ATAGACGCGGCCGCAAGGAAGAGGAGACTCTG
VEGFA_3UTR2_HindIII_rev	ATAGACAAGCTTAAAATAGAGATATTTATTTTTATATATATATAATATATATATATATAAATG
VEGFA_3UTR3_NotI_fwd	ATAGACGCGGCCGCGCAAGGCCAGGGCATGGGG
VEGFA_3UTR_mid_HindIII_rev3	ATAGACAAGCTTCTTCCAACAATGTGTCTCTTCTCTTCGCCGGGACAT
VEGFA_5UTR_MluI_fwd	ATAGACACGCGTGGAGGCTTGGGGCAGCCGG
VEGFA_5UTR_MluI_rev	ATAGACACGCGTCGCGACTGGTCAGCTGCGGG

Table 7-6: Plasmids generated in this study.

Plasmid	**Description**
pCMV-MBNL2-38	overexpression of MBNL2-38
pCMV-MBNL2-39	overexpression of MBNL2-39
pCMV-MBNL2-40	overexpression of MBNL2-40
pCMV-MBNL2-41	overexpression of MBNL2-41

pDL-ALDOC-3'UTR	complete *ALDOC* 3' UTR in 3' orientation of the firefly luciferase for luciferase reporter gene assay
pDL-ITGA5-3'UTR	complete *ITGA5* 3' UTR in 3' orientation of the firefly luciferase for luciferase reporter gene assay
pDL-ITGA5-5'UTR	complete *ITGA5* 5' UTR in 3' orientation of the firefly luciferase for luciferase reporter gene assay
pDL-LOX-3'UTR	3' part of the *LOX* 3' UTR in 3' orientation of the firefly luciferase for luciferase reporter gene assay
pDL-LOX-5'UTR	complete *LOX* 5' UTR in 3' orientation of the firefly luciferase for luciferase reporter gene assay
pDL-VEGFA-3'UTR1	Part of the *VEGFA* 3' UTR containing potential MBNL2 binding site 1 in 3' orientation of the firefly luciferase for luciferase reporter gene assay
pDL-VEGFA-3'UTR2	Part of the *VEGFA* 3' UTR containing potential MBNL2 binding site 2 in 3' orientation of the firefly luciferase for luciferase reporter gene assay
pDL-VEGFA-3'UTR3	Part of the *VEGFA* 3' UTR containing potential MBNL2 binding site 3 in 3' orientation of the firefly luciferase for luciferase reporter gene assay
pDL-VEGFA-5'UTR	complete *VEGFA* 5' UTR in 3' orientation oft he firefly luciferase for luciferase reporter gene assay

Table 7-7: siRNAs used in this study.

Specificity	**Sequence 5' -> 3'**
Nonsilencing control (CTRL)	UUCUCCGAACGUGUCACGU[dT][dT]
HNRNPD	GGGUCCCUCUGAAGUUUAA[dT][dT] AGACUGCACUCUGAAGUUA[dT][dT] GAAGGUGAUUGAUCCUAAA[dT][dT]
HNRNPDL	GGGUAUAACUAUGGGAACU[dT][dT]
MBNL1	AAGGACGAGGUCAUUAGCCAU[dT][dT]
MBNL2	CACCGUAACCGUUUGUAUG[dT][dT] [286]

Table 7-8: Antibodies used in this study.

Specificity	Manufacturer
GFP	Sigma (118144600)
hnRNP A0	Cell Signaling Technology (D8A5 XP)
hnRNP A1	Millipore (05-1521)
hnRNP C	Santa Cruz (sc-32308)
hnRNP D	Millipore (07-260)
hnRNP DL	Sigma (AV40585)
hnRNP E2	Abcam (ab184962)
hnRNP L	Santa Cruz (sc-32317)
hnRNP M	Santa Cruz (sc-20002)
HSP60	Abcam (ab6530)
MBNL1	Wolfson Centre for Inherited Neuromuscular Disease (CIND; MB1a(4A8))[287]
MBNL2	Santa Cruz (sc-136167)
Mouse	Jackson ImmunoResearch
Rabbit	Jackson ImmunoResearch
VCAM1	Cell Signaling Technology (E1E8X)

8 Methods

8.1 Cell culture, hypoxia treatment and transfection

HeLa, A549 and MCF-7 cells were obtained from the Deutsche Sammlung von Mikroorganismen und Zellkulturen (DSMZ; no.: ACC 57, no. ACC-107 and no. ACC-115). The cell lines were cultured in T75 flasks in DMEM (HeLa, A549) or RPMI-1640 medium (MCF-7), respectively, supplemented with 10% FCS, 1 mM sodium pyruvate and Penicillin Streptomycin.

HeLa "Flp-in" Host Cell Line HF1-3 cells, stably expressing GFP or the GFP-hnRNP DL fusion protein[147], were cultured in DMEM medium supplemented with 10% FCS, 1 mM sodium pyruvate, Penicillin Streptomycin and 150 µg/ml hygromycine B. In the following method descriptions, HF1-3 cells are also referred to as HeLa cells.

HUVEC cells (Lonza, CC-2519) were cultured in T75 flasks in EBM medium supplemented with 10% FCS and EGM single quots (hEGF, Hydrocortison, GA-1000, bovine brain extract). HUVECs were splitted once a week and only passages 2 and 3 were used for experiments.

HUVECs are primary cells and change their characteristics, when they are cultured for longer periods.

For hypoxia experiments, $1x10^5$ A549 cells or $2x10^5$ MCF-7 cells were seeded in 12 well plates and incubated under normoxic conditions (37°C, 5% CO_2, 21% O_2) for 24 h. Then, cells were transferred to the hypoxia incubation chamber (37°C, 5% CO_2, 0.5% O_2, Eppendorf Galaxy 48 R incubator). RNA samples were prepared 48 h later as described below.

For siRNA transfection of HeLa cells, $6x10^4$ cells were seeded in 12 well plates. 24 h later, transfection was performed using Lipofectamine RNAiMAX according to the manufacturer's protocol together with 4 pmol siRNA in DMEM medium.

For siRNA transfection of HUVECs, $3.5x10^5$ cells were seeded in 60 mm cell culture dishes. 24 h later, transfection was performed using Lipofectamine RNAiMAX according to the manufacturer's protocol together with 60 pmol siRNA in OptiMEM medium. After 4 h the transfection mixes were removed and fresh medium was added.

For reverse siRNA transfections, $1x10^5$ A549 or $2x10^5$ MCF-7 were transfected using Lipofectamine RNAiMAX according to the manufacturer's protocol and 200 pmol siRNA. Cells were mixed with the transfection mix and were seeded directly in 12 well plates. 24 h later, the transfection mixes were removed and fresh medium was added. Then, cells were transferred to the hypoxia incubation chamber.

For MBNL2 overexpression and luciferase reporter gene assays, $1x10^5$ MCF-7 cells were transfected using Lipofectamine 2000 according to the manufacturer's protocol and 100 ng plasmid. Cells were mixed with the transfection mix and were seeded directly in 12 well plates.

8.2 RNA sequencing and data analyses

RNA sequencing was performed by the Core Unit Systems Medicine at the University of Würzburg. Ribosomal RNA was depleted from the total RNA samples from normoxic and hypoxic A549 and MCF-7 cells (n=2, RiboZero, Illumina). Strand-specific cDNA libraries were generated using TruSeq stranded mRNA library preparation kit from Illumina according to the manufacturer's protocol omitting the polyA enrichment step. The cDNA libraries were sequenced on a NextSeq 500 (Illumina). Approximately 100 million 75 nt single-end reads were obtained per sample.

RNA sequencing after *MBNL2* knockdown in MCF-7 cells was performed identically except for the polyA enrichment, which was performed instead of the rRNA depletion. Here, 80 million 75 nt single-end reads were obtained per sample.

RNA sequencing data from A549, MCF-7 and *MBNL2* knockdown experiments is available in the Gene Expression Omnibus Database (GEO, www.ncbi.nlm.nih.gov/geo/) under the accession numbers GSE131378 and GSE136231.

Reads were mapped to the human genome (GRCh38/hg38 assembly) using the splice-aware aligner STAR version 2.4.5a.[288] Reads were counted within genes annotated in GENCODE version 24 using the htseq-count script from the HTSeq python package version 0.6.1.[289] The R/Bioconductor package DESeq2[193] was used to analyze differential gene expression between hypoxic and normoxic conditions or between *MBNL2* knockdown and control cells. Differentially expressed genes were considered, when they had an adjusted P value < 0.05 and an absolute fold change > 1.5. The rMATS version 3.2.5[194] was used to detect AS events. AS events were considered as changed, when they had an adjusted P value < 0.05 and an absolute change in PSI > 10%. For both differentially expressed genes and AS events, only genes with a minimum expression level of > 1 transcript per million (TPM) in at least one of the four samples obtained for each cell type/condition were considered. The enrichGO function in clusterProfiler package version 3.6.0[290] in R (version 3.4.3) was used to analyze gene ontology (GO) enrichment.

8.3 RNA extraction and reverse transcription

Total RNA from HeLa cells was isolated using TRIzol reagent, followed by TURBO DNase treatment.

Total RNA from HUVECs was isolated using the miRNeasy Mini kit, including the optional on-column DNA digestion with the RNase-Free DNase Set.

Total RNA from A549 and MCF-7 cells was isolated either using TRIzol reagent, followed by TURBO DNase treatment or by using the miRNeasy Mini kit, including the optional on-column DNA digestion with the RNase-Free DNase Set.

In general, miRNeasy Mini kit was used as described in the manufacturer's protocol. For RNA extractions using TRIzol the procedure was conducted as follows. Cells were washed with

1x PBS and TRIzol was added directly into the cell culture plate or dish. The liquid was mixed and transferred into a reaction tube. 80 µl chloroform was added and the mixture was vortexed for 15 s. After 3 min at RT, the mixture was centrifuged at 13,300 rpm and 4°C for 15 min. The upper phase was transferred into a new reaction tube. A second extraction was performed using 200 µl chloroform. After centrifugation at 13,300 rpm and 4°C for 15 min the upper phase was transferred into a new reaction tube. 200 µl isopropanol and 0.75 µl Glycoblue were added to the solution. The RNA was precipitated for 10 min at RT and was then centrifuged at 13,300 rpm and 4°C for 30 min. The pellet was washed with 70% ethanol. After another centrifugation step at 13,300 rpm and 4°C for 15 min, the RNA pellet was dissolved in 35 µl dH_2O. 4 µl TURBO DNase buffer and 1 µl TURBO DNase were added to the RNA. After DNase digestion for 15 min at RT, 200 µl absolute ethanol and 4 µl sodium acetate were added for precipitation. The RNA was precipitated at -80°C for 1 h or overnight. The RNA solution was then centrifuged at 13,300 rpm and 4°C for 30 min. The pellet was washed with 70% ethanol. After another centrifugation step at 13,300 rpm and 4°C for 15 min, the RNA pellet was dissolved in 20 µl dH_2O.

After isolation, RNA concentration was determined using the nanodrop system. 500 ng RNA were quality checked on a 1% agarose gel.

cDNA was synthesized using the SuperScript III Reverse Transcriptase kit according to the manufacturer's protocol. 1 µg RNA was reverse transcribed. The reverse transcription mix and the corresponding program are shown in Table 8-1. Finally, the cDNA was diluted by adding 180 µl H_2O.

Table 8-1: Reverse transcription (RT) mix and program.

RT mix		**RT program**	
1 µg	RNA	Denaturation	65°C for 5 min
ad 11 µl	MQ water	Cool down /Annealing	on ice for 1 min
1 µl	dNTPs, 10 mM each	Reverse Transcription	25°C for 5 min
1 µl	random hexamers		50°C for 30 min
added after Annealing	Mastermix for all samples		70°C for 15 min
4 µl	5x First Strand buffer	Storage	8°C ∞
1 µl	Dithiothreitol, 0.1 M		
1 µl	Ribolock		
1 µl	SuperScript III		

8.4 RT-PCR

Splicing analyses were performed using Taq polymerase. Oligonucleotide sequences are listed in Table 7-4. A typical RT-PCR mix and RT-PCR program are shown in Table 8-2.

Table 8-2: RT-PCR mix and program.

PCR mix		**PCR program**	
17.5 μl	dH_2O	Denaturation	95°C for 5 min
3 μl	10x ThermoPol buffer	Denaturation	95°C for 30 s (30-35 cycles)
1 μl	oligonucleotide fwd (10 μM)	Annealing	55°C for 30 s (30-35 cycles)
1 μl	oligonucleotide rev (10 μM)	Elongation	72°C for 30 s (30-35 cycles)
0.6 μl	dNTPs, 10 mM each	Final elongation	72°C for 7 min
5 μl	cDNA	Storage	8°C ∞
0.3 U	Taq DNA polymerase		

8.5 *ATP2A1* minigene splicing assay

Mouse Embryonic Fibroblasts (MEFs) with *MBNL1* and *MBNL2* double knock-out were a gift from MS Swanson.[167] The growth conditions of MEFs are described in [202]. Prior to transfection, the cells were plated in 12 well plates and transfected at 50-60% confluence with Lipofectamine 3000 according to the manufacturer's protocol. Co-transfection was conducted with 200 ng of a minigene and 750 ng of GFP-MBNL1-40, GFP-MBNL2-38, GFP-MBNL2-40 or GFP expression vectors, which are described in [170]. Cells were harvested 42 h after transfection. Total RNA was isolated using TRI reagent according to the manufacturer's protocol. cDNA was synthesized using the SuperScript III Reverse Transcriptase kit. Splicing analysis was performed using GoTaq DNA polymerase.

8.6 Quantitative RT-PCR

RT-qPCR was used to quantify mRNA levels. RT-qPCR samples contained 5 µl cDNA, 10 µl 2x Fast SYBR green master mix and 1 µl forward and reverse oligonucleotide each (10 µM). A StepOnePlus Real Time PCR instrument with standard settings for Fast SYBR green mixes including melting temperature was used. All measurements were carried out in

technical duplicates. RT-qPCR analysis was done using the ΔΔCt method.[291] All PCR products were verified by sequencing. Oligonucleotide sequences are listed in Table 7-3.

8.7 Protein extraction and Western blot analyses

In order to obtain protein extract, cells were lysed in lysis buffer (137 mM NaCl, 10% glycerol, 20 mM Tris-HCl pH 8.0, 2 mM EDTA pH 8.0, 1% Igepal, 5 µl protease inhibitor cocktail) for 20 min on ice. Cell debris were removed after centrifugation at 17,000 g, 4°C for 15 min.

Protein content of extracts was determined using the Bradford protein assay.[292] By binding of Coomassie brilliant blue G-250, the absorption maximum of proteins shifts from 465 to 595 nm. Thus, the absorption increase at 595 nm is a measure of the protein concentration of the extract. A calibration curve with a known protein concentration of BSA was created. 2 μl of the protein extracts were diluted in 1 ml Bradford reagent, which was diluted 1:5. After 10 min incubation at RT, the absorption was measured at 595 nm. The concentration of the protein extract could be determined using the linear equation resulting from the calibration curve. The measurement was carried out in technical triplicates.

10 μg protein extract were used for Western blot analyses. The protein samples were mixed with 4x protein loading dye, boiled for 5 min at 95°C and cooled down to RT. 10 μg were loaded on 10% SDS gels. 4 μl Precision Plus All blue protein standard (Bio-Rad) were used as size standard. The gels were pre-stained using TCE (2,2,2-trichloroethanol) in the collecting gel. Thus, total lane protein loading could be detected before blotting. The gels were activated and photographed using the ChemiDoc MP System (Bio-Rad) and the Image Lab software. Then, proteins were transferred to a PVDF membrane using the Trans-Blot Turbo Transfer System (Bio-Rad). The transfer was performed in the fast blot apparatus for 7 min. After the transfer, the membrane was blocked for 1 h in 2% (w/v) skim milk in 1x TBS-T. The membrane was then incubated with the primary antibody, dissolved in 2% (w/v) skim milk in 1x TBS-T, for 1 h at RT. Then, the membrane was washed 3 times with 1x TBS-T. The membrane was incubated with the secondary antibody for 1 h at RT. The membrane was washed 3 times with 1x TBS-T and then developed with ECL substrate. For strong signals, the ECL system from Bio-Rad and for weak signals, the ECL Select System from Life technologies were used. The membrane was incubated with substrate for 5 min and then developed using

the ChemiDoc MP System (Bio-Rad) and the Image Lab software. Membranes were stored in 1x TBS-T at 4°C.

8.8 RNA-binding protein immunoprecipitation

RIPs were performed using the Magna RIP kit (Millipore) followed by DNase I digestion according to the manual. $4x10^6$ HIF1-3 cells (overexpressing GFP or a GFP-hnRNP DL fusion protein) were used per RIP. 10% of each precipitate was used for Western blot analyses. Mouse IgG and anti-snRNP70 antibody were included in the kit.

8.9 Plasmid construction

Starting vectors for construction of the MBNL2 overexpression plasmids, containing the sequences of the several MBNL2 isoforms[170] were a kind gift from K. Sobczak (Adam Mickiewicz University, Poznan, Poland). MBNL2 sequences were amplified using Q5 High-Fidelity DNA polymerase. Obtained fragments and pCMV-MS vector[293] (**Figure 11-4**) were digested using XhoI-HF and XbaI-HF. Vector and insert were ligated using T4 DNA ligase. Plasmids were transformed into *E. coli* DH5α. *E. coli* were cultured on/in LB medium supplemented with 100 μg/ml ampicillin (Amp). Plasmids were isolated using the QIAprep Miniprep Kit according to the manual.

For the luciferase reporter gene assays, 3' UTRs from *ALDOC*, *ITGA5*, *LOX* (3' part of the 3' UTR) and *VEGFA* (three parts, which contain one potential MBNL2 binding site) as well as complete 5' UTRs from *ITGA5*, *LOX* and *VEGFA* were cloned into the bidirectional luciferase reporter gene vector pDL (**Figure 11-3**).[293] Sequences were amplified from MCF-7 genomic DNA using Q5 High-Fidelity DNA polymerase. NotI-HF and HindIII-HF/SalI-HF (3' UTRs) or BamHI and MluI (5' UTRs) were used for digestion, respectively. Plasmids were transformed into *E. coli* Top10. *E. coli* were cultured on/in LB medium supplemented with 100 μg/ml ampicillin. Plasmids were isolated using QIAprep Miniprep Kit according to the manual.

All oligonucleotides used for cloning are listed in Table 7-5.

8.10 DNA Sequencing

Plasmid sequencing was conducted by Seqlab according to the Sanger procedure. 1 μg plasmid was sent to Seqlab in a 1.5 ml reaction tube together with 30 pmol sequencing oligonucleotide in a final volume of 15 μl.

8.11 Isolation of genomic DNA

Genomic DNA for the amplification of 3' UTRs was isolated using the DNeasy Blood & Tissue kit (Qiagen) according to the manufacturer's protocol.

8.12 Polymerase chain reaction

The polymerase chain reaction (PCR) was used for example to amplify DNA fragments from genomic DNA or plasmids for cloning in this study. A typical PCR mix and a typical PCR program are described in Table 8-3. The annealing temperature depends on the melting temperature of the used oligonucleotides. Elongation time was adjusted according to the amplified fragment length (1 min per 2kb).

Table 8-3: PCR mix and program.

PCR mix		**PCR program**	
1 x	Q5 buffer	Denaturation	98°C for 3 min
30 pmol	oligonucleotide fwd	Denaturation	98°C for 30 s (35 cycles)
30 pmol	oligonucleotide rev	Annealing	55°C for 30 s (35 cycles)
100 ng	template DNA	Elongation	72°C for 30 s (35 cycles)
20 nmol	dNTPs	Final elongation	72°C for 7 min
2 U	Q5 DNA polymerase	Storage	8°C ∞
ad 100 μl	dH_2O		

8.13 Transformation of *E. coli*

$CaCl_2$ competent *E. coli* cells were used for transformation of plasmid DNA. The competent cells were thawed on ice. 100 μl of competent cells were added to a ligation mix. The ligation mix contained 25 ng of a digested plasmid, the fivefold molar amount of insert and 2 U T4 DNA ligase in 1x T4 DNA ligase buffer. The ligation mix was incubated for 30 min at RT. The

ligation mix, together with the competent *E. coli* cells, was incubated on ice for 30 min. Then, the cells were heat-shocked at 42°C for 90 s. The mix was incubated on ice for 10 min. Then, 900 μl LB medium was added and the mix was incubated at 37°C for 1 h with constant shaking at 950 rpm in an Eppendorf thermomixer. Cells were centrifuged at 13,300 rpm for 1 min. The supernatant was removed. Cells were resuspended in the remaining medium and were plated onto LB agar containing 100 μg/ml ampicillin.

8.14 Colony PCR

To analyze, whether *E. coli* colonies had the desired plasmid, colony PCR was performed. Fragments were subsequently analyzed on 1% agarose gels. A typical PCR mix and a typical PCR program are described in Table 8-4.

Table 8-4: Colony PCR mix and program.

PCR mix		**PCR program**	
1 x	ThermoPol buffer	Denaturation	96°C for 4 min
7.5 pmol	oligonucleotide fwd	Denaturation	96°C for 30 s (30 cycles)
7.5 pmol	oligonucleotide rev	Annealing	50°C for 30 s (30 cycles)
20 nmol	dNTPs	Elongation	72°C for 30 s (30 cycles)
1.25 U	Taq DNA polymerase	Final elongation	72°C for 7 min
ad 25 μl	dH_2O	Storage	8°C ∞
	E. coli cells from one colony		

8.15 Generation of $CaCl_2$ competent *E. coli* cells

For the generation of competent cells, a fresh culture of the *E. coli* cell stock was prepared on LB agar. A 4 ml overnight culture was inoculated. 16 h later, the overnight culture was transferred to 200 ml LB medium in a 1 l flask. The culture was incubated at 37°C with shaking at 180 rpm until the oD_{600} had reached a value between 0.4 and 0.5. The cells were then incubated on ice for 30 min and divided into 4 centrifuge tubes (50 ml each). All subsequent steps were performed on ice. Cells were centrifuged at 6,000 rpm for 5 min and the supernatant was removed. Cell pellets were washed with 25 ml of a 0.1 M $CaCl_2$ solution and were centrifuged again at 6,000 rpm for 5 min. The cells were resuspended in 20 ml of a 0.1 M $CaCl_2$ solution and were incubated on ice for 1 h. Glycerol (100%) was added to a final concentration of 15% and cells were aliquoted into 1.5 ml reaction tubes with

330 µl competent *E. coli* cells each. The cells were shocked-frosted immediately in liquid nitrogen. Competent *E. coli* cells were stored at -80°C.

8.16 Luciferase reporter gene assay

Luciferase activity in MCF-7 cells (control cells, MBNL2 overexpression or *MBNL2* knockdown) was measured after 48 h of hypoxia treatment. The medium was removed and 100 µl DMEM without phenol red was added. 100 µl Dual-Glo luciferase substrate was added. The Dual-Glo reagent contains the luciferase substrate, but also substances, which lead to cell disruption. The cell disruption allows for the reaction of the firefly luciferase with its substrate in the supernatant. After 10 min incubation at RT, the solution was transferred into a white 96 well plate. The chemiluminescence was determined using the TECAN infinite M 200 Pro plate reader (default setting: luminescence, no attenuation, 1000 ms integration time). To measure the activity of the *Renilla* luciferase, which serves as internal standard, 100 µl of the Dual-Glo Stop&Glo reagent was added. After 5 min incubation at RT the chemiluminescence was determined. The relative light units were determined by calculating the quotient of firefly and *Renilla* luciferase.

8.17 mRNA decay assay

Directly after hypoxia treatment (48 h) and 72 h after transfection, MCF-7 cells were treated with 5 µg/ml actinomycin D for 30 min. Actinomycin D was then removed and RPMI-1640 medium was added. MCF-7 cells were incubated under hypoxic conditions. Total RNA was prepared before hypoxia incubation (0 h sample) and after 2 and 4 h. MRNA levels were quantified by RT-qPCR, normalized to *RPLP0* mRNA levels and plotted against time.

8.18 Enzyme-linked immunosorbent assay (ELISA)

Human VEGF-A ELISA Kit (Sigma-Aldrich) was used to determine secreted human VEGF-A protein levels in cell culture supernatants. Protein detection was performed according to the manufacturer's protocol. Cell culture supernatants were obtained from normoxic and hypoxic (48 h, 0.5% O_2) A549 and MCF-7 cells transfected either with a nonsilencing control siRNA

(siCTRL) or an siRNA targeting *MBNL2* (siMBNL2) and were diluted 1:2 in Sample Diluent Buffer B.

8.19 Cell viability assay

The crystal violet assay was used to determine the viability of cells. The cells were washed with 1x PBS and fixed for 5 min with 0.5% formaldehyde in PBS. Cells were stained for 5 min with 0.5% crystal violet in PBS. After three washing steps with 1x PBS the cells were incubated with 33% acetic acid for 5 min. Samples were transferred to a 96 well plate. Absorption at 570 nm was measured in a TECAN infinite M 200 Pro plate reader.[294] Absorption was normalized to normoxic control cells.

In experiments with cisplatin, A549 and MCF-7 cells were transfected as described and were incubated under normoxic or hypoxic conditions (48 h, 0.5% O_2). 24 h later, cisplatin was added at final concentrations of 10 or 20 µM. 24 h later, crystal violet assay was performed. Here, the absorption was normalized to normoxic control cells with the respective cisplatin concentration.

8.20 Cell migration assay

HUVECs (si_ctrl/si_DL) were serum-starved (EBM medium without FCS) 24 h after transfection. 24 h later, HUVECs were washed with 1x PBS and detached using 40 µl Trypsin-EDTA (0.05% trypsin, 0.02% EDTA in 1x PBS). HUVECs were resuspended in starvation medium (EBM medium without FCS). $5x10^4$ cells in 100 µl starvation medium were seeded per insert in a 24 well transwell chamber (Thincert cell culture inserts, pore diameter 8 µm, translucent PET membrane, Greiner). Transwell inserts were placed into a lower well containing 700 µl EBM medium with supplements or starvation medium as a negative control. After 5 h under normoxic conditions, cells were removed from the inner side of the insert with a cotton swab. Migrated cells (at the outer side of the insert) were washed with 1x PBS and fixed with methanol. Migrated cells were stained using crystal violet (0.5% in 1x PBS) and the membranes were mounted using Pertex (Histolab). No cells were detected in the negative control. Migrated cells in six fields per well from random sites of the transwell insert membrane were counted using Image J software.

A549 cells (si_CTRL/si_MBNL2) were serum-starved (DMEM medium without FCS) and transferred to the hypoxia incubation chamber (48 h, 0.5% O_2) 24 h after transfection. 48 h later, A549 cells were washed with 1 x PBS and detached using 40 µl Trypsin-EDTA (0.05% trypsin, 0.02% EDTA in 1 x PBS). A549 cells were resuspended in starvation medium (DMEM medium without FCS). $5x10^4$ cells in 100 µl starvation medium were seeded per insert in a 24 well transwell chamber. Transwell inserts were placed into a lower well containing 700 µl DMEM medium supplemented with 10% FCS, 1 mM sodium pyruvate and Penicillin Streptomycin without or with 100 ng/µl hEGF as a positive control or starvation medium as a negative control. After 5 h under hypoxic conditions, cells were removed from the inner side of the insert with a cotton swab and were washed, fixed and stained as described above.

8.21 Spheroid sprouting assay

24 h after transfection, HUVECs were detached using Trypsin-EDTA (0.05% trypsin, 0.02% EDTA in 1x PBS). 500 HUVECs were seeded per 50 μl drop as hanging drop culture in a 15 cm plate (**Figure 8-1**) in EBM medium supplemented with 20% EBM-methylcellulose medium (1.2% w/v methylcellulose in EBM medium without supplements). Approximately 100 drops were created for each condition (si_ctrl/si_DL). 24 h later, spheroids were transferred to a collagen matrix. The collagen mix was prepared for all samples, so that the pH is the same for every condition. Collagen is mixed with 10% 10x M199 medium. Methylcellulose-FCS (20% FCS, 80% EBM-methylcellulose medium) was prepared. Spheroids were harvested in 1x PBS and centrifuged for 3 min with 500 g. The supernatant is removed. 2.6 ml methylcellulose-FCS were added to the spheroids. The sample for every condition (si_ctrl/si_DL) was split between two reaction tubes. Spheroids in one of the two reaction tubes were stimulated with 0.05 mg/ml VEGF-A protein. The collagen medium mix was then neutralized until the indicator turned from orange to pink. 1.3 ml collagen mix were added to each spheroid sample. Samples were transferred immediately into the inner wells of a 24 well plate (4 wells per sample) without producing air bubbles and incubated for 24 h at 37°C, 5% CO_2, 21% O_2. Outer wells of the 24 well plate were previously filled with 1x PBS to prevent draining of the spheroids. 24 h later, spheroids and their sprouts were photographed using an Axiovert 200 microscope (10x objective). At least 10 spheroids per condition were analyzed using Image J software. The spheroids were not allowed to be too close to each

other or to the edge of the well to be evaluated. Analysis was performed as a blind study by S. Peter. For analysis, the cumulative sprout length in pixels was measured using the Image J software.

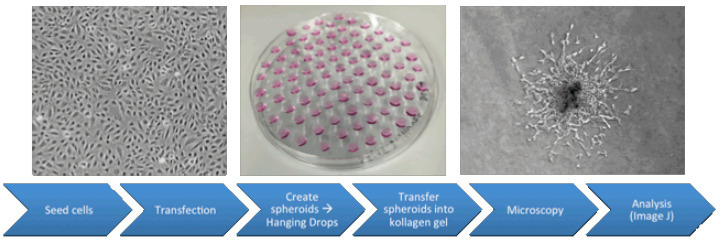

Figure 8-1: Spheroid sprouting assay workflow. The experiment workflow is explained in the blue boxes. The left picture shows a HUVEC monolayer in 2D culture. The middle picture is showing hanging drop cultures, which are created to build the HUVEC spheroids. The right picture shows a HUVEC spheroid with sprouts, which can be used for evaluation at the last day of the experiment.

9 Abbreviations

Table 9-1: Abbreviations.

Abbreviation	Explanation
3’	3’ OH end
5’	5’ phosphate end
A3SS	alternative 3’ splice site
A5SS	alternative 5’ splice site
AS	alternative splicing
AS-NMD	alternative splicing coupled to nonsense-mediated decay
bp	base pair
CE	cassette exon
CTRL	control
circRNA	circular RNA
dH_2O	distilled water
Da	Dalton
DM	myotonic dystrophy
DMSO	dimethyl sulfoxide
DNA	deoxyribonucleic acid
dNTP	deoxynucleoside triphosphate
E. coli	*Escherichia coli*
FCS	fetal calf serum
FDR	false discovery rate
fwd	forward
gDNA	genomic DNA
GO	gene ontology
h	hour
hEGF	human epidermal growth factor
HIF	hypoxia inducible factor
hnRNP	heterogenous nuclear ribonucleoprotein
HRE	HIF-responsive element
IRES	internal ribosome entry site
LB	lysogeny broth
lncRNA	long non-coding RNA
MBNL	muscleblind-like
min	minute
miRNA	micro RNA
mORF	main open reading frame
MQ	Milli-Q
mRNA	messenger RNA

MXE	mutually exclusive exon
n.d.	not detectable
NLS	nuclear localization signal
NMD	nonsense-mediated decay
nt	nucleotide
ori	origin of replication
padj	adjusted P value
PBS	phosphate buffered saline
PCR	polymerase chain reaction
PSI	percent spliced-in
PTC	premature termination codon
P value	probability value
qPCR	quantitative PCR
RBP	RNA-binding protein
rel.	relative
rev	reverse
rHRE	ribosomal HIF-responsive element
RI	retained intron
RIP	RNA-binding protein immunoprecipitation
RNA	ribonucleic acid
RNAi	RNA interference
RRM	RNA recognition motif
rRNA	ribosomal RNA
RT	real time
RT	reverse transcriptase
RT	room temperature
s	second
SF	splicing factor
siCTRL	nonsilencing control siRNA
siRNA	short interfering RNA
snoRNA	small nucleolar RNA
snRNA	small nuclear RNA
snRNP	small nuclear ribonucleoprotein
SR	serine and arginine-rich
SS	splice site
TPM	transcripts per million
tRNA	transfer RNA
uORF	upstream open reading frame
UTR	untranslated region
vs.	versus

10 References

[1] Dunwoodie SL. The role of hypoxia in development of the Mammalian embryo. Dev Cell 17, 755-73 (2009).

[2] Li W, Li Y, Guan A, Fan J, Cheng CF, Bright AM, Chinn C, Chen M & Woodley DT. Extracellular heat shock protein-90alpha: linking hypoxia to skin cell motility and wound healing. EMBO J 26, 1221-33 (2007).

[3] Simonson TS, Yang Y, Huff CD, Yun H, Qin G, Witherspoon DJ, Bai Z, Lorenzo FR, Xing J, Jorde LB, Prchal JT & Ge R. Genetic Evidence for High-Altitude Adaptation in Tibet. Science 329, 72-75 (2010).

[4] Bodamyali T, Stevens CR, Billingham MEJ, Ohta S & Blake DR. Influence of hypoxia in inflammatory synovitis. Ann Rheum Dis 57, 703-710 (1998).

[5] Stenmark KR, Fagan KA & Frid MG. Hypoxia-Induced Pulmonary Vascular Remodeling: Cellular and Molecular Mechanisms. Circ Res 99, 675-691 (2006).

[6] Höckel M & Vaupel P. Tumor Hypoxia: Definitions and Current Clinical, Biologic, and Molecular Aspects. J of National Cancer Institute 93, No. 4, 266-276 (2001).

[7] Evans RG, Goddard D, Eppel GA & O'Connor PM. Factors that render the kidney susceptible to tissue hypoxia in hypoxemia. Am J Physiol Regul Integr Comp Physiol 300: R931-R940 (2011).

[8] Fraisl P, Mazzone M, Schmidt T & Carmeliet P. Regulation of Angiogenesis by Oxygen and Metabolism. Developmental Cell 16, 167-179 (2009).

[9] Potente M, Gerhardt H & Carmeliet P. Basic and Therapeutic Aspects of Angiogenesis. Cell 146, 873-887 (2011).

[10] Semenza GL. HIF-1: mediator of physiological and pathophysiological responses to hypoxia. J Appl Physiol (1985) 88, 1474-1480 (2000).

[11] Carroll VA & Ashcroft M. Targeting the molecular basis for tumour hypoxia. Expert rev Mol Med 7, 1-16 (2005).

[12] Chee NT, Lohse I & Brothers SP. mRNA-to-protein translation in hypoxia. Mol Cancer 18, 49 (2019).

[13] Schito L & Semenza GL. Hypoxia-inducible factors: Master regulators of cancer progression. Trends Cancer 2, 758–770 (2016).

[14] Koh MY, Lemos R, Liu X & Powis G. The hypoxia-associated factor switches cells from HIF-1α– to HIF-2α–dependent signaling promoting stem cell characteristics, aggressive tumor growth and invasion. Cancer Res 71, 4015–27 (2011).

[15] Meijer TWH, Kaanders JHAM, Span PN & Bussink J. Targeting Hypoxia, HIF-1, and Tumor Glucose Metabolism to Improve Radiotherapy Efficacy. Clin Cancer Res 18, 5585-94 (2012).

[16] Cui XG, Han ZT, He SH, Wu XD, Chen TR, Shao CH, Chen DL, Su N, Chen YM, Wang T, Wang J, Song DW, Yan WJ, Yang XH, Liu T, Wie HF & Xiao J. HIF1/2α mediates hypoxia-induced LDHA expression in human pancreatic cancer cells. Oncotarget 8, 24840-24852 (2017).

[17] Haase VH. Regulation of erythropoiesis by hypoxia-inducible factors. Blood Rev 27, 41-53 (2013).

[18] Lin C, McGough R, Aswad B, Block JA & Terek R. Hypoxia induces HIF-1alpha and VEGF expression in chondrosarcoma cells and chondrocytes. J Orthop Res 22, 1175-81 (2004).

[19] Holmquist-Mengelbier L, Fredlund E, Löfstedt T, Noguera R, Navarro S, Nilsson H, Pietras A, Vallon-Christersson J, Borg A, Gradin K, Poellinger L & Pahlmann S. Recruitment of HIF-1alpha and HIF-2alpha to common target genes is differentially regulated in neuroblastoma: HIF-2alpha promotes an aggressive phenotype. Cancer Cell 10, 413-23 (2006).

[20] Makino Y, Cao R, Svensson K, Bertilsson G, Asman M, Tanaka H, Cao Y, Berkenstam A & Poellinger L. Inhibitory PAS domain protein is a negative regulator of hypoxia-inducible gene expression. Nature 414, 550–4 (2001).

[21] Galbán S, Kuwano Y, Pullmann RJr, Martindale JL, Kim HH, Lai A, Abdelmohsen K, Yang X, Dang Y, Liu JO, Lewis SM, Holcik M & Gorospe M. RNA-Binding Proteins HuR and PTB Promote the Translation of Hypoxia-Inducible Factor 1α. Mol and Cell Biol 28, 93-107 (2008).

[22] Carraway KR, Johnson EM, Kauffmann TC, Fry NJ & Mansfield KD. Hypoxia and Hypoglycemia synergistically regulate mRNA stability. RNA Biol 14, 938-951 (2017).
[23] Chee NT, Lohse I & Brothers SP. mRNA-to-protein translation in hypoxia. Mol Cancer 18, 49 (2019).
[24] Ivanova IG, Park CV & kenneth NS. Translating the Hypoxic Response—The Role of HIF Protein Translation in the Cellular Response to Low Oxygen. Cells 8, 114 (2019).
[25] Sheflin LG, Zou AP & Spaulding SW. Androgens regulate the binding of endogenous HuR to the AU-rich 3′UTRs of HIF-1α and EGF mRNA. Biochem and Biophys Res Comm 322, 644-651 (2004).
[26] Gorospe M, Tominaga K, Wu X, Fähling M & Ivan M. Post-transcriptional control of the hypoxic response by RNA-binding proteins and microRNAs. Front Mol Neurosci 4, 7 (2011).
[27] Schepens B, Tinton SA, Bruynooghe Y, Beyaert R & Cornelis S. The polypyrimidine tract-binding protein stimulates HIF-1α IRES-mediated translation during hypoxia. Nucleic Acids Research 33, 6884-6894 (2005).
[28] Yancoupoulos GD, Davis S, Gale NW, Rudge JS, Wiegand SJ & Holash J. Vascular-specific growth factors and blood vessel formation. Nature 407, 242-8 (2000).
[29] Masuda K, Abdelmohsen K & Gorospe M. RNA-binding proteins implicated in the hypoxic response. J Cell Mol Med 13, 2759-2769 (2009).
[30] Coles LS, Bartley MA, Bert A, Hunter J, Polyan S, Diamond P, Vadas MA & Goodall GJ. A multi-protein complex containing cold shock domain (Y-box) and polypyrimidine tract binding proteins forms on thevascularendothelial growth factormRNAPotential role in mRNA stabilization. Eur J Biochem 271, 648-660 (2004).
[31] Yao P, Wu J, Lindner D & Fox PL. Interplay between miR-574-3p and hnRNP L regulates VEGFA mRNA translation and tumorigenesis. Nucleic Acids Res 45, 7950-64 (2017).
[32] Iacono M, Mignone F & Pesole G. uAUG and uORFs in human and rodent 5'untranslated mRNAs. Gene 349, 97-105 (2005).
[33] Somers J, Pöyry T & Willis AE. A perspective on mammalian upstream open reading frame function. Int J Biochem Cell Biol 45, 1690-700 (2013).
[34] Komar AA & Hatzoglou M. Cellular IRES-mediated translation: the war of ITAFs in pathophysiological states. Cell Cycle 10, 229-40 (2011).
[35] Uniacke J, Holterman CE, Lachance G, Franovic A, Jacob MD, Fabian MR, Payette J, Holcik M, Pause A & Lee S. An oxygen-regulated switch in the protein synthesis machinery. Nature 486, 126-9 (2012).
[36] Staudacher JJ, Naarmann-de Vries IS, Ujvari SJ, Klinger B, Kasim M, Benko E, Ostareck-Lederer A, Ostareck DH, Bondke Persson A, Lorenzen S, Meier JC, Blüthgen N, Persson PB, Henrion-Caude A, Mrowka R & Fähling M. Hypoxia-induced gene expression results from selective mRNA partitioning to the endoplasmic reticulum. Nucleic Acids Res 43, 3219–3236 (2015).
[37] Hettiarachchi GK, Katneni UK, Hunt RC, Kames JM, Athey JC, Bar H, Sauna ZE, McGill JR, Ibla JC & Kimchi-Sarfaty C. Translational and transcriptional responses in human primary hepatocytes under hypoxia. Am J Physiol Gastrointest Liver Physiol 316, G720-G734 (2019).
[38] Voellenkle C, Garcia-Manteiga JM, Pedrotti S, Perfetti A, De Toma I, Da Silva D, Maimone B, Greco S, Fasanaro P, Creo P, Zaccagnini G, Gaetano C & Martelli F. Implication of Long noncoding RNAs in the endothelial cell response to hypoxia revealed by RNA-sequencing. Scientific Reports 6, 24141 (2016).
[39] Fiedler J, Baker AH, Dimmeler S, Heymans S, Mayr M & Thum T. Non-coding RNAs in vascular disease – from basic science to clinical applications: scientific update from the Working Group of Myocardial Function of the European Society of Cardiology. Cardiovascular Res 114, 1281-86 (2018).
[40] Chen LL & Yang L. Regulation of circRNA biogenesis. RNA Biol 12, 381-388 (2015).
[41] Boeckel JN, Jaé N, Heumüller AW, Chen W, Boon RA, Stellos K, Zeiher AM, John D, Uchida S & Dimmeler S. Identification and Characterization of Hypoxia-Regulated Endothelial Circular RNA. Circ Res 117, 884-890 (2015).

[42] Liang G, Liu Z, Tan L, Su A, Jiang WG & Gong C. HIF1α-associated circDENND4C Promotes Proliferation of Breast Cancer Cells in Hypoxic Environment. Anticancer Res 37, 4337-43 (2017).
[43] Ma L, Bajic VB & Zhang Z. On the classification of long non-coding RNA. RNA Biol 10, 924-933 (2013).
[44] Engreitz JM, Haines JE, Perez EM, Munson G, Chen J, Kane M, McDonel PE, Guttman M & Lander ES. Local regulation of gene expression by lncRNA promoters, transcription, and splicing. Nature 539, 452-455 (2016).
[45] Han P & Chang CP. Long non-coding RNA and chromatin remodeling. RNA Biol 12, 1094-98 (2015).
[46] Chang YN, Zhang K, Hu ZM, Qi HX, Shi ZM, Han XH, Han YW & Hong W. Hypoxia-regulated lncRNAs in cancer. Gene 575, 1-8 (2016).
[47] Takahashi K, Yan IK, Haga H & Patel T. Modulation of hypoxia-signaling pathways by extracellular linc-RoR. J of Cell Science 127, 1585-94 (2014).
[48] Wang Y, Liu X, Zhang H, Sun L, Zhou Y, Jin H, Zhang Ho, Zhang Hu, Liu J, Guo H, Nie Y, Wu K, Fan D, Zhang He & Liu L. Hypoxia-Inducible lncRNA-AK058003 Promotes Gastric Cancer Metastasis by Targeting γ-Synuclein. Neoplasis 16, 1094-1106 (2014).
[49] Liu H, Zhang Z, Xiong W, Zhang L, Du Y, Liu Y & Xiong X. Long non-coding RNA MALAT1 mediates hypoxia-induced pro-survival autophagy of endometrial stromal cells in endometriosis. J of Cell and Mol Med 23, 439-452 (2019).
[50] Yang F, Huo X, Yuan S, Zhang L, Zhou W, Wang F & Sun S. Repression of the Long Noncoding RNA-LET by Histone Deacetylase 3 Contributes to Hypoxia-Mediated Metastasis. Mol Cell 49, 1083-96 (2013).
[51] Tripathi V, Ellis JD, Shen Z, Song DY, Pan Q, Watt AT, Freier SM, Bennett CF, Sharma A, Bubulya PA, Blencowe BJ, Prasanth SG & Prasanth KV. The Nuclear-Retained Noncoding RNA MALAT1 Regulates Alternative Splicing by Modulating SR Splicing Factor Phosphorylation. Mol Cell 39, 925-938 (2010).
[52] Xu C, Yang M, Tian J, Wang X & Li Z. MALAT-1: A long non-coding RNA and its important 3' end functional motif in colorectal cancer metastasis. Int J Oncology 39, 169-175 (2011).
[53] Ying L, Chen Q, Wang Y, Zhou Z, Huang Y & Qiu F. Upregulated MALAT-1 contributes to bladder cancer cell migration by inducing epithelial-to-mesenchymal transition. Mol BioSystems 8, 2289-2294 (2012).
[54] Schmidt LH, Spieker T, Koschmieder S, Humberg J, Jungen D, Bulk E, Hascher A, Wittmer D, Marra A, Hillejan L, Wiebe K, Berdel WE, Wiewrodt R & Müller-Tidow C. The Long Noncoding MALAT-1 RNA Indicates a Poor Prognosis in Non-small Cell Lung Cancer and Induces Migration and Tumor Growth. J of Thoracic Oncology 6, 1984-1992 (2011).
[55] Iorio MV & Croce CM. MicroRNA dysregulation in cancer: diagnostics, monitoring and therapeutics. A comprehensive review. EMBO Mol Med 4, 143-159 (2012).
[56] Berezikov E, Chung WJ, Willis J, Cuppen E & Lai EC. Mammalian Mirtron Genes. Mol Cell 28, 328-336 (2007).
[57] Bhayani MK, Calin GA & Lai SY. Functional relevance of miRNA* sequences in human disease. Mutat Res 731, 14-19 (2012).
[58] Chan YC, Banerjee J, Choi SY & Sen CK. miR-210: The Master Hypoxamir. Microcirc 19, 215-223 (2012).
[59] Fasanaro P, D'Alessandra Y, Di Stefano V, Melchionna R, Romani S, Pompillo G, Capogrossi MC & Martelli F. MicroRNA-210 modulates endothelial cell response to hypoxia and inhibits the receptor tyrosine kinase ligand Ephrin-A3. J Biol Chem 283, 15878-83 (2008).
[60] Hua Z, Lv Q, Ye W, Wong CKA, Cai G, Gu D, Ji Y, Zhao C, Wang J, Yang BB & Zhang Y. MiRNA-Directed Regulation of VEGF and Other Angiogenic Factors under Hypoxia. PLoS ONE 1, e116 (2006).
[61] Jafarifar F, Yao P, Eswarappa SM & Fox PL. Repression of VEGFA by CA-rich element-binding microRNAs is modulated by hnRNP L. EMBO J 30, 1324-1334 (2011).

[62] Martin SK, Diamond P, Gronthos S, Peet DJ & Zannettino ACW. The emerging role of hypoxia, HIF-1 and HIF-2 in multiple myeloma. Leukemia 25, 1533-1542 (2011).
[63] Brown JM & Wilson WR. Exploiting Tumour Hypoxia In Cancer Treatment. Nature Reviews 4, 437-447 (2004).
[64] Harris AL. Hypoxia — A Key Regulatory Factor In Tumour Growth. Nature Reviews Cancer 2, 38-47 (2002).
[65] Noman MZ, Janji B, Berchem G, Mami-Chouaib F & Chouaib S. Hypoxia-induced autophagy: A new player in cancer immunotherapy? Autophagy 8, 704-706 (2012).
[66] Wilson WR & Hay MP. Targeting hypoxia in cancer therapy. Nature Reviews Cancer 11, 393-410 (2011).
[67] Harper SJ & Bates DO. VEGF-A splicing: the key to anti-angiogenic therapeutics? Nature Reviews Cancer 8, 880-7 (2008).
[68] Will CL & Lührmann R. Spliceosome Structure and Function. Cold Spring Harb Perspect Biol 3, 7 (2011).
[69] Cieply B & Carstens RP. Functional roles of alternative splicing factors in human disease. WIREs RNA 6, 311-326 (2015).
[70] De Conti L, Baralle M & Buratti E. Exon and intron definition in pre-mRNA splicing. Wiley Interdiscip Rev RNA 4, 49-60 (2013).
[71] Deckert J, Hartmuth K, Boehringer D, Behzadnia N, Will CL, Kastner B, Stark H, Urlaub H & Lührmann R. Protein Composition and Electron Microscopy Structure of Affinity-Purified Human Spliceosomal B Complexes Isolated under Physiological Conditions. Molecular and Cellular Biology 26, 5528-5543 (2006).
[72] Wahl MC, Will CL & Lührmann R. The Spliceosome: Design Principlesof a Dynamic RNP Machine. Cell 136, 701-718 (2009).
[73] Fox-Walsh KL, Dou Y, Lam BJ, Hung S, Baldi PF & Hertel KJ. The architecture of pre-mRNAs affects mechanisms of splice-site pairing. PNAS 102, 16176-16181 (2005).
[74] Pan Q, Shai O, Lee LJ, Frey BJ & Blencowe BJ. Deep surveying of alternative splicing complexity in the human transcriptome by high-throughput sequencing. Nature Genetics 40, 1413-1415 (2008).
[75] Wang ET, Sandberg R, Luo S, Khrebtukova I, Zhang L, Mayr C, Kingsmore SF, Schroth GP & Burge CB. Alternative isoform regulation in human tissue transcriptomes. Nature 456, 470-476 (2008).
[76] Kelemen O, Convertini P, Zhang Z, Wen Y, Shen M, Falaleeva M & Stamm S. Function of alternative splicing. Gene 1, 1-30 (2013).
[77] Gallego-Paez LM, Bordone MC, Leote AC, Saraiva-Agostinho N, Ascensao-Ferreira M & Barbosa-Morais NL. Alternative splicing: the pledge, the turn, and the prestige - The key role of alternative splicing in human biological systems. Hum Genet 136, 1015-1042 (2017).
[78] Scotti MM & Swanson MS. RNA mis-splicing in disease. Nature Rev Genetics 17, 19-32 (2016).
[79] McManus CJ & Graveley BR. RNA structure and the mechanisms of alternative splicing. Curr Opin Genet Dev 21, 373-379 (2011).
[80] Chen M & Manley JL. Mechanisms of alternative splicing regulation: insights from molecular and genomics approaches. Nat Rev Mol Cell Biol 10, 741-54 (2009).
[81] Anczuków O & Krainer AR. Splicing-factor alterations in cancers. RNA 22, 1285-1301 (2016).
[82] Biamonti G, Catillo M, Pignataro D, Montecucco A & Ghigna C. The alternative splicing side of cancer. Sem in Cell & Dev Biol 32, 30-36 (2014).
[83] Kurosaki T & Maquat LE. Nonsense-mediated mRNA decay in humans at a glance. J Cell Sci 129, 461-467 (2016).
[84] Hillman RT, Green RE & Brenner SE. An unappreciated role for RNA surveillance. Genome Biology 5, R8 (2004).
[85] Ge Y & Porse BT. The functional consequences of intron retention: Alternative splicing coupled to NMD as a regulator of gene expression. Bioessays 36, 236-243 (2013).

[86] Green RE, Lewis BP, Hillman RT, Blanchette M, Lareau LF, Garnett AT, Rio DC & Brenner SE. Widespread predicted nonsense-mediated mRNA decay of alternatively-spliced transcripts of human normal and disease genes. Bioinformatics 19 Suppl 1, 118-21 (2003).

[87] Pan Q, Saltzman AL, Kim YK, Misquitta C, Shai Q, Maquat LE, Frey BJ & Blencowe BJ. Quantitative microarray profiling provides evidence against widespread coupling of alternative splicing with nonsense-mediated mRNA decay to control gene expression. Genes Dev 15, 153-8 (2006).

[88] Wittmann J, Hol EM & Jäck HM. hUPF2 silencing identifies physiologic substrates of mammalian nonsense-mediated mRNA decay. Mol Cell Biol 26, 1272-87 (2006).

[89] Kurosaki T & Maquat LE. Nonsense-mediated mRNA decay in humans at a glance. J of Cell Sci 129, 461-467 (2016).

[90] Lareau LF, Inada M, Green RE, Wengrod JC & Brenner SE. Unproductive splicing of SR genes associated with highly conserved and ultraconserved DNA elements. Nature 446, 926-9 (2007).

[91] Saltzman AL, Kim YK, Pan Q, Fagnani MM, Maquat LE & Blencowe BJ. Regulation of multiple core spliceosomal proteins by alternative splicing-coupled nonsense-mediated mRNA decay. Mol Cell Biol 28, 4320-30 (2008).

[92] Ni JZ, Grate L, Donohue JP, Preston C, Nobida N, O'Brien G, Shiue L, Clark TA, Blume JE & Ares M Jr. Ultraconserved elements are associated with homeostatic control of splicing regulators by alternative splicing and nonsense-mediated decay. Genes & Dev 21, 708-718 (2007).

[93] Stoilov P, Daoud R, Nayler O & Stamm S. Human tra2-beta1 autoregulates its protein concentration by influencing alternative splicing of its pre-mRNA. Hum Mol Genet 13, 509-24 (2004).

[94] Jumaa H & Nielsen PJ. The splicing factor SRp20 modifies splicing of its own mRNA and ASF/SF2 antagonizes this regulation. EMBO J. 16, 5077-5085 (1997).

[95] Rahman L, Bliskovski V, Kaye FJ & Zajak-Kaye M. Evolutionary conservation of a 2-kb intronic sequence flanking a tissue-specific alternative exon in the PTBP2 gene. Genomics 83, 76-84 (2004).

[96] Wilson GM, Sun Y, Sellers J, Lu H, Penkar N, Dillard G & Brewer G. Regulation of AUF1 expression via conserved alternatively spliced elements in the 3' untranslated region. Mol Cell Biol 19, 4056-64 (1999).

[97] Kemmerer K, Fischer S & Weigand JE. Auto- and cross-regulation of the hnRNPs D and DL. RNA 24, 324-331 (2018).

[98] Spellman R, Llorian M & Smith CW. Crossregulation and functional redundancy between the splicing regulator PTB and its paralogs nPTB and ROD1. Mol Cell 27, 420-34 (2007).

[99] Rossbach O, Hung LH, Schreiner S, Grishina I, Heiner M, Hui J & Bindereif A. Auto- and cross-regulation of the hnRNP L proteins by alternative splicing. Mol Cell Biol 29, 1442-51 (2009).

[100] Venables JP. Aberrant and Alternative Splicing in Cancer. Cancer Res 64, 7647-7654 (2004).

[101] Chabot B & Shkreta L. Defective control of pre–messenger RNA splicing in human disease. J Cell Biol 212, 13-27 (2016).

[102] Holmilla R, Fouquet C, Cadranel J, Zalcman G & Soussi T. Splice mutations in the p53 gene: case report and review of the literature. Hum Mutat 21, 101-2 (2003).

[103] Broeks A, Urbanus JH, de Knijff P, Devilee P, Nicke M, Klöpper K, Dörk T, Floore AN & van't Veer LJ. IVS10-6T>G, an ancient ATM germline mutation linked with breast cancer. Hum Mutat 21, 521-8 (2003).

[104] Hoffman JD, Hallam SE, Venne VL, Lyon E & Ward K. Implications of a novel cryptic splice site in the BRCA1 gene. Am J Med Genet 80, 140-4 (1998).

[105] Musolini A, Bella MA, Bortesi B, Michiara M, Naldi N, Zanelli P, Capeletti M, Pezzuolo D, Camisa R, Savi M, Neri TM & Ardizzoni A. BRCA mutations, molecular markers, and clinical variables in early-onset breast cancer: A population-based study. The breast 16, 280-292 (2007).

[106] Hollander MC, Blumenthal GM & Dennis PA. PTEN loss in the continuum of common cancers, rare syndromes and mouse models. Nature Reviews Cancer 11, 289-301 (2011).

[107] Carracedo A, Alimonti A & Pandolfi PP. PTEN Level in Tumor Suppression: How Much Is Too Little? Cancer Res 71, 629-33 (2011).
[108] Agrawal S & Eng C. Differential expression of novel naturally occurring splice variants of PTEN and their functional consequences in Cowden syndrome and sporadic breast cancer. Hum Mol Gen 15, 777-787 (2006).
[109] Xu Y, Gau XD, Lee JH, Huang H, Tan H, Ahn J, Reinke LM, Peter ME, Feng Y, Gius D, Siziopikou KP, Peng J, Xiao X & Cheng C. Cell type-restricted activity of hnRNPM promotes breast cancer metastasis via regulating alternative splicing. Genes & Dev 28, 1191-1203 (2014).
[110] Bonomi S, Gallo S, Catillo M, Pignataro D, Biamonti G & Ghigna C. Oncogenic Alternative Splicing Switches: Role in Cancer Progression and Prospects for Therapy. Int J Cell Biol 2013, 1-17 (2013).
[111] Nowak DG, Woolard J, Amin EM, Konopatskaya O, Saleem MA, Churchill AJ, Ladomery MR, Harper SJ & Bates DO. Expression of pro- and anti-angiogenic isoforms of VEGF is differentially regulated by splicing and growth factors. J Cell Sci 121, 3487-95 (2008).
[112] Faustino NA & Cooper TA. Pre-mRNA splicing and human disease. Genes Dev 17, 419-37 (2003).
[113] Garcia-Blanco MA, Baraniak AP & Lasda EL. Alternative splicing in disease and therapy. Nat Biotechnol 22, 535-46 (2004).
[114] Lee SCW & Abdel-Wahab O. Therapeutic targeting of splicing in cancer. Nature Med 22, 976-86 (2016).
[115] Lin JC. Therapeutic Applications of Targeted Alternative Splicing to Cancer Treatment. Int J of Mol Sci 19, 75 (2018).
[116] Havens MA & Hastings ML. Splice-switching antisense oligonucleotides as therapeutic drugs. Nucleic Acids Res 44, 1141-1172 (2016).
[117] Lim KR, Maruyama R & Yokota T. Eteplirsen in the treatment of Duchenne muscular dystrophy. Drug Des Dev Ther 11, 533-545 (2017).
[118] Wilfond BS, Morales C & Taylor HA. Expanded access for nusinersen in patients with spinal muscular atrophy: Negotiating limited data, limited alternative treatments, and limited hospital resources. Am J of Bioeth 17, 66-67 (2017).
[119] Gerstberger S, Hafner M & Tuschl T. A census of human RNA-binding proteins. Nature Reviews Genetics 15, 829-845 (2014).
[120] Hentze MW, Castella A, Schwarzl T & Preiss T. A brave new world of RNA-binding proteins. Nature Reviews Molecular Cell Biology 19, 327-341 (2018).
[121] Glisovic T, Bachorik JL, Yong J & Dreyfuss G. RNA-binding proteins and post-transcriptional gene regulation. FEBS letters 582, 1977-1986 (2008).
[122] Howard JM & Sanford JR. The RNAissance family: SR proteins as multifaceted regulators of gene expression. Wiley Interdiscip Rev RNA 6, 93-110 (2015).
[123] Manley JL & Krainer AR. A rational nomenclature for serine/arginine-rich protein splicing factors (SR proteins). Genes Dev 24, 1073-4 (2010).
[124] Geuens T, Bouhy D & Timmermann V. The hnRNP family: insights into their role in health and disease. Hum Genet 135, 851-867 (2016).
[125] Han SP, Tang YH & Smith R. Functional diversity of the hnRNPs: past, present and perspectives. Biochemical J 430, 379-392 (2010).
[126] Kalsotra A, Xiao X, Ward AJ, Castle JC, Johnson JM, Burge CB & Cooper TA. A postnatal switch of CELF and MBNL proteins reprograms alternative splicing in the developing heart. PNAS 105, 20333-20338 (2008).
[127] Gabut M, Chaudhry S & Blencowe BJ. SnapShot: The splicing regulatory machinery. Cell 133, 192.e1 (2008).
[128] Matlin AJ, Clark F & Smith CW. Understanding alternative splicing: towards a cellular code. Nat Rev Mol Cell Biol 5, 386-98 (2005).
[129] Dassi E. Handshakes and Fights: The Regulatory Interplay of RNA-Binding Proteins. Front Mol Biosci 4, 67 (2017).

[130] Wang ET, Ward AJ, Cherone JM, Giudice J, Wang TT, Treacy DJ, Lambert NJ, Freese P, Saxena T, Cooper TA & Burge CB. Antagonistic regulation of mRNA expression and splicing by CELF and MBNL proteins. Genome Res 25, 858-871 (2015).

[131] Kedde Martijn & Agami Reuven. Interplay between microRNAs and RNA-binding proteins determines developmental processes. Cell Cycle 7, 899-903 (2008).

[132] Kamei D, Tsuchiya N, Yamazaki M, Meguro H & Yamada M. Two forms of expression and genomic structure of the human heterogeneous nuclear ribonucleoprotein D-like JKTBP gene (HNRPDL). Gene 228, 13-22 (1999).

[133] Tsuchiya N, Kamei D, Takano A, Matsui T & Yamada M. Cloning and characterization of a cDNA encoding a novel heterogeneous nuclear ribonucleoprotein-like protein and its expression in myeloid leukemia cells. J Biochem 123, 499-507 (1998).

[134] Lal A, Mazan-Mamczarz K, Kawai T, Yang X, Martindale JL & Gorospe M. Concurrent versus individual binding of HuR and AUF1 to common labile target mRNAs. EMBO J 23, 3092-102 (2004).

[135] Li X, Johansson C, Glahder J, Mossberg AK & Schwartz S. Suppression of HPV-16 late L1 5'-splice site SD3632 by binding of hnRNP D proteins and hnRNP A2/B1 to upstream AUAGUA RNA motifs. Nucleic Acids Res 41, 10488-508 (2013).

[136] Reboll MR, Oumard A, Gazdag AC, Renger I, Ritter B, Schwarzer M, Hauser H, Wood M, Yamada M, Resch K & Nourbakhsh M. NRF IRES activity is mediated by RNA binding protein JKTBP1 and a 14-nt RNA element. RNA 13, 1328-1340 (2007).

[137] Nourbakhsh M & Hauser H. Constitutive silencing of IFN-b promoter is mediated by NRF (NF-kB-repressing factor), a nuclear inhibitor of NF-kB. EMBO J 18, 6415-6425 (1999).

[138] Nourbakhsh M, Kalble S, Dorrie A, Hauser H, Resch K & Kracht M. The NF-kb repressing factor is involved in basal repression and interleukin (IL)-1-induced activation of IL-8 transcription by binding to a conserved NF-kb-flanking sequence element. J Biol Chem 276, 4501-4508 (2001).

[139] Feng X, Guo Z, Nourbakhsh M, Hauser H, Ganster R, Shao L & Geller DA. Identification of a negative response element in the human inducible nitric oxide synthase (hiNOS) promoter: The role of NF-kB repressing factor (NRF) in basal repression of the hiNOS gene. PNAS 99, 14212-14217 (2002).

[140] Omnus DJ, Mehrtens S, Ritter B, Resch K, Yamada M, Frank R, Nourbakhsh & Reboll MR. JKTBP1 Is Involved in Stabilization and IRES-Dependent Translation of NRF mRNAs by Binding to 5′ and 3′ Untranslated Regions. J of Mol Biol 407, 492-504 (2011).

[141] Bosch FX, Lorincz A, Munoz N, Meijer CJ & Shah KV. The causal relation between human papillomavirus and cervical cancer. J Clin Pathol 55, 244-265 (2002).

[142] Boopathi E, Lenka N, Prabu SK, Fang JK, Wilkinson F, Atchison M, Giallongo A & Avadhani NG. Regulation of murine cytochrome c oxidase Vb gene expression during myogenesis: YY-1 and heterogeneous nuclear ribonucleoprotein D-like protein (JKTBP1) reciprocally regulate transcription activity by physical interaction with the BERF-1/ZBP-89 factor. J Biol Chem 279, 35242-54 (2004).

[143] Akagi T, Kamei D, Tsuchiya N, Nishina Y, Horiguchi H, Matsui M, Kamma H & Yamada M. Molecular characterization of a mouse heterogeneous nuclear ribonucleoprotein D-like protein JKTBP and its tissue-specific expression. Gene 245, 267-273 (2000).

[144] Loflin P, Chen CYA & Shyu AB. Unraveling a cytoplasmic role for hnRNP D in the in vivo mRNA destabilization directed by the AU-rich element. Genes & Dev 13, 1884-1897 (1999).

[145] Kawamura H, Tomozoe Y, Akagi T, Kamei D, Ochiai M & Yamada M. Identification of the Nucleocytoplasmic Shuttling Sequence of Heterogeneous Nuclear Ribonucleoprotein D-like Protein JKTBP and Its Interaction with mRNA. J Biol Chem 277, 2732-2739 (2002).

[146] Lomonaco V, Martoglia R, Mandreoli F, Anderlucci L, Emmett W, Bicciato S & Taccioli C. UCbase 2.0: ultraconserved sequences database (2014 update). Database 2014, bau062 (2014).

[147] Kemmerer K. Alternatives Spleißen unter Hypoxie in humanen Endothelzellen. Doctoral thesis, Technische Universität Darmstadt (2016).

[148] Fischer S. Untersuchung von konservierten Elementen in nicht translatierten Bereichen der mRNA bei Sauerstoffmangel. Bachelor thesis. Technische Universität Darmstadt (2013).

[149] Hang X, Li P, Li Z, Qu W, Yu Y, Li H, Shen Z, Zheng H, Gao Y, Wu Y, Deng M, Sun Z & Zhang C. Transcription and splicing regulation in human umbilical vein endothelial cells under hypoxic stress conditions by exon array. BMC Genomics 10, 126 (2009).

[150] Kemmerer K. Analyse von RNA-Sekundärstrukturelementen in nichtkodierenden Bereichen. Diploma thesis, Goethe-Universität Frankfurt am Main (2011).

[151] Suzuki T, Shimizu T, Satoh K, Sugibayashi R & Takeda K. Differential expression of genes during TPA-induced differentiation of human prostatic cancer TSU-Pr1 cells. Int J Mol Med 10, 735-9 (2002).

[152] Wu YY, Li H, Lv XY, Wie Q, Li X, Liu XY, Zhou Q & Wie YQ. Overexpression of JKTBP1 induces androgen-independent LNCaP cell proliferation through activation of epidermal growth factor-receptor (EGF-R). Cell Biochem Funct 26, 467-477 (2008).

[153] Zhou H, Ge Y, Sun L, Ma W, Wu J, Zhang X, Hu X, Eaves CJ, Wu D & Zhao Y. Growth arrest specific 2 is upregulated in chronic myeloid leukemia cells and required for their growth. PLoS One 9, e86195 (2014).

[154] Ji D, Zhang P, Ma W, Fei Y, Xue W, Wang Y, Zhang X, Zhou H & Zhao Y. Oncogenic heterogeneous nuclear ribonucleoprotein D-like modulates the growth and imatinib response of human chronic myeloid leukemia CD34+ cells via pre-B-cell leukemia homeobox 1. Oncogene, ePub ahead of print (2019).

[155] Wang C, Zheng M, Wang S, Nie X, Guo Q, Gao L, Li X, Qi Y, Liu J & Lin B. Whole Genome Analysis and Prognostic Model Construction Based on Alternative Splicing Events in Endometrial Cancer. BioMed Res Int 2019, Article ID 2686875, 10 pages (2019).

[156] Vieira NM, Naslavsky MS, Licinio L, Kok F, Schlesinger D, Vainzof M, Sanchez N, Kitajima JP, Gal L, Cavacana N, Serafini PR, Chuartzman S, Vasquez C, Mimbacas A, Nigro V, Pavanello RC, Schuldiner M, Kunkel LM & Zatz M. A defect in the RNA-processing protein HNRPDL causes limb-girdle muscular dystrophy 1G (LGMD1G). Hum Mol Gen 23, 4103-10 (2014).

[157] Pascual M, Vicente M, Monferrer L & Artero R. The Muscleblind family of proteins: an emerging class of regulators of developmentally programmed alternative splicing. Differentiation 74, 65-80 (2006).

[158] Teplova M & Patel D. Structural insights into RNA recognition by the alternative-splicing regulator muscleblind-like MBNL1. Nat Struct Mol Biol 15, 1343-1351 (2008).

[159] Goers E, Purcell J, Voelker R, Gates D & Berglund J. MBNL1 binds GC motifs embedded in pyrimidines to regulate alternative splicing. Nucleic Acids Res 38, 2467-2484 (2010).

[160] Konieczny P, Stepniak-Konieczna E & Sobczak K. MBNL proteins and their target RNAs, interaction and splicing regulation. Nucleic Acids Research 42, 10873-10887 (2014).

[161] Witten JT & Ule J. Understanding splicing regulation through RNA splicing maps. Trends in Genetics 27, 89-97 (2011).

[162] Taylor K, Sznaijder LJ, Cywoniuk P, Thomas JD, Swanson MS & Sobczak K. MBNL splicing activity depends on RNA binding site structural context. Nucleic Acids Research 46, 9119-9133 (2018).

[163] Adereth Y, Dammai V, Kose N, Li R & Hsu T. RNA-dependent integrin alpha3 protein localization regulated by the Muscleblind-like protein MLP1. Nat Cell Biol 7, 1240-1247 (2005).

[164] Du H, Cline MS, Osborne RJ, Tuttle DL, Clark TA, Donohue JP, Hall MP, Shiue L, Swanson MS, Thornton CA & Ares MJr. Aberrant alternative splicing and extracellular matrix gene expression in mouse models of myotonic dystrophy. Nat Struct Mol Biol 17, 187-193 (2010).

[165] Masuda A, Andersen HS, Doktor TK, Okamoto T, Ito M, Andresen BS & Ohno K. CUGBP1 and MBNL1 preferentially bind to 3' UTRs and facilitate mRNA decay. Sci Rep 2, 209 (2012).

[166] Zu T, Cleary JD, Liu Y, Banez-Coronel M, Bubenik JL, Ayhan F, Ashizawa T, Xia G, Clark HB, Yachnis AT, Swanson MS & Ranum LPW. RAN Translation Regulated by Muscleblind Proteins in Myotonic Dystrophy Type 2. Neuron 95, 1292-1305 (2017).

[167] Batra R, Charizanis K, Manchanda M, Mohan A, Li M, Finn DJ, Goodwin M, Zhang C, Sobczak K, Thornton CA & Swanson MS. Loss of MBNL leads to disruption of developmentally regulated alternative polyadenylation in RNA-mediated disease. Mol Cell, 56, 311-322 (2014).

[168] Rau F, Freyermuth F, Fugier C, Villemin JP, Fischer MC, Jost B, Dembele D, Gourdon G, Nicole A, Duboc D Wahbi K, Day JW, Fujimura H, Takahashi MP, Auboeuf D, Dreumont N, Furling D & Charlet-Berguerand N. Misregulation of miR-1 processing is associated with heart defects in myotonic dystrophy. Nat Struct Mol Biol 18, 840-845 (2011).

[169] Wang ET, Cody NAL, Jog S, Biancolella M, Wang TT, Treacy DJ, Luo S, Schroth GP, Housman DE, Reddy S, Lécuyer E & Burge CB. Transcriptome-wide Regulation of Pre-mRNA Splicing and mRNA Localization by Muscleblind Proteins. Cell 150, 710-724 (2012).

[170] Sznaijder LJ, Michalak M, Taylor K, Cywoniuk P, Kabza M, Wojtkowiak-Szlachcic A, Matloka M, Konieczny P & Sobczak K. Mechanistic determinants of MBNL activity. Nucleic Acids Research 44, 10326-10342 (2016).

[171] Konieczny P, Stepniak-Konieczna E & Sobczak K. MBNL expression in autoregulatory feedback loops. RNA Biol 15, 1-8 (2018).

[172] Miller JW, Urbinati CR, Teng-Umnuay P, Stenberg MG, Byrne BJ, Thornton CA & Swanson MS. Recruitment of human muscleblind proteins to (CUG)(n) expansions associated with myotonic dystrophy. EMBO J 19, 4439-48 (2000).

[173] Lee KY, Li M, Manchanda M, Batra R, Charizanis K, Mohan A, Warren SA, Chamberlain CM, Finn D, Hong H, Ashraf H, Kasahara H, Ranum LP & Swanson MS. Compound loss of muscleblind-like function in myotonic dystrophy. EMBO Mol Med 5, 1887-1900 (2013).

[174] Sznajder LJ & Swanson MS. Short Tandem Repeat Expansions and RNA-Mediated Pathogenesis in Myotonic Dystrophy. Int J Mol Sci 20, pii: E3365 (2019).

[175] Tang R, Qi Q, Wu R, Zhou X, Wo D, Zhou H, Mao Y, Li R, Liu C, Wang L, Chen W, Hua D, Zhang H & Wang W. The polymorphic terminal-loop of pre-miR-1307 binding with MBNL1 contributes to colorectal carcinogenesis via interference with Dicer1 recruitment. Carcinogenesis 36, 867-875 (2015).

[176] Fish L, Pencheva N, Goodarzi H, Tran H, Yoshida M & Tavazoie SF. Muscleblind-like 1 suppresses breast cancer metastatic colonization and stabilizes metastasis suppressor transcripts. Genes & Dev. 30, 386-398 (2016).

[177] Tang L, Zhao P & Kong D. Muscleblind‐like 1 destabilizes Snail mRNA and suppresses the metastasis of colorectal cancer cells via the Snail/E‐cadherin axis. Int J Oncol 54, 955-965 (2019).

[178] Tabaglio T, Low DHP, Teo WKL, Goy PA, Cywoniuk P, Wollmann H, Ho J, Tan D, Aw J, Pavesi A, Sobczak K Wee DKB & Guccione E. MBNL1 alternative splicing isoforms play opposing roles in cancer. Life Science Alliance online (2018).

[179] Chen A, Sceneay J, Gödde N, Kinwel T, Ham S, Thompson EW, Humbert PO & Möller A. Intermittent hypoxia induces a metastatic phenotype in breast cancer. Oncogene online (2018).

[180] Lee YH, Jhuang YL, Chen YL, Jeng YM & Yuan RH. Paradoxical overexpression of MBNL2 in hepatocellular carcinoma inhibits tumor growth and invasion. Oncotarget 7, 65589-65601 (2016).

[181] Perron G, Jandaghi P, Solanki S, Safisamghabadi M, Storoz C, Karimzadeh M, Papadakis AI, Arsenault M, Scelo G, Banks RE, Trost J, Lanthrop M, Tanguay S, Brazma A, Huang S, Brimo F, Najafabadi H & Riazalhosseini Y. A General Framework for Interrogation of mRNA Stability Programs Identifies RNA-Binding Proteins that Govern Cancer Transcriptomes. Cell Reports 23, 1639-1650 (2018).

[182] Zhang J, Zheng Z, Wu M, Zhang L, Wang J, Fu W, Xu N, Zhao Z, Lao Y & Xu H. The natural compound neobractatin inhibits tumor metastasis by upregulating the RNA-binding-protein MBNL2. Cell Death Dis 10, 554 (2019).

[183] Yuan J, Liu X, Wang T, Pan W, Tao Q, Zhou W, Wang F & Sun S. The MBNL3 splicing factor promotes hepatocellular carcinoma by increasing PXN expression through the alternative splicing of lncRNA-PXN-AS1. Nature Cell Biology 19, 820-832 (2017).

[184] Weigand JE, Boeckel JN, Gellert P & Dimmeler S. Hypoxia-Induced Alternative Splicing in Endothelial Cells. PLoS ONE 7, e42697 (2012).
[185] Hu X, Wu R, Shehadeh LA, Zhou Q, Jiang C, Huang X, Zhang L, Gao F, Liu X, Yu H, Webster KA & Wang J. Severe hypoxia exerts parallel and cell-specific regulation of gene expression and alternative splicing in human mesenchymal stem cells. BMC Genomics 15, 303 (2014).
[186] Sena JA, Wang L, Heasley LE & Hu CJ. Hypoxia regulates alternative splicing of HIF and non-HIF target genes. Mol Cancer Res 12, 1233-43 (2014).
[187] Weigand JE. Unpublished data (2016).
[188] Kim I, Moon SO, Park SK, Chae SW & Koh GY. Angiopoietin-1 Reduces VEGF-Stimulated Leukocyte Adhesion to Endothelial Cells by Reducing ICAM-1, VCAM-1, and E-Selectin Expression. Circ Res 89, 477-479 (2001).
[189] Fearnley GW, Odell AF, Latham AM, Mughal NA, Bruns AF, Burgoyne NJ, Homer-Vanniasinkam S, Zachary IC, Hollstein MC, Wheatcroft SB & Ponnambalam S. VEGF-A isoforms differentially regulate ATF-2–dependent VCAM-1 gene expression and endothelial–leukocyte interactions. Mol Biol Cell 25, 2315-37 (2014).
[190] Gimbel AT. Identification of novel mRNA-RBP interactions. Master thesis. Technische Universität Darmstadt (2017).
[191] Bray F, Ferlay J, Soerjomataram I, Siegel RL, Torre LA & Jemal A. Global cancer statistics 2018: GLOBOCAN estimates of incidence and mortality worldwide for 36 cancers in 185 countries. CA Cancer J Clin 68, 394-424 (2018).
[192] Siegel RL, Miller KD & Jemal A. Cancer statistics, 2019. CA Cancer J Clin 69, 7-34 (2019).
[193] Love MI, Huber W & Anders S. Moderated estimation of fold change and dispersion for RNA-seq data with DESeq2. Genome Biol 15, 550 (2014).
[194] Shen S, Park JW, Lu ZX, Lin L, Henry MD, Wu YN, Zhou Q & Xing Y. rMATS: robust and flexible detection of differential alternative splicing from replicate RNA-Seq data. PNAS 111, E5593-5601 (2014).
[195] Conesa A, Madrigal P, Tarazona S, Gomez-Cabrero D, Cervera A, McPherson A, Wojciech Szczésniak M, Gaffney DJ, Elo LL, Zhang X & Mortazavi A. A survey of best practices for RNA-seq data analysis. Genome Biol 17, 13 (2016).
[196] Wagner GP, Kin K & Lynch VJ. Measurement of mRNA abundance using RNA-seq data: RPKM measure is inconsistent among samples. Theory Biosci 131, 281-285 (2012).
[197] Li B, Ruotti V, Stewart RM, Thomson JA & Dewey CN. RNA-Seq gene expression estimation with read mapping uncertainty. Bioinformatics 26, 493-500 (2010).
[198] Schafer S, Miao K, Benson GC, Heinig M, Cook SA & Hubner N. Alternative Splicing Signatures in RNA-seq Data: Percent Spliced in (PSI). Curr Prot in Human Gen 87, 11.16.1-11.16.14 (2015).
[199] Gerhardus JS. Alternatives Spleißen in Antwort auf Sauerstoffmangel in Krebszellen. Bachelor thesis. Technische Universität Darmstadt (2017).
[200] Ray D, Kazan H, Cook KB, Weirauch MT, Najafabadi HS, Li X, Gueroussov S, Albu M, Zheng H, Yang A, Na H, Irimia M, Matzat LH, Dale RK, Smith SA, Yarosh CA, Kelly SM, Nabet B, Mecenas D, Li W, Laishram RS, Qiao M, Lipshitz HD, Piano F, Corbett AH, Carstens RP, Frey BJ, Anderson RA, Lynch KW, Penalva LOF, Lei EP, Fraser AG, Blencowe BJ, Morris Q & Hughes TR. A compendium of RNA-binding motifs for decoding gene regulation. Nature 499, 172-177 (2013).
[201] Lambert N, Robertson A, Jangi M, McGeary S, Sharp PA & Burge CB. RNA Bind-n-Seq: quantitative assessment of the sequence and structural binding specificity of RNA binding proteins. Mol Cell 54, 887-900 (2014).
[202] Cywoniuk P, Taylor K, Sznajder LJ & Sobczak K. Hybrid splicing minigene and antisense oligonucleotides as efficient tools to determine functional protein/RNA interactions. Sci Rep 7, 17587 (2017).
[203] Amable L. Cisplatin resistance and opportunities for precision medicine. Pharmacological Res 106, 27-36 (2016).

[204] Dasari S & Tchounwou PB. Cisplatin in cancer therapy: Molecular mechanisms of action. Eur J of Pharmacology 740, 364-378 (2014).
[205] Galluzzi L, Senovilla L, Vitale I, Michels J, Martins I, Kepp O, Castedo M & Kroemer G. Molecular mechanisms of cisplatin resistance. Oncogene 31, 1869-83 (2012).
[206] Wlotzka K. Regulation des RNA-Bindeproteins MBNL2 unter Hypoxie. Bachelor thesis. Technische Universität Darmstadt (2018).
[207] Hafner M, Landthaler M, Burger L, Khorshid M, Haussner J, Berninger P, Rothballer A, Ascano M, Jungkamp AC, Munschauer M, Ulrich A, Wardle GS, Dewell S, Zavolan M & Tuschl T. Transcriptome-wide Identification of RNA-Binding Protein and MicroRNA Target Sites by PAR-CLIP. Cell 141, 129-141 (2010).
[208] Avendano-Vazquez SE, Dhir A, Bembich S, Buratto E, Proudfoot N & Baralle FE. Autoregulation of TDP-43 mRNA levels involves interplay between transcription, splicing, and alternative polyA site selection. Genes & Dev 26, 1679-1684 (2012).
[209] Bergeron D, Pal G, Beaulieu YB, Chabot B & Bachand F. Regulated Intron Retention and Nuclear Pre-mRNA Decay Contribute to *PABPN1* Autoregulation. Mol Cell Biol 35, 2503-17 (2015).
[210] Loflin P, Chen CYA & Shyu AB. Unraveling a cytoplasmic role for hnRNP D in the in vivo mRNA destabilization directed by the AU-rich element. Genes & Dev 13, 1884-97 (1999).
[211] Raineri I, Wegmueller D, Gross B, Certa U & Moroni C. Roles of AUF1 isoforms, HuR and BRF1 in ARE-dependent mRNA turnover studied by RNA interference. Nucleic Acids Res 32, 1279-88 (2004).
[212] Lu JY & Schneider RJ. Tissue distribution of AU-rich mRNA-bind- ing proteins involved in regulation of mRNA decay. J Biol Chem 279, 12974–79 (2004).
[213] Laroia G, Cuesta R, Brewer G & Schneider RJ. Control of mRNA decay by heat shock-ubiquitin-proteasome pathway. Science 284, 499–502 (1999).
[214] Zucconi BE & Wilson GM. Modulation of neoplastic gene regulato- ry pathways by the RNA-binding factor AUF1. Front Biosci (Landmark Ed) 16, 2307–25 (2011).
[215] Lal A, Mazan-Mamczarz K, Kawai T, Yang X, Martindale JL & Gorospe M. Concurrent versus individual binding of HuR and AUF1 to common labile target mRNAs. EMBO J 23, 3092-3102 (2004).
[216] Gao R, Yu Y, Inoue A, Widodo N, Kaul SC & Wadhwa R. Heterogeneous Nuclear Ribonucleoprotein K (hnRNP-K) Promotes Tumor Metastasis by Induction of Genes Involved in Extracellular Matrix, Cell Movement, and Angiogenesis. J Biol Chem 288, 15046-56 (2013).
[217] Moran-Jones K, Grindlay J, Jones M, Smith R & Norman JC. hnRNP A2 Regulates Alternative mRNA Splicing of TP53INP2 to Control Invasive Cell Migration. Cancer Res 69, 9219-27 (2009).
[218] Babic I, Sharma S & Black DL. A Role for Polypyrimidine Tract Binding Protein in the Establishment of Focal Adhesions. Mol Cell Biol 29, 5564-77 (2009).
[219] Al-Khalaf HH & Aboussekhra A. MicroRNA-141 and MicroRNA-146b-5p Inhibit the Prometastatic Mesenchymal Characteristics through the RNA-binding Protein AUF1 Targeting the Transcription Factor ZEB1 and the Protein Kinase AKT. J Biol Chem 289, 31433-47 (2014).
[220] Chang SH & Hla T. Gene regulation by RNA binding proteins and microRNAs in angiogenesis. Trends in Mol Med 17, 650-658 (2011).
[221] Fellows A, Griffin ME, Petrella BL, Zhong L, Parvin-nejad FP, Fava R, Morganelli P, Robey RB & Nichols RC. AUF1/hnRNP D represses expression of VEGF in macrophages. Mol Biol Cell 23, 1414-22 (2012).
[222] Huang CY, Shih CM, Tsao NW, Chen YH, Li CY, Chang YJ, Chang NC, Ou KL, Lin CY, Lin YW, Nien CH & Lin FY. GroEL1, from Chlamydia pneumoniae, Induces Vascular Adhesion Molecule 1 Expression by p37 AUF1 in Endothelial Cells and Hypercholesterolemic Rabbit. PLoS One 7, e42808 (2012).
[223] Cerami E, Gao J, Dogrusoz U, Gross BE, Sumer SO, Aksoy BA, Jacobsen A, Byrne CJ, Heuer ML, Larsson E, Antipin Y, Reva B, Goldberg AP, Sander C & Schultz N. The cBio Cancer Genomics

Portal: An Open Platform for Exploring Multidimensional Cancer Genomics Data. Cancer Discovery 2, 401-404 (2012).
224 Gao J, Aksoy BA, Dogrusoz U, Dresdner G, Gross B, Sumer SO, Sun Y, Jacobsen A, Sinha R, Larsson E, Cerami E, Sander C & Schultz N. Integrative analysis of complex cancer genomics and clinical profiles using the cBioPortal. Sci Signal 6, pl1 (2013).
225 Das S & Krainer AR. Emerging Functions of SRSF1, Splicing Factor and Oncoprotein, in RNA Metabolism and Cancer. Mol Cancer Res 12, 1195-204 (2014).
226 Shinojima T, Oya M, Takayanagi A, Mizuno R, Shimizu N & Murai M. Renal cancer cells lacking hypoxia inducible factor (HIF)-1α expression maintain vascular endothelial growth factor expression through HIF-2α. Carcinogenesis 28, 529-536 (2007).
227 Morris MR, Hughes DJ, Tian Y, Ricketts CJ, Lau KW, Gentle D, Shuib S, Serrano-Fernandez P, Lubinski J, Wiesener MS, Pugh CW, Latif F, Ratcliffe PJ & Maher ER. Mutation Analysis of Hypoxia-inducible Factors HIF1A and HIF2A in Renal Cell Carcinoma. Anticancer Res 29, 4337-43 (2009).
228 Muz B, de la Puente P, Azab F & Azab AK. The role of hypoxia in cancer progression, angiogenesis, metastasis, and resistance to therapy. Hypoxia 3, 83-92 (2015).
229 Ravi M, Paramesh V, Kaviya SR, Anuradha E & Paul Solomon FD. 3D Cell Culture Systems: Advantages and Applications. J of Cellular Physiol 230, 16-26 (2015).
230 Sutherland RM, Sordat B, Bamat J, Gabbert H, Bourrat B & Mueller-Klieser W. Oxygenation and Differentiation in Multicellular Spheroids of Human Colon Carcinoma. Cancer Research 46, 5320-29 (1986).
231 Breslin S & O'Driscoll L. The relevance of using 3D cell cultures, in addition to 2D monolayer cultures, when evaluating breast cancer drug sensitivity and resistance. Oncotarget 7, 45745-56 (2016).
232 Imamura Y, Mukohara T, Shimono Y, Funakoshi Y, Chayahara N, Toyoda M, Kiyota N, Takao S, Kono S, Nakatsura T & Minami H. Comparison of 2D- and 3D-culture models as drug-testing platforms in breast cancer. Oncology Reports 33, 1837-43 (2015).
233 Riedl A, Schlederer M, Pudelko K, Stadler M, Walter S, Unterleuthner D, Unger C, Kramer N, Hengstschläger M, Kenner L, Pfeiffer D, Krupitza G & Dolznig H. Comparison of cancer cells in 2D vs 3D culture reveals differences in AKT–mTOR–S6K signaling and drug responses. J of Cell Sci 130, 203-218 (2017).
234 Stock K, Estrada MF, Vidic S, Gjerde K, Rudisch A, Santo VE, Barbier M, Blom S, Arundkar SC, Selvam I, Osswald A, Stein Y, Gruenewald S, Brito C, van Weerden W, Rotter V, Boghaert E, Oren M, Sommergruber W, Chong Y, de Hoogt R & Graeser R. Capturing tumor complexity *in vitro*: Comparative analysis of 2D and 3D tumor models for drug discovery. Nature Sci Reports 6, 28951 (2016).
235 Ord JJ, Streeter EH, Roberts ISD, Cranston D & Harris AL. Comparison of hypoxia transcriptome in vitro with in vivo gene expression in human bladder cancer. Br J of Cancer 93, 346-354 (2005).
236 Vaupel P & Mayer A. Hypoxia in cancer: significance and impact on clinical outcome. Cancer Metastasis Rev 26, 225-239 (2007).
237 Bayer C & Vaupel P. Acute versus chronic hypoxia in tumors. Strahlentherapie und Onkologie 188, 616-627 (2012).
238 Rofstad EK, Gaustad JV, Egeland TAM, Mathiesen B & Galappathi K. Tumors exposed to acute cyclic hypoxic stress show enhanced angiogenesis, perfusion and metastatic dissemination. Cancer Cell Biol 127, 1535-46 (2010).
239 Henze AT & Acker T. Feedback regulators of hypoxia-inducible factors and their role in cancer biology. Cell cycle 9, 2749-63 (2010).
240 Moroz E, Carlin S, Dyomina K, Burke S, Thaler HAT, Blasberg R & Serganova I. Real-Time Imaging of HIF-1α Stabilization and Degradation. PLoS One 4, e5077 (2009).
241 Cui P, Lin Q, Ding F, Xin C, Gong W, Zhang L, Geng J, Zhang B, Yu X, Yang J, Hu S & Yu J. A comparison between ribo-minus RNA-sequencing and polyA-selected RNA-sequencing. Genomics 96, 259-265 (2010).

[242] Zhao W, He X, Hoadley KA, Parker JS, Hayes DN & Perou CM. Comparison of RNA-Seq by poly (A) capture, ribosomal RNA depletion, and DNA microarray for expression profiling. BMC Genomics 15, 419 (2014).
[243] Benes V, Blake J & Doyle K. Ribo-Zero Gold Kit: improved RNA-seq results after removal of cytoplasmic and mitochondrial ribosomal RNA. Nature Methods 8, 982 (2011).
[244] Sengupta S, Bolin JM, Ruotti V, Nguyen BK, Thomson JA, Elwell AL & Stewart R. Single Read and Paired End mRNA-Seq Illumina Libraries from 10 Nanograms Total RNA. J Vis Exp 56, e3340 (2011).
[245] Meyerson M, Gabriel S & Getz G. Advances in understanding cancer genomes through second-generation sequencing. Nature Rev Gen 11, 685-696 (2010).
[246] Cieslik M & Chinnaiyan AM. Cancer transcriptome profiling at the juncture of clinical translation. Nature Rev Gen 19, 93-103 (2018).
[247] Rhodes DR, Kalyana-Sundaram S, Mahavisno V, Varambally R, Yu J, Briggs BB, Barrette TR, Anstet MJ, Kincead-Beal C, Kulkami P, Varambally S, Ghosh D & Chinnaiyan AM. Oncomine 3.0: Genes, Pathways, and Networks in a Collectionof 18,000 Cancer Gene Expression Profiles. Neoplasia 9, 166-180 (2007).
[248] Rhodes DR & Chinnaiyan AM. Oncomine 3.0: Genes, Pathways, and Networks in a Collectionof 18,000 Cancer Gene Expression Profiles. Nature Gen 37, S31-S37 (2005).
[249] Han J, Li J, Ho JC, Chia GS, Kato H, Jha S, Yang H, Poellinger L & Lee KL. Hypoxia is a Key Driver of Alternative Splicing in Human Breast Cancer Cells. Scientific Reports 7, 4108 (2017).
[250] Nakayama K & Kataoka N. Regulation of Gene Expression under Hypoxic Conditions. Int J Mol Sci 20, 3278 (2019).
[251] Jakubauskiene E, Vilys L, Makino Y, Poellinger L & Kanopka A. Increased Serine-Arginine (SR) Protein Phosphorylation Changes Pre-mRNA Splicing in Hypoxia. J Biol Chem 290, 18079-89 (2015).
[252] Bowler E, Porazinski S, Uzor S, Thibault P, Durand M, Lapointe E, Rouschop KMA, Hancock J, Wilson I & Ladomery M. Hypoxia leads to significant changes in alternative splicing and elevated expression of CLK splice factor kinases in PC3 prostate cancer cells. BMC Cancer, 18, 355 (2018).
[253] Biamonti G & Caceres JF. Cellular stress and RNA splicing. Trends in Biochem Sci 34, 146-153 (2009).
[254] Wang F, Zheng Y, Orange M, Yang C, Yang B, Liu J, Tan T, Ma X, Chen T, Yin X, Tang X & Zhu H. PTRF suppresses the progression of colorectal cancers. Oncotarget 8, 48650-59 (2017).
[255] Regazzetti C, Dumas K, Lacas-Gervais S, Pastor F, Peraldi P, Bonnafous S, Dugail I, Le Lay S, Valet P, Le Marchand-Brustel Y, Tran A, Gual P, Tantl JF, Cormont M & Giorgetti-Peraldi S. Hypoxia inhibits Cavin-1 and Cavin-2 expression and down-regulates caveolae in adipocytes. Endocrinology 156, 789-801 (2014).
[256] Pinder BD & Smibert CA. Smaug: an unexpected journey into the mechanisms of post-transcriptional regulation. Fly (Austin) 7, 142-5 (2013).
[257] Klejewski A, Swierczewska M, Zaorska K, Brazert M, Nowicki M, Zabel M & Januchowski R. New and Old Genes Associated with Topotecan Resistance Development in Ovarian Cancer Cell Lines. Anticancer Res 37, 1625-1636 (2017).
[258] Beppu K, Nakamura K, Linehan WM, Rapisarda A & Thiele CJ. Topotecan blocks hypoxia-inducible factor-1alpha and vascular endothelial growth factor expression induced by insulin-like growth factor-I in neuroblastoma cells. Cancer Res 65, 4775-81 (2005).
[259] Brady LK, Wang H, Radens CM, Bi Y, Radovich M, Maity A, Ivan C, Ivan M, Barash Y & Koumenis C. Transcriptome analysis of hypoxic cancer cells uncovers intron retention in EIF2B5 as a mechanism to inhibit translation. PLoS Biol 15, e2002623 (2017).
[260] Moseley PL. Heat shock proteins and heat adaptation of the whole organism. J of Applied Physiol 83, 1413-17 (1997).
[261] El-Arabey AA, Salama SA & Abd-Allah AR. CENP-E as a target for cancer therapy: Where are we now?. Life Sci 208, 192-200 (2018).

[262] He X, Pool M, Darcy KM, Lim SB, Auersperg N, Coon JS & Beck WT. Knockdown of polypyrimidine tract-binding protein suppresses ovarian tumor cell growth and invasiveness *in vitro*. Oncogene 26, 4961-68 (2007).

[263] Xu W, Rao Q, An Y, Li M & Zhang Z. Identification of biomarkers for Barcelona Clinic Liver Cancer staging and overall survival of patients with hepatocellular carcinoma. PLoS One 13, e0202763 (2018).

[264] Ghigna C, Giordano S, Shen H, Benvenuto F, Castiglioni F, Comoglio PM, Green MR, Riva S & Biamonti G. Cell Motility Is Controlled by SF2/ASF through Alternative Splicing of the Ron Protooncogene. Mol Cell 20, 881-890 (2005).

[265] Krishnamachary B, Penet MF, Nimmagadda S, Mironchik Y, Raman V, Solaiyappan M, Semenza GL, Pomper MG & Bhujwalla ZM. Hypoxia Regulates CD44 and Its Variant Isoforms through HIF-1α in Triple Negative Breast Cancer. PLoS One 7, e44078 (2012).

[266] Shi X, Liu Z, Liu Z, Feng X, Hua F, Hu X, Wang B, Lu K & Nie F. Long noncoding RNA PCAT6 functions as an oncogene by binding to EZH2 and suppressing LATS2 in non-small-cell lung cancer. EBioMedicine 37, 177-187 (2018).

[267] Wan L, Zhang L, Fan K, Cheng ZX, Sun QC & Wang JJ. Knockdown of Long Noncoding RNA PCAT6 Inhibits Proliferation and Invasion in Lung Cancer Cells. Onco Res Feat Preclin and Clin Cancer Ther 24, 161-170 (2016).

[268] Xu Z, Yang F, Wie D, Liu B, Chen C, Bao Y, Wu Z, Wu D, Han T, Li J, Wang J, Liu J, Qu L & Wang L. Long noncoding RNA-SRLR elicits intrinsic sorafenib resistance via evoking IL-6/STAT3 axis in renal cell carcinoma. Oncogene 36, 1965-77 (2017).

[269] Di Liddo A, de Oliveira Freitas Machado C, Fischer S, Ebersberger S, Heumüller AW, Weigand JE, Müller-McNicoll M and Zarnack K. A combined computational pipeline to detect circular RNAs in human cancer cells under hypoxic stress. Journal of Molecular Cell Biology, Epub ahead of print, doi: 10.1093/jmcb/mjz094.(2019).

[270] Song Y, Zheng S, Wang J, Long H, Fang L, Wang G, Li Z, Que T, Liu Y, Li Y, Zhang X, Fang W & Qi S. Hypoxia-induced PLOD2 promotes proliferation, migration and invasion via PI3K/Akt signaling in glioma. Oncotarget 8, 41947-62 (2017).

[271] Lee JH, Song SY, Kim MS, Yoo NJ & Lee SH. Frameshift mutations of a tumor suppressor gene ZNF292 in gastric and colorectal cancers with high microsatellite instability. J Patho, Microbiol and Immonol 124, 556-560 (2016).

[272] Satoh J, Asahina N, Kitano S & Kino Y. Bioinformatics data mining approach indicates the expression ofchromatin immunoprecipitation followed by deep sequencing(ChIP-Seq)-based hypoxia-inducible factor-1atarget genes inperiplaque lesions of multiple sclerosis. Clin and Exp Neuroimmunol 6, 156-169 (2015).

[273] Adachi M, Taki T, Higashiyama M, Kohno N, Inufusa H & Miyake M. Significance of Integrin α5 Gene Expression as a Prognostic Factor in Node-negative Non-Small Cell Lung Cancer. Clin Cancer Res 6, 96-101 (2000).

[274] Liu JL, Wie W, Tang W, Jiang Y, Hang HW, Li JT & Zhou X. Silencing of Lysyl Oxidase Gene Expression by RNA Interference Suppresses Metastasis of Breast Cancer. Asian Pacific J of Cancer Prevention 13, 3507-11 (2012).

[275] Kathagen A, Schulte A, Balcke G, Phillips HS, Martens T, Matschke J, Günther HS, Soriano R, Modrusan Z, Sandmann T, Kuhl C, Tissier A, Holz M, Krawinkel LA, Glatzel M, Westphal M & Lamszus K. Hypoxia and oxygenation induce a metabolic switch between pentose phosphate pathway and glycolysis in glioma stem-like cells. Acta Neuropathologica 126, 763-780 (2013).

[276] Axelson H, Fredlund E, Ovenberger M, Landberg G & Pahlman S. Hypoxia-induced dedifferentiation of tumor cells – A mechanism behind heterogeneity and aggressiveness of solid tumors. Sem in Cell & Dev Biol 16, 554-563 (2005).

[277] Seubwai W, Kraiklang R, Wongkham C & Wongkham S. Hypoxia Enhances Aggressiveness of Cholangiocarcinoma Cells. Asian Pacific J of Cancer Prevention 13, 53-58 (2012).

[278] Erler JT, Bennewith KL, Nicolau M, Dornhöfer N, Kong C, Le QT, Chi JTA, Jeffrey SS & Giaccia AJ. Lysyl oxidase is essential for hypoxia-induced metastasis. Nature 440, 1222-26 (2006).

[279] Charizanis K, Lee KY, Batra R, Goodwin M, Zhang C, Yuan Y, Shiue L, Cline M, Scotti MM, Xia G, Kumar A, Ashizawa T, Clark HB, Kimura T, Takahashi MP, Fujimura H, Jinnai K, Yoshikawa H, Gomes-Pereira M, Gourdon G, Sakai N, Nishino S, Foster TC, Ares M, Darnell RB & Swanson MS. Muscleblind-like 2-Mediated Alternative Splicingin the Developing Brain and Dysregulationin Myotonic Dystrophy. Neuron 75, 437-450 (2012).

[280] Arif A, Yao P, Terenzi F, Jia J, Ray PS & Fox PL. The GAIT translational control system. Wiley Interdiscip Rev RNA 9, e1441 (2018).

[281] Yao P, Potdar AA, Ray PS, Eswarappa SM, Flagg AC, Willard B & Fox PL. The HILDA complex coordinates a conditional switch in the 3'-untranslated region of the VEGFA mRNA. PLoS Biol 11, e1001635 (2013).

[282] Pu JJ, Teye EK, Sido A, Kawasawa YI, Xin P, Finnberg NK, El-Deiry WS & Shimko S. PIGN gene expression aberration weakens chromosomal stability via altering its interaction with the spindle assembly checkpoint protein complex during leukemogenesis. Clin Res 77, 13 (2017).

[283] Nadiradze G, Giger-Pabst U, Zieren J, Strumberg D, Solass W & Reymond MA. Pressurized Intraperitoneal Aerosol Chemotherapy (PIPAC) with Low-Dose Cisplatin and Doxorubicin in Gastric Peritoneal Metastasis. J Gastrointestinal Surgery 20, 367-373 (2016).

[284] Thorn CF, Oshiro C, Marsh S, Hernandez-Boussard T, McLeod H, Klein TE & Altman RB. Doxorubicin pathways: pharmacodynamics and adverse effects. Pharmacogenet Genomics 21, 440-446 (2012).

[285] Yoon JH, De S, Srikantan S, Abdelmohsen K, Grammatikakis I, Kim J, Kim KM, Noh JH, White EJF, Martindale JL, Yang X, Kang MJ, Wood 3rd WH, Hooten NN, Evans MK, Becker KG, Tripathi V, Prasanth KV, Wilson GM, Tuschl T, Ingolia NT, Hafner M & Gorospe M. PAR-CLIP analysis uncovers AUF1 impact on target RNA fate and genome integrity. Nature Communications 5, 5248 (2014).

[286] Paul S, Dansithong W, Kim D, Rossi J, Webster NJ, Comai L & Reddy S. Interaction of muscleblind, CUG-BP1 and hnRNP H proteins in DM1-associated aberrant IR splicing. EMBO J 25, 4271-4283 (2006).

[287] Holt I, Mittal S, Furling D, Butler-Browne GS, Brook JD & Morris GE. Defective mRNA in myotonic dystrophy accumulates at the periphery of nuclear splicing speckles. Genes Cells, 12, 1035-1048 (2007).

[288] Dobin A, Davis CA, Schlesinger F, Drenkow J, Zaleski C, Jha S, Batut P, Chaisson M & Gingeras TR. STAR: ultrafast universal RNA-seq aligner. Bioinformatics 29, 15-21 (2013).

[289] Anders S, Pyl PT & Huber W. HTSeq - a Python framework to work with high-throughput sequencing data. Bioinformatics 31, 166-169 (2015).

[290] Yu G, Wang LG, Han Y & He QY. clusterProfiler: an R package for comparing biological themes among gene clusters. OMICS 16, 284-287 (2012).

[291] Pfaffl MW. A new mathematical model for relative quantification in real-time RT-PCR. Nucleic Acids Res 29, e45 (2001).

[292] Bradford MM. A rapid and sensitive method for the quantitation of microgram quantities of protein utilizing the principle of protein-dye binding. Anal Biochem 72, 248-54 (1976).

[293] Kemmerer K & Weigand JE. Hypoxia reduces MAX expression in endothelial cells by unproductive splicing. FEBS letters 588, 4784-4790 (2014).

[294] Feoktistova M, Geserick P & Leverkus M. Crystal Violet Assay for Determining Viability of Cultured Cells. Cold Spring Harbor Prot 2016, 4 (2016).

11 Supplementary Figures

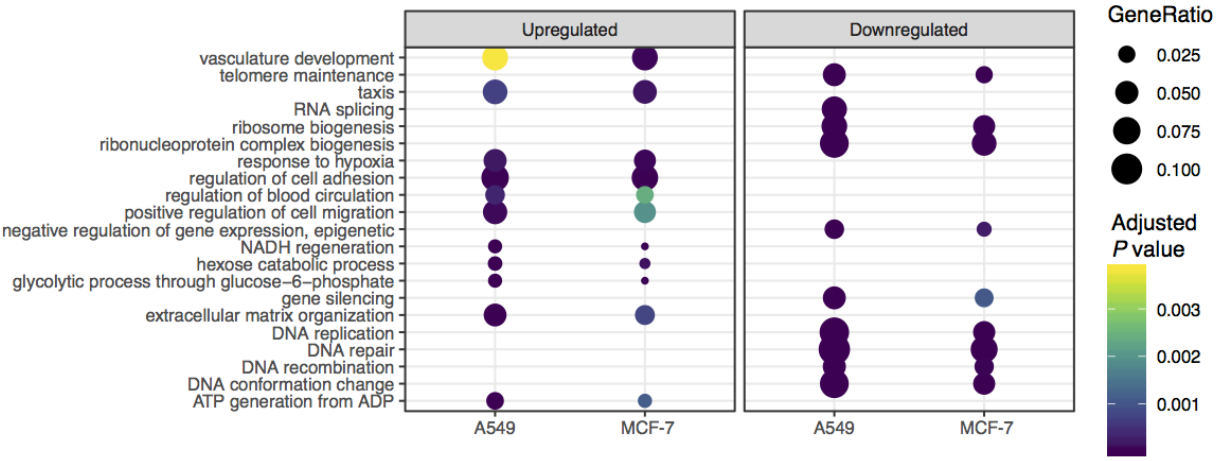

Figure 11-1: GO analyses of differentially expressed genes under hypoxia. As expected, hypoxia response genes were induced and genes associated with DNA repair, replication etc. were reduced.

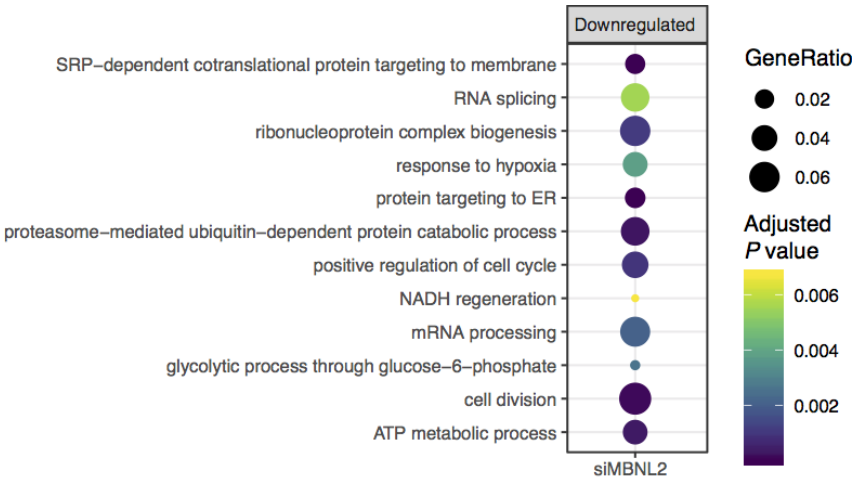

Figure 11-2: GO analyses of differentially expressed genes after MBNL2 knockdown. No GO terms were significantly induced after *MBNL2* knockdown.

Table 11-1: Aligned *MBNL2* sequences. CLUSTAL Omega (1.2.4) multiple sequence alignment was used to create sequence alignment. Alignment was manually modified to increase clarity. Exon 5 is marked in blue, exon 8 is marked in yellow. Stop codons are indicated in grey.

```
MBNL2-39        ATGGCTTTGAACGTTGCCCCAGTCAGAGATACAAAATGGCTGACATTAGAAGTCTGCAGA      60
MBNL2-41        ATGGCTTTGAACGTTGCCCCAGTCAGAGATACAAAATGGCTGACATTAGAAGTCTGCAGA      60
MBNL2-38        ATGGCTTTGAACGTTGCCCCAGTCAGAGATACAAAATGGCTGACATTAGAAGTCTGCAGA      60
MBNL2-40        ATGGCTTTGAACGTTGCCCCAGTCAGAGATACAAAATGGCTGACATTAGAAGTCTGCAGA      60
                ************************************************************


MBNL2-39        CAGTTTCAAAGAGGAACATGCTCACGCTCTGATGAAGAATGCAAATTTGCTCATCCCCCC      120
MBNL2-41        CAGTTTCAAAGAGGAACATGCTCACGCTCTGATGAAGAATGCAAATTTGCTCATCCCCCC      120
MBNL2-38        CAGTTTCAAAGAGGAACATGCTCACGCTCTGATGAAGAATGCAAATTTGCTCATCCCCCC      120
MBNL2-40        CAGTTTCAAAGAGGAACATGCTCACGCTCTGATGAAGAATGCAAATTTGCTCATCCCCCC      120
                ************************************************************
```

```
MBNL2-39      AAAAGTTGTCAGGTTGAAAATGGAAGAGTAATTGCCTGCTTTGATTCCCTAAAGGGCCGT    180
MBNL2-41      AAAAGTTGTCAGGTTGAAAATGGAAGAGTAATTGCCTGCTTTGATTCCCTAAAGGGCCGT    180
MBNL2-38      AAAAGTTGTCAGGTTGAAAATGGAAGAGTAATTGCCTGCTTTGATTCCCTAAAGGGCCGT    180
MBNL2-40      AAAAGTTGTCAGGTTGAAAATGGAAGAGTAATTGCCTGCTTTGATTCCCTAAAGGGCCGT    180
              ************************************************************


MBNL2-39      TGTTCGAGAGAGAACTGCAAGTATCTTCACCCTCCGACACACTTAAAAACTCAACTAGAA    240
MBNL2-41      TGTTCGAGAGAGAACTGCAAGTATCTTCACCCTCCGACACACTTAAAAACTCAACTAGAA    240
MBNL2-38      TGTTCGAGAGAGAACTGCAAGTATCTTCACCCTCCGACACACTTAAAAACTCAACTAGAA    240
MBNL2-40      TGTTCGAGAGAGAACTGCAAGTATCTTCACCCTCCGACACACTTAAAAACTCAACTAGAA    240
              ************************************************************


MBNL2-39      ATTAATGGAAGGAACAATTTGATTCAGCAAAAAACTGCAGCAGCAATGCTTGCCCAGCAG    300
MBNL2-41      ATTAATGGAAGGAACAATTTGATTCAGCAAAAAACTGCAGCAGCAATGCTTGCCCAGCAG    300
MBNL2-38      ATTAATGGAAGGAACAATTTGATTCAGCAAAAAACTGCAGCAGCAATGCTTGCCCAGCAG    300
MBNL2-40      ATTAATGGAAGGAACAATTTGATTCAGCAAAAAACTGCAGCAGCAATGCTTGCCCAGCAG    300
              ************************************************************


MBNL2-39      ATGCAATTTATGTTTCCAGGAACACCACTTCATCCAGTGCCCACTTTCCCTGTAGGTCCC    360
MBNL2-41      ATGCAATTTATGTTTCCAGGAACACCACTTCATCCAGTGCCCACTTTCCCTGTAGGTCCC    360
MBNL2-38      ATGCAATTTATGTTTCCAGGAACACCACTTCATCCAGTGCCCACTTTCCCTGTAGGTCCC    360
MBNL2-40      ATGCAATTTATGTTTCCAGGAACACCACTTCATCCAGTGCCCACTTTCCCTGTAGGTCCC    360
              ************************************************************


MBNL2-39      GCGATAGGGACAAATACGGCTATTAGCTTTGCTCCTTACCTAGCACCTGTAACCCCTGGA    420
MBNL2-41      GCGATAGGGACAAATACGGCTATTAGCTTTGCTCCTTACCTAGCACCTGTAACCCCTGGA    420
MBNL2-38      GCGATAGGGACAAATACGGCTATTAGCTTTGCTCCTTACCTAGCACCTGTAACCCCTGGA    420
MBNL2-40      GCGATAGGGACAAATACGGCTATTAGCTTTGCTCCTTACCTAGCACCTGTAACCCCTGGA    420
              ************************************************************


MBNL2-39      GTTGGGTTGGTCCCAACGGAAATTCTGCCCACCACGCCTGTTATTGTTCCCGGAAGTCCA    480
MBNL2-41      GTTGGGTTGGTCCCAACGGAAATTCTGCCCACCACGCCTGTTATTGTTCCCGGAAGTCCA    480
MBNL2-38      GTTGGGTTGGTCCCAACGGAAATTCTGCCCACCACGCCTGTTATTGTTCCCGGAAGTCCA    480
MBNL2-40      GTTGGGTTGGTCCCAACGGAAATTCTGCCCACCACGCCTGTTATTGTTCCCGGAAGTCCA    480
              ************************************************************


MBNL2-39      CCGGTCACTGTCCCGGGCTCAACTGCAACTCAGAAACTTCTCAGGACTGACAAACTGGAG    540
MBNL2-41      CCGGTCACTGTCCCGGGCTCAACTGCAACTCAGAAACTTCTCAGGACTGACAAACTGGAG    540
MBNL2-38      CCGGTCACTGTCCCGGGCTCAACTGCAACTCAGAAACTTCTCAGGACTGACAAACTGGAG    540
MBNL2-40      CCGGTCACTGTCCCGGGCTCAACTGCAACTCAGAAACTTCTCAGGACTGACAAACTGGAG    540
              ************************************************************


MBNL2-39      GTATGCAGGGAGTTCCAGCGAGGAAACTGTGCCCGGGGAGAGACCGACTGCCGCTTTGCA    600
MBNL2-41      GTATGCAGGGAGTTCCAGCGAGGAAACTGTGCCCGGGGAGAGACCGACTGCCGCTTTGCA    600
MBNL2-38      GTATGCAGGGAGTTCCAGCGAGGAAACTGTGCCCGGGGAGAGACCGACTGCCGCTTTGCA    600
MBNL2-40      GTATGCAGGGAGTTCCAGCGAGGAAACTGTGCCCGGGGAGAGACCGACTGCCGCTTTGCA    600
              ************************************************************


MBNL2-39      CACCCCGCAGACAGCACCATGATCGACACAAGTGACAACACCGTAACCGTTTGTATGGAT    660
MBNL2-41      CACCCCGCAGACAGCACCATGATCGACACAAGTGACAACACCGTAACCGTTTGTATGGAT    660
MBNL2-38      CACCCCGCAGACAGCACCATGATCGACACAAGTGACAACACCGTAACCGTTTGTATGGAT    660
MBNL2-40      CACCCCGCAGACAGCACCATGATCGACACAAGTGACAACACCGTAACCGTTTGTATGGAT    660
              ************************************************************
```

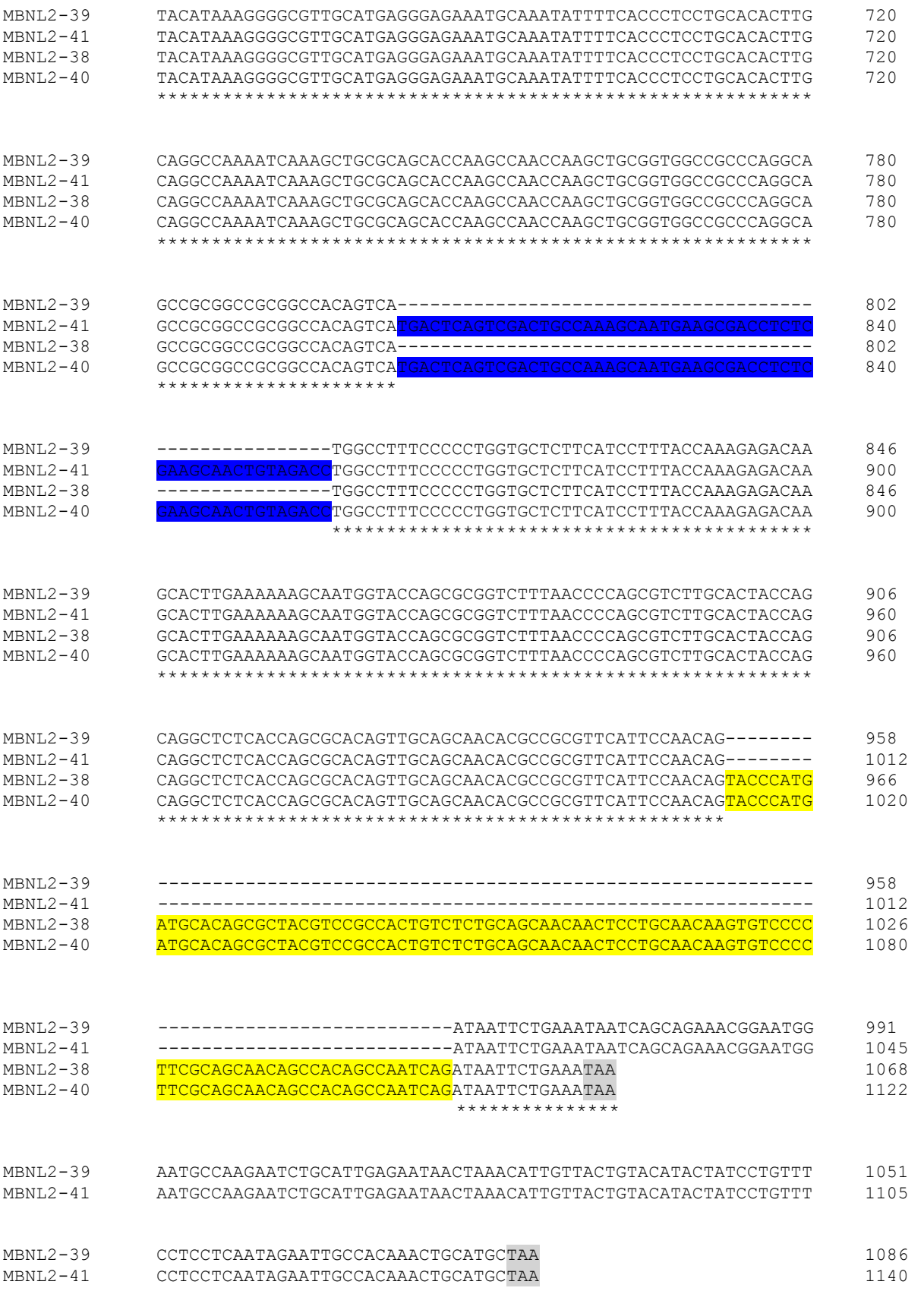
MBNL2-39 TACATAAAGGGGCGTTGCATGAGGGAGAAATGCAAATATTTTCACCCTCCTGCACACTTG 720
MBNL2-41 TACATAAAGGGGCGTTGCATGAGGGAGAAATGCAAATATTTTCACCCTCCTGCACACTTG 720
MBNL2-38 TACATAAAGGGGCGTTGCATGAGGGAGAAATGCAAATATTTTCACCCTCCTGCACACTTG 720
MBNL2-40 TACATAAAGGGGCGTTGCATGAGGGAGAAATGCAAATATTTTCACCCTCCTGCACACTTG 720
MBNL2-39 CAGGCCAAAATCAAAGCTGCGCAGCACCAAGCCAACCAAGCTGCGGTGGCCGCCCAGGCA 780
MBNL2-41 CAGGCCAAAATCAAAGCTGCGCAGCACCAAGCCAACCAAGCTGCGGTGGCCGCCCAGGCA 780
MBNL2-38 CAGGCCAAAATCAAAGCTGCGCAGCACCAAGCCAACCAAGCTGCGGTGGCCGCCCAGGCA 780
MBNL2-40 CAGGCCAAAATCAAAGCTGCGCAGCACCAAGCCAACCAAGCTGCGGTGGCCGCCCAGGCA 780
MBNL2-39 GCCGCGGCCGCGGCCACAGTCA---------- 802
MBNL2-41 GCCGCGGCCGCGGCCACAGTCATGACTCAGTCGACTGCCAAAGCAATGAAGCGACCTCTC 840
MBNL2-38 GCCGCGGCCGCGGCCACAGTCA---------- 802
MBNL2-40 GCCGCGGCCGCGGCCACAGTCATGACTCAGTCGACTGCCAAAGCAATGAAGCGACCTCTC 840
MBNL2-39 ----------TGGCCTTTCCCCCTGGTGCTCTTCATCCTTTACCAAAGAGACAA 846
MBNL2-41 GAAGCAACTGTAGACCTGGCCTTTCCCCCTGGTGCTCTTCATCCTTTACCAAAGAGACAA 900
MBNL2-38 ----------TGGCCTTTCCCCCTGGTGCTCTTCATCCTTTACCAAAGAGACAA 846
MBNL2-40 GAAGCAACTGTAGACCTGGCCTTTCCCCCTGGTGCTCTTCATCCTTTACCAAAGAGACAA 900
MBNL2-39 GCACTTGAAAAAAGCAATGGTACCAGCGCGGTCTTTAACCCCAGCGTCTTGCACTACCAG 906
MBNL2-41 GCACTTGAAAAAAGCAATGGTACCAGCGCGGTCTTTAACCCCAGCGTCTTGCACTACCAG 960
MBNL2-38 GCACTTGAAAAAAGCAATGGTACCAGCGCGGTCTTTAACCCCAGCGTCTTGCACTACCAG 906
MBNL2-40 GCACTTGAAAAAAGCAATGGTACCAGCGCGGTCTTTAACCCCAGCGTCTTGCACTACCAG 960
MBNL2-39 CAGGCTCTCACCAGCGCACAGTTGCAGCAACACGCCGCGTTCATTCCAACAG-------- 958
MBNL2-41 CAGGCTCTCACCAGCGCACAGTTGCAGCAACACGCCGCGTTCATTCCAACAG-------- 1012
MBNL2-38 CAGGCTCTCACCAGCGCACAGTTGCAGCAACACGCCGCGTTCATTCCAACAGTACCCATG 966
MBNL2-40 CAGGCTCTCACCAGCGCACAGTTGCAGCAACACGCCGCGTTCATTCCAACAGTACCCATG 1020
MBNL2-39 ---------- 958
MBNL2-41 ---------- 1012
MBNL2-38 ATGCACAGCGCTACGTCCGCCACTGTCTCTGCAGCAACAACTCCTGCAACAAGTGTCCCC 1026
MBNL2-40 ATGCACAGCGCTACGTCCGCCACTGTCTCTGCAGCAACAACTCCTGCAACAAGTGTCCCC 1080
MBNL2-39 ----------ATAATTCTGAAATAATCAGCAGAAACGGAATGG 991
MBNL2-41 ----------ATAATTCTGAAATAATCAGCAGAAACGGAATGG 1045
MBNL2-38 TTCGCAGCAACAGCCACAGCCAATCAGATAATTCTGAAATAA 1068
MBNL2-40 TTCGCAGCAACAGCCACAGCCAATCAGATAATTCTGAAATAA 1122
MBNL2-39 AATGCCAAGAATCTGCATTGAGAATAACTAAACATTGTTACTGTACATACTATCCTGTTT 1051
MBNL2-41 AATGCCAAGAATCTGCATTGAGAATAACTAAACATTGTTACTGTACATACTATCCTGTTT 1105
MBNL2-39 CCTCCTCAATAGAATTGCCACAAACTGCATGCTAA 1086
MBNL2-41 CCTCCTCAATAGAATTGCCACAAACTGCATGCTAA 1140

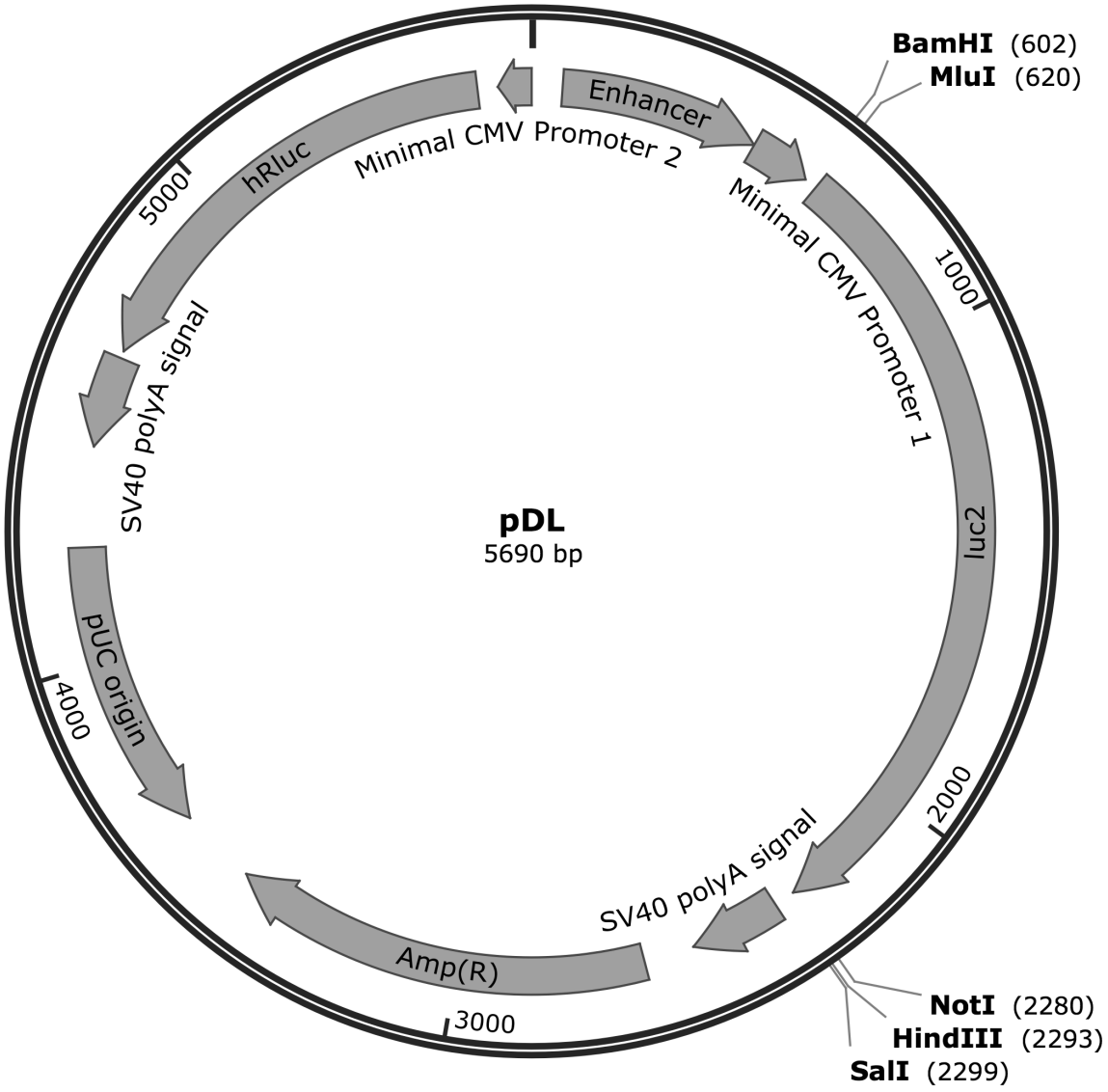

Figure 11-3: pDL plasmid map. The plasmid contains the coding sequence of the ß-lactamase [Amp(R)], firefly luciferase (luc2) and *Renilla* luciferase (hRluc) with CMV promoters (Minimal CMV Promoter 1/2) and an enhancer element (Enhancer). The restriction sites for *BamHI* and *MluI* were used for restriction cloning of 5' UTRs. *NotI* and *HindIII* or *SalI* were used for restriction cloning of 3' UTRs. Figure was created using SnapGene.

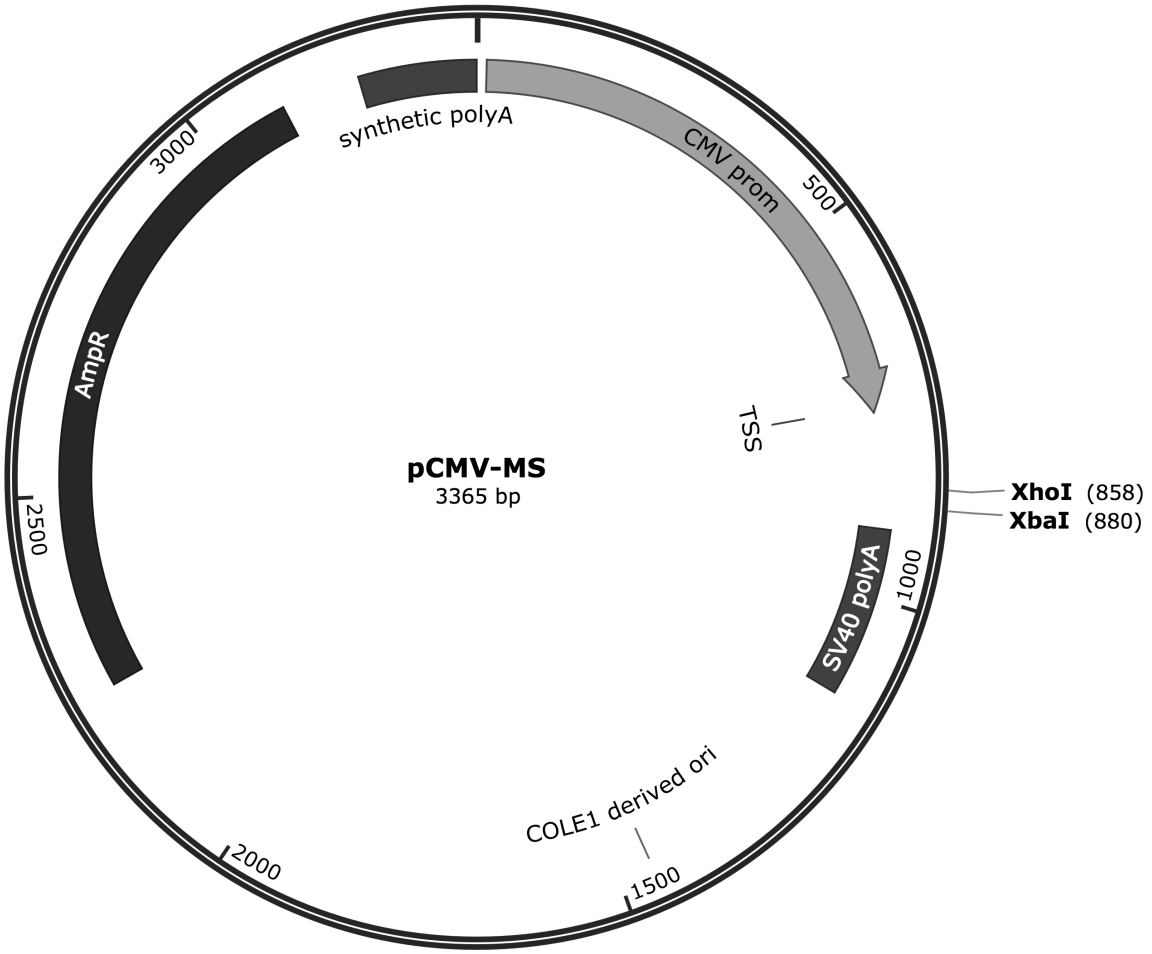

Figure 11-4: pCMV plasmid map. The plasmid contains the coding sequence of the ß-lactamase [Amp(R)] and a CMV promoter (Minimal CMV Promoter 1/2). *XhoI* and *XbaI* restriction sites were used for restriction cloning. Figure was created using SnapGene.

12 List of Figures

13 Acknowledgement

An dieser Stelle möchte ich allen danken, die mich bei der Arbeit an meinem Promotionsprojekt unterstützt haben.
Mein besonderer Dank gilt:

Dr. Julia Weigand
Ich danke Dir für die Vergabe des Themas und die hervorragende Betreuung meiner Arbeit. Außerdem bin ich dankbar für die Freiheiten, die ich bei meiner Arbeit hatte, und für die vielen Möglichkeiten, die Du mir gegeben hast, um meine fachlichen und persönlichen Kompetenzen zu verbessern wie z.B. die Teilnahme an Tagungen und Weiterbildungen.

Prof. Dr. Beatrix Süß
Ich danke Dir dafür, dass ich meine Arbeit in Deinem Labor durchführen durfte und für die vielen hilfreichen Diskussionen.

Prof Dr. Alexander Löwer
Ich danke Ihnen für die freundliche Übernahme des Zweitgutachtens.

Dr.-Ing. Wilhelm und Maria Kirmser Stiftung
Ich danke der Dr.-Ing. Wilhelm und Maria Kirmser Stiftung für die finanzielle Unterstützung.

SFB902
Ich danke dem SFB902 für die finanzielle Unterstützung und den Mitgliedern des SFB902 für hilfreiches Feedback zu meiner Forschung.

Dr. Katrin Kemmerer
Ich danke Dir für alle Vorarbeiten im hnRNP DL-Projekt und dafür, dass Du bereits zu Zeiten meiner Bachelorarbeit meine Begeisterung für das Thema geweckt hast.

Dr. Kathi Zarnack und Antonella Di Liddo
Ich danke Euch für die Durchführung der bioinformatischen Analysen und für die konstruktiven Diskussionen während unserer Zusammenarbeit.

Dr. Michaela Müller-McNicholl und Camila de Oliveira Freitas Machado
Ich danke Euch für die Zusammenarbeit und das hilfreiche Feedback zu meiner Arbeit.

Prof. Dr. Krzysztof Sobzak und Katarzyna Taylor
I am thankful for your scientific support and for the transfer of MBNL2 overexpression plasmids.

Prof. Dr. Stefanie Dimmeler und Dr. Larissa Pfisterer
Ich bin dankbar, dass ich in Ihrem Labor neue Methoden erlernen durfte.

Weigand-Lab: Britta Kluge, Stephen Peter und Dr. Johannes Braun
Ich danke Euch für die hervorragende Zusammenarbeit, die gegenseitige Unterstützung und die allzeit gute Stimmung.

Maria Fauth, Jamina Gerhardus, Anna Theresa Gimbel und Karolin Wlotzka
Ich danke Euch für die Mitarbeit an meinen Projekten. Ich hätte mir keine besseren Studenten wünschen können.

Anne Emmerich, Anett Hegewald und Julia Wellstein
Ich danke Euch für unvergessliche Mittagspausen und mentalen Beistand in allen Phasen der Doktorarbeit (vor allem Pinguin-in-Badewanne-Phase).

Süß-Lab: Dr. Janina Atanasov, Claudia Baier, Dr. Isabell Baumann, Dr. Cristina Bofill-Bosch, Dr. Adrien Boussebayle, Kai Breitwieser, Franzi Engel, Anne Groher, Dr. Florian Groher, Dr. Stella Hedrich, Jeannine Jäger, Dr. Thea Lotz, Dr. Adam Mol, Dr. Martin Rudolph, Dr. Meike Saul, Dr. Christopher Schneider, Britta Schreiber, Dunja Sehn, Caroline Sellerberg, Dr. Michi Vockenhuber, Dr. Marc Vogel, Eva Wolf & alle Anderen
Ich danke Euch für die angenehme Arbeitsatmosphäre und für die gegenseitige Motivation.

Ute und Armin
Ihr habt mir ermöglicht, diesen Weg zu gehen und Ihr standet immer hinter mir, egal welche Entscheidungen ich in meinem Leben getroffen habe. Dafür bin ich Euch sehr dankbar!

Christian
Du hast mich immer unterstützt und glaubst an mich. Du gibst mir so viel Kraft. Danke!

13 Curriculum Vitae

Personal Information

Name:	Sandra Fischer
Date of birth:	10.09.1990 (in Hanau)
Address:	Martin-Niemöller-Straße 26 64354 Reinheim

Experience

07/2016 - today	Doctoral candidate Working Group Süß/Weigand Technische Universität, Darmstadt
03/2016 - 06/2016	Research Engineer BRAIN AG, Zwingenberg
04/2015 - 12/2015	Master Student BRAIN AG, Zwingenberg
10/2013 - 10/2014	Research Associate Working Group Süß/Weigand Technische Universität, Darmstadt
04/2013 - 07/2013	Bachelor Student Working Group Süß/Weigand Technische Universität, Darmstadt

Education

10/2013 - 01/2016	Technische Universität, Darmstadt Degree: Master of Science in Biomolecular Engineering (Final grade: 1,18)
10/2010 - 07/2013	Technische Universität, Darmstadt Degree: Bachelor of Science in Biomolecular Engineering (Final grade: 1,67)
09/2001 - 07/2010	Grimmelshausen-Gymnasium, Gelnhausen
09/1997 - 07/2001	Kinzigtalschule, Gründau-Lieblos

Reinheim, 14.10.2019

14 Publications and Presentations

Publications

Kemmerer K*, **Fischer S*** and Weigand JE. (2018) Auto- and cross-regulation of the hnRNPs D and DL. RNA. (* Shared first author)

Braun J, **Fischer S**, Xu ZZ, Sun H, Ghoneim DH, Gimbel AT, Plessmann U, Urlaub H, Mathews DH and Weigand JE. (2018) Identification of new high affinity targets for Roquin based on structural conservation. Nucleic Acids Research.

Ertongur-Fauth T, **Fischer S**, Hartmann D, Brüggemann A, Seeger V, Kleber A and Krohn M. (2018) Towards novel bioactive antiperspirants for cosmetic applications. IFSCC Magazine. (**Top Award in Applied Research**)

Di Liddo A, de Oliveira Freitas Machado C, **Fischer S**, Ebersberger S, Heumüller AW, Weigand JE, Müller-McNicoll M and Zarnack K (2019) A combined computational pipeline to detect circular RNAs in human cancer cells under hypoxic stress. Journal of Molecular Cell Biology.

Fischer S, Di Liddo A, Taylor K, Sobczak K, Zarnack K and Weigand JE. (2019) Muscleblind-like 2 controls the hypoxia response of cancer cells. RNA. (*in revision*)

Posters and Presentations

Perspectives in vascular biology (2016), Frankfurt
Poster: “Alternative splicing in response to hypoxia”

Hallmarks of cancer: Focus on RNA (2017), Prag
Poster: “Alternative splicing in response to hypoxia”

35. Rabensteiner Kolleg (2017), Pottenstein
Presentation: “Crossregulation of the hnRNPs D and DL”

2. RMU RNA-Salon - Ribonomics for every taste (2017), Frankfurt
Poster: “Alternative splicing in response to hypoxia”

Symposium on Nucleic acid modifications (2017), Mainz
Poster: “Hypoxia-driven alternative splicing in cancer“

SFB 902 Symposium - RNA Biology (2017), Friedrichsdorf
Presentation: “Auto- and crossregulation of the hnRNPs D and DL” (**Best Talk 3. Prize**)

SFB 902 Symposium - Understanding RNA-based Regulation in Cells (2018), Frankfurt
Poster: “Hypoxia-driven alternative splicing in cancer“

SFB 902 Audit (2018), Frankfurt
Poster: “Identification of regulatory elements based on structural conservation“

GBM RNA Biochemistry Meeting (2018), Bonn
Poster: “Hypoxia-driven alternative splicing in cancer“

15 Ehrenwörtliche Erklärung

Ich erkläre hiermit ehrenwörtlich, dass ich die vorliegende Arbeit entsprechend den Regeln guter wissenschaftlicher Praxis selbstständig und ohne unzulässige Hilfe Dritter angefertigt habe.

Sämtliche aus fremden Quellen direkt oder indirekt übernommenen Gedanken sowie sämtliche von Anderen direkt oder indirekt übernommenen Daten, Techniken und Materialien sind als solche kenntlich gemacht. Die Arbeit wurde bisher bei keiner anderen Hochschule zu Prüfungszwecken eingereicht.

Darmstadt, den __.__._____

_____

Sandra Fischer